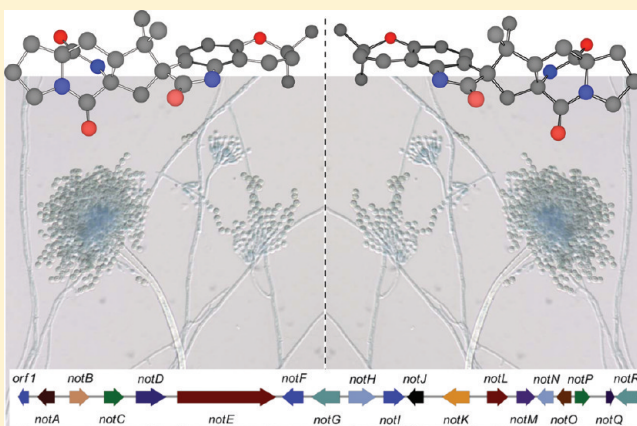


# Natural Products Synthesis: Enabling Tools To Penetrate Nature's Secrets of Biogenesis and Biomechanism<sup>†</sup>

Robert M. Williams\*

Department of Chemistry, Colorado State University, Fort Collins, Colorado 80523, United States

**ABSTRACT:** Selected examples from our laboratory of how synthetic technology platforms developed for the total synthesis of several disparate families of natural products was harnessed to penetrate biomechanistic and/or biosynthetic queries is discussed. Unexpected discoveries of biomechanistic reactivity and/or penetrating the biogenesis of naturally occurring substances were made possible through access to substances available only through chemical synthesis. Hypothesis-driven total synthesis programs are emerging as very useful conceptual templates for penetrating and exploiting the inherent reactivity of biologically active natural substances. In many instances, new enabling synthetic technologies were required to be developed. The examples demonstrate the often untapped richness of complex molecule synthesis to provide powerful tools to understand, manipulate and exploit Nature's vast and creative palette of secondary metabolites.



## INTRODUCTION

Natural products have constituted a resplendent source of chemical value to medicine, both modern and traditional, and have also provided a seemingly limitless supply of challenging structures for the synthetic chemist. Natural products have been one of the main drivers for the development of modern asymmetric methodology and have been used as a testing ground for ever more innovative strategies and concepts for complex molecule synthesis. Many practitioners of the art of total synthesis have limited their often breathtaking conquest of a natural product to assembly of the single natural substance itself and have rarely harnessed the power of the total synthesis technology they have labored to develop for penetrating the mode of action of biologically relevant natural products and/or the biogenesis of the natural compound or the larger family of natural agents to which it belongs. Our laboratory has long held an interest in how biologically active natural substances exert their effects in living systems and also how Nature constructs these beautiful and complex materials. In this Perspective, we will show examples selected from our laboratory of how total synthesis platforms can be exploited to penetrate some of Nature's closely guarded secrets of molecular construction and molecular action.

### I. BICYCLOMYCIN

Our first foray into natural products total synthesis was the *Streptomyces* sp. metabolite bicyclomycin (bicozamycin) (Scheme 1).<sup>1</sup> We devised an electrophilic glycine species (**1**) that was used to address the installation of the branched isoleucine

bridge constituting the bicyclo[4.2.2]diazadecane ring system.<sup>2</sup> Conversion of lactone **3** into the bicyclic substrate **4** was followed by regioselective bridgehead carbanion oxidation and double diastereo-differentiating aldol condensation. The overall synthesis constituted just twelve steps from commercially available glycine anhydride.

Bicyclomycin represented a structurally new class of antimicrobial agent, and its mechanism of action was later elucidated by Widger and co-workers in an extensive series of publications to act on the ATP-dependent motor protein Rho.<sup>3</sup>

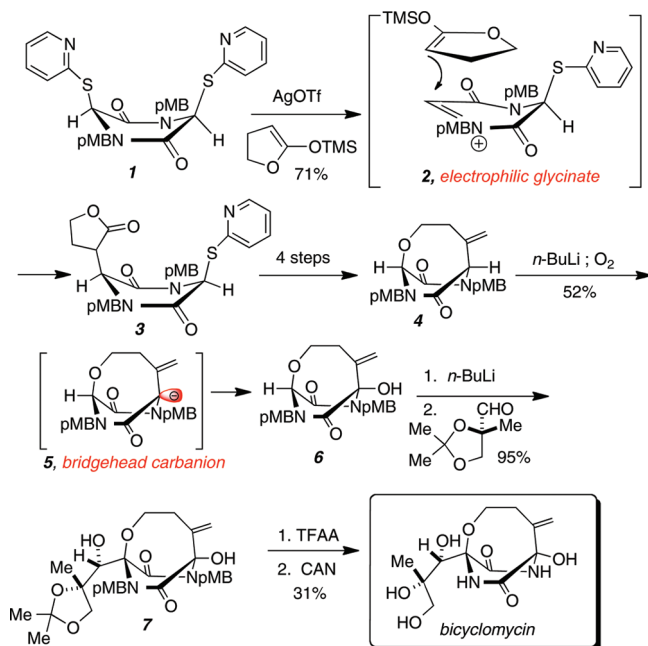
At the time, it was known that the *exo*-methylene moiety was essential for antimicrobial activity,<sup>[3–5]</sup> and we wondered whether the *exo*-methylene and adjacent carbinolamine could participate in the formation of a highly electrophilic pyruvamide system (**10**, Scheme 2).

Iseki and co-workers at Fujisawa first demonstrated that thiols added irreversibly to the *exo*-methylene moiety to provide the thiol-addition species **11** with the bicyclo[4.2.2] core structure intact,<sup>4</sup> a process whose mechanism was first proposed and studied by our laboratory.<sup>5</sup> Kohn and co-workers subsequently discovered that, depending on the pH of the medium, different thiol-addition products were produced, including an interesting Claisen rearrangement product **13**.<sup>6</sup> On the basis of the interesting and novel chemical (and later, biochemical) reactivity of bicyclomycin that was emerging, we wondered if the bridging ether oxygen atom was obligatory for antimicrobial activity or was a spectator atom (Figure 1).

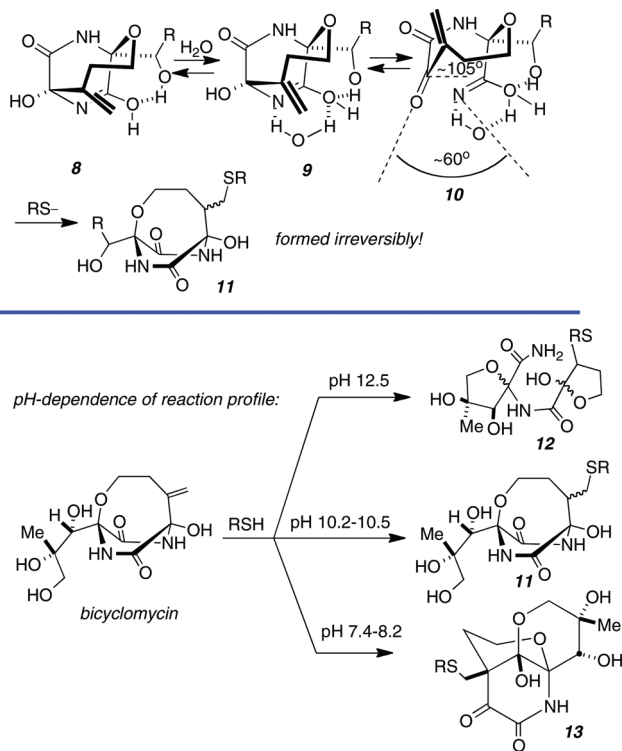
Received: February 18, 2011

Published: March 25, 2011

## Scheme 1. Total Synthesis of Bicyclomycin



## Scheme 2. Bicyclomycin: A Latent Michael Acceptor and pH-Dependence



This turned out to be the first instance where we attempted to harness the total synthesis technology platform we had developed to construct the natural product to prepare a single analogue (“carba”bicyclomycin).<sup>7</sup> The objective was to answer the question concerning the relevance of the bridging ether

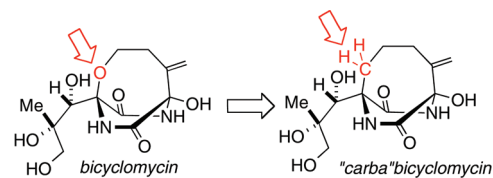
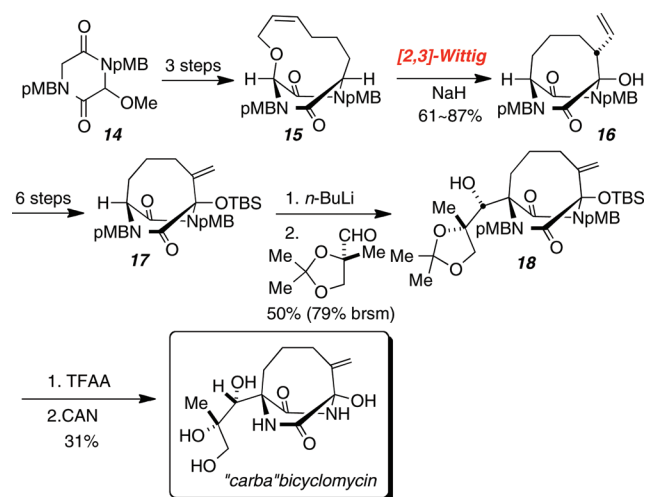


Figure 1. Design of isosteric “carba”bicyclomycin analogue.

## Scheme 3. Synthesis of “Carba” Bicyclomycin

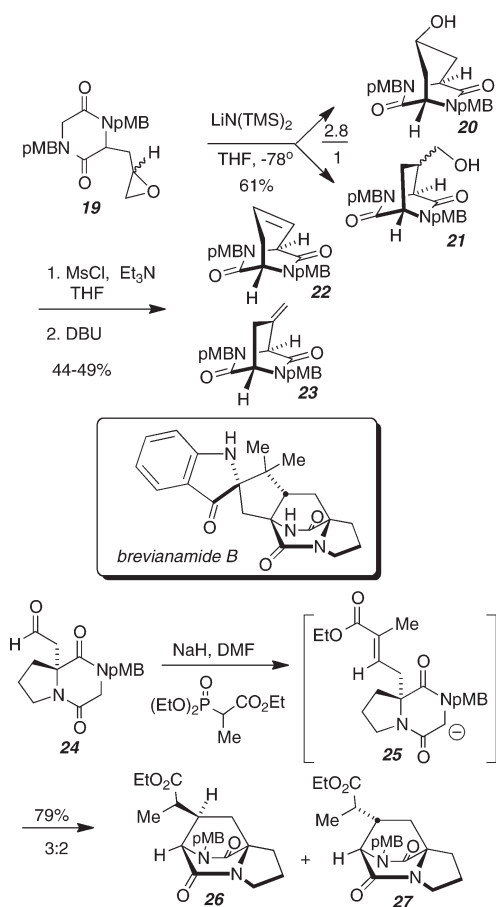


oxygen atom, as two of the three thiol-addition structures discovered by Kohn et al.<sup>6</sup> require participation of that oxygen atom. As shown in Scheme 3, we developed a rather unique solution to constructing the bicyclo[4.2.2] ring structure by deploying a 2, 3-Wittig ring contraction (15 to 16). Bridgehead carbanion generation from 17 and double-diastereodifferentiating aldol condensation and deprotection furnished “carba”bicyclomycin. While still reactive with respect to thiolate addition to the *exomethylene* moiety, this compound turned out to lack antimicrobial activity and clearly indicated the structural requirement for the bridging oxygen atom.<sup>8</sup> This type of interrogation became a major thematic paradigm in our laboratory to the present time. In other words, we sought to extract maximum value from developing a total synthesis platform by exploiting that powerful synthetic technology to prepare mechanistically inspired analogs as mechanistic probes.

## II. PRENYLATED INDOLE ALKALOIDS

An outgrowth of attempts to make more reactive latent Michael-type acceptors based on the bicyclomycin structure, we had prepared the bicyclo[2.2.2] diazaoctane system 23 via the intramolecular enolate–epoxide ring-opening reaction shown in Scheme 4.<sup>9</sup> We were aware of the existence of the brevianamides, isolated by Arthur Birch in the late 1960s,<sup>10</sup> and decided to devise methodology to construct the bicyclo[2.2.2] diazaoctane core of the brevianamides. The first foray was a nonsterecontrolled intramolecular Michael addition on system 25,<sup>11</sup> which led us to develop a stereocontrolled intramolecular S<sub>N</sub>2' cyclization reaction (Scheme 5) that culminated in the first asymmetric synthesis of brevianamide B,<sup>12</sup> a minor metabolite of *Penicillium brevicompactum*.

Scheme 4. Early Synthetic Studies on Bicyclo[2.2.2]diazaoctanes

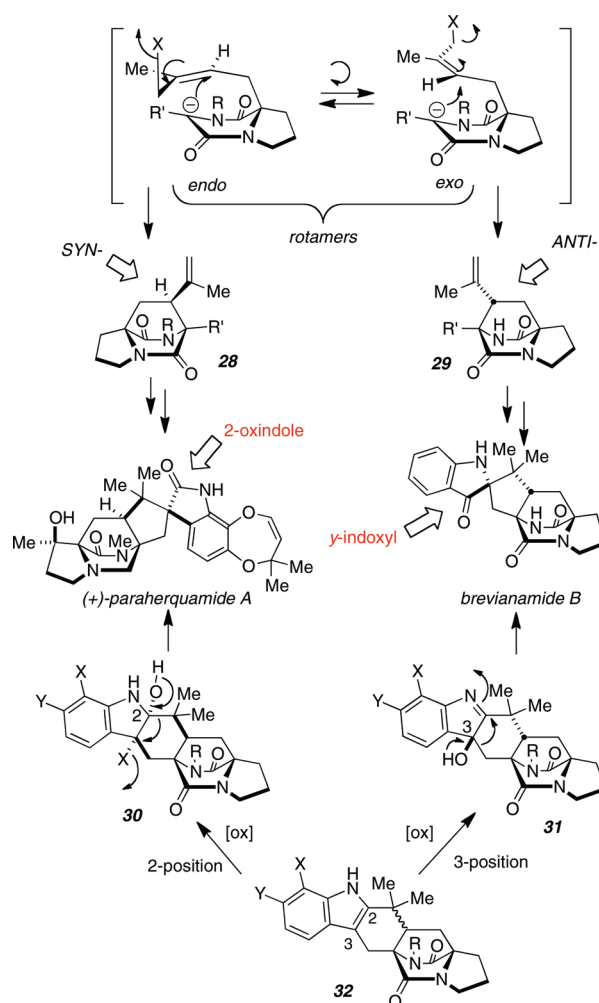


Right around the time we initiated studies on the synthesis of brevipanamides A and B, new members of what has become an enormous family of prenylated indole alkaloids from various genera of fungi, the structures of the paraherquamides<sup>13</sup> and marcfortines<sup>14</sup> were published. A “unified” retrosynthesis was devised to accommodate the differences in relative stereochemistry at the bridging isoprene-derived stereogenic center between the brevipanamides and paraherquamides. The goal was to selectively access the two possible reactive rotamers (*endo* and *exo*) for the intramolecular  $S_N2'$  cyclization reaction. This process would install an isopropenyl residue that could then participate in an olefin–cation cyclization to give the generalized 2,3-disubstituted indole. Chemoselective oxidation of 2,3-disubstituted indoles was well-known in the literature to furnish either the spiro- $\psi$ -indoxyl of the brevipanamides or the spiro-oxindole of the paraherquamides.

The brevipanamide project turned out to be a fortuitous choice, as we stumbled on a surprising discovery regarding the absolute stereochemistry of this natural product, which in turn led us into the larger field of secondary metabolite biosynthesis.

It was found that the diastereofacial selectivity of the intramolecular  $S_N2'$  cyclization reaction could be exquisitely controlled to provide the *syn*-relative stereochemistry (paraherquamides) by running the reaction in a poorly coordinating solvent such as benzene, which we suggested proceeded via a closed transition state as shown in Scheme 6.<sup>12</sup> The diastereoselectivity could be reversed to favor the corresponding *anti*-stereochemistry by the addition of a

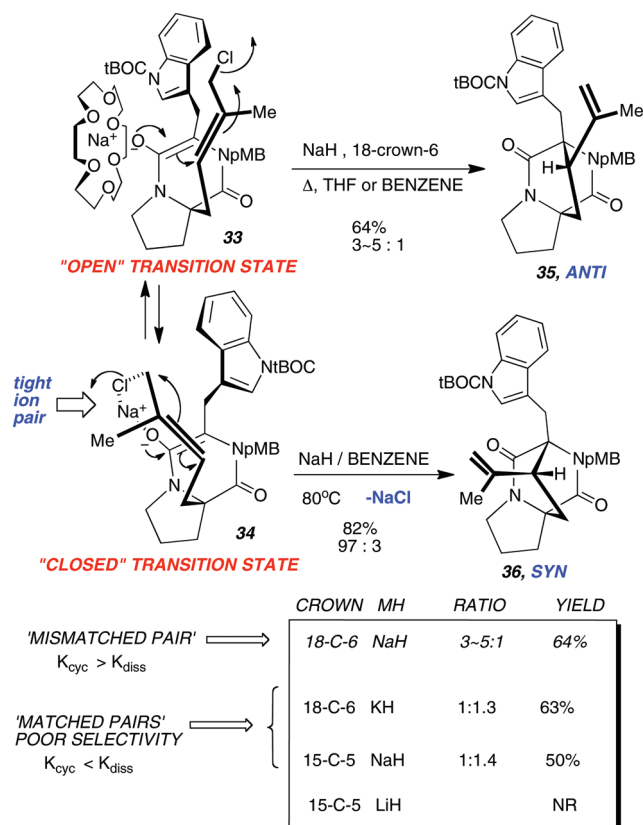
Scheme 5. “Unified” Retrosynthesis for the Brevipanamides and Paraherquamides



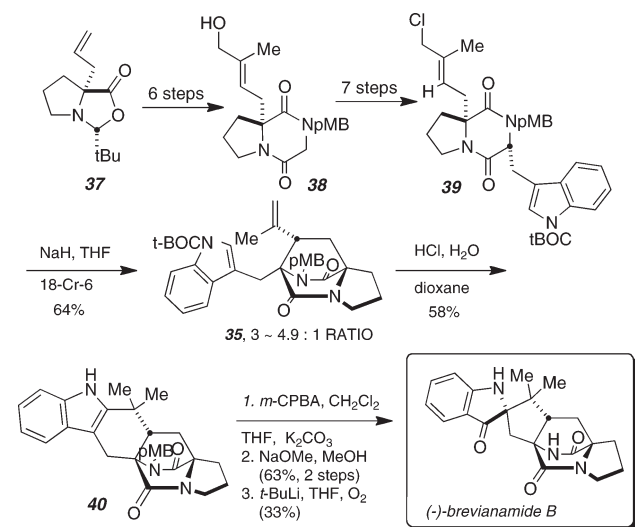
“mis-matched” crown ether, and selectivities as high as 10:1 favoring the anti-isomer were observed.

The asymmetric synthesis of (–)-brevipanamide B was completed by this approach, as summarized in Scheme 7. The intramolecular  $S_N2'$  reaction proved effective in delivering the desired *anti*-diastereomer in up to a 4.9:1 ratio. The planned olefin–cation cyclization worked smoothly, and the peracid oxidation of the 2,3-disubstituted indole was entirely diastereoselective, giving a single 3(*S*)-hydroindolenine that rearranged smoothly to the corresponding spiroindoxyl. We encountered significant difficulty in removing the *N*-*p*-methoxybenzyl group and eventually found that formation of the dipole-stabilized benzylic carbanion, generated through treatment with excess *tert*-butyllithium and quenching with molecular oxygen, effected the removal of this difficult to cleave protecting residue.

When the synthesis was completed, attempts to obtain an authentic sample of (–)-brevipanamide B from Prof. Birch and other laboratories that had isolated the natural compound were fruitless. On the other hand, the major metabolite, (+)-brevipanamide A, whose absolute configuration was established by X-ray crystallographic analysis,<sup>10i</sup> was made available. Prof. Birch had reported the semisynthetic conversion of brevipanamide A into brevipanamide B by a redox process which we followed to obtain an authentic sample of (–)-brevipanamide B.<sup>10c</sup>

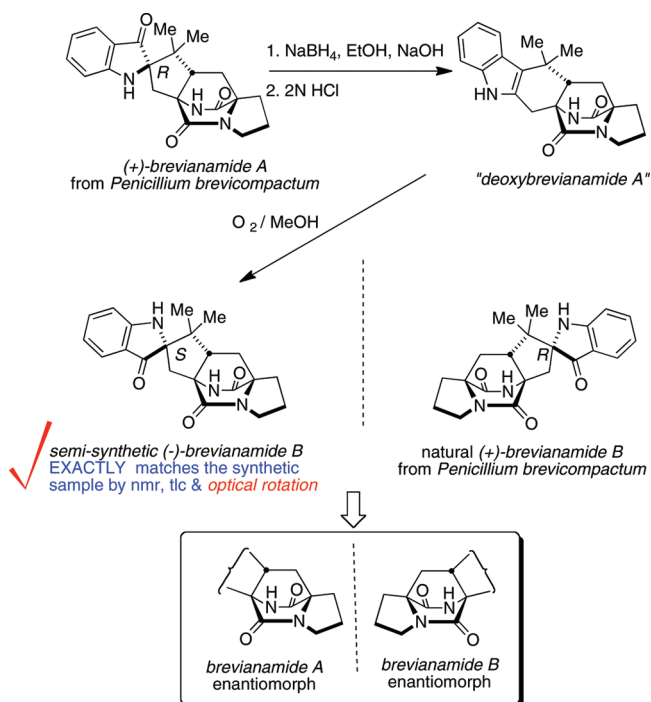
Scheme 6. Diastereoselective Intramolecular  $S_N2'$  Cyclization Reactions

Scheme 7. Asymmetric Synthesis of (–)-Brevianamide B



The semisynthetic and totally synthetic samples of (–)-brevianamide B proved identical by all spectroscopic methods and had the same sign and magnitude of optical rotation, revealing that these substances possessed the same absolute configuration. Due to the initial difficulty we encountered in locating a sample of brevianamide B, our laboratory endeavored to acquire cultures of *Penicillium brevicompactum* which were grown and harvested to

Scheme 8. Discovery of the Enantio-divergent Biogenesis of Brevianamides A and B



provide natural brevianamide A (the major metabolite) and a small amount of natural brevianamide B. Much to our surprise, the absolute configuration of the natural brevianamide B turned out to be the (+)-enantiomer and was thus antipodal to the semisynthetic material. This clearly revealed that Nature had constructed these two diastereomeric natural substances in two enantiomeric forms (Scheme 8). This discovery was quite fascinating to us and drew us to ponder how the two pseudo-enantiomeric brevianamides arose in Nature. We also learned a very powerful lesson from this exercise: namely, that had we not endeavored to isolate the natural compound ourselves, directly from the producing organism, we would have never stumbled on the puzzling absolute stereochemical differences between brevianamides A and B. This accidental discovery drew us irresistibly into learning the origin of this enantio-divergent biogenesis.

In 1970, Porter and Sammes were the first to speculate on the biogenetic origin of the bicyclo[2.2.2]diazaoctane ring system of brevianamides A and B, wherein the intramolecular Diels–Alder reaction of the reverse-prenylated indole-derived azadiene was invoked (Figure 2).<sup>15</sup> Interestingly, Birch later proposed an alternative biogenesis invoking the intermediacy of an epidithia-piperazinedione species.<sup>16</sup>

Birch then carried out radiolabeled precursor incorporation experiments in *Penicillium brevicompactum* and demonstrated that cyclo-L-Trp-L-Pro (brevianamide F) was incorporated intact into brevianamide A.<sup>17</sup> On the basis of this important result, he suggested that brevianamide F was reverse-prenylated to deoxybrevianamide E, which in turn was oxidized and cyclized to give brevianamides A and B.

Combining the results from Birch and considering the Sammes IMDA biogenetic proposal,<sup>15</sup> we suggested the modified biogenetic pathway shown in Scheme 9, wherein the azadiene species is *achiral*, which should give rise (in the absence of enzyme mediation) to a *racemic* Diels–Alder product. Inferring the



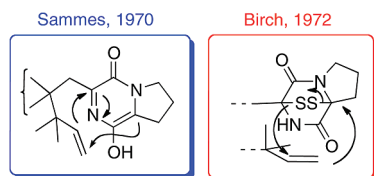
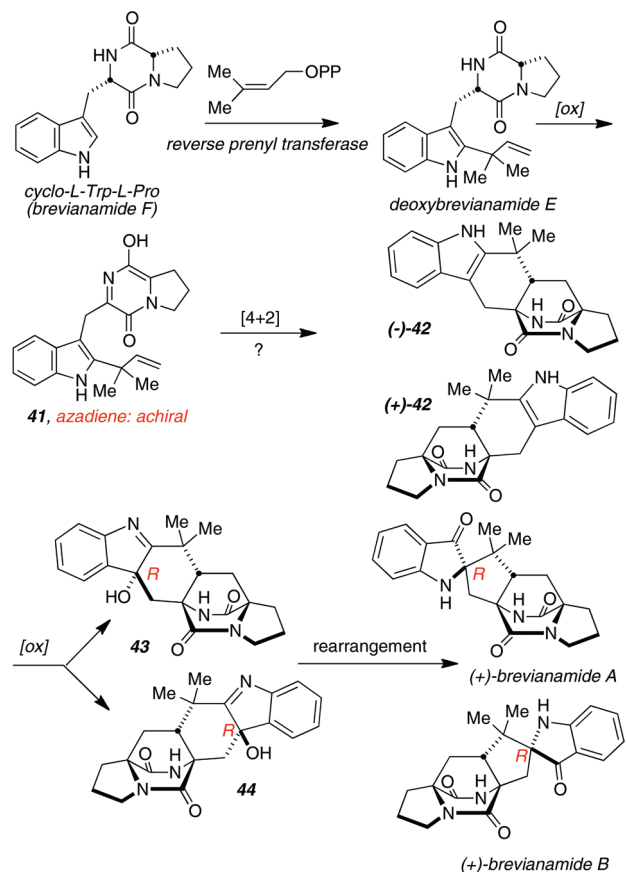


**Figure 2.** Sammes and Birch proposals for the construction of the bicyclo[2.2.2]diazaoctane core structure.

### Scheme 9. Modified Biogenetic Proposal to Accommodate the Natural Stereochemistries of Brevianamides A and B



presence of an *R*-selective indole oxidase, the presumed racemic intermediate would be converted into two optically pure, diastereomeric 3*R*-hydroxyindolenines suffering a Pinacol-type rearrangement that would give the observed natural substances (–)-brevianamide A and (+)-brevianamide B. As our synthesis passed through the presumed hexacyclic Diels–Alder adduct **42**, our total synthesis platform provided us with the tools to probe this interesting stereochemical puzzle. To interrogate this biogenetic pathway, we had to (ironically) adapt our asymmetric synthesis to prepare isotopically labeled, *racemic* cycloadduct **42** and determine if this was a biosynthetic precursor to the brevianamides. This was accomplished, and the requisite racemic, authentic <sup>13</sup>C-labeled cycloadduct **42** was used as a reference standard to screen culture extracts for the presence of this species and was also deployed in a precursor incorporation experiment.

Despite how soundly our proposal appeared on paper in terms of accommodating the relative and absolute stereochemistry of

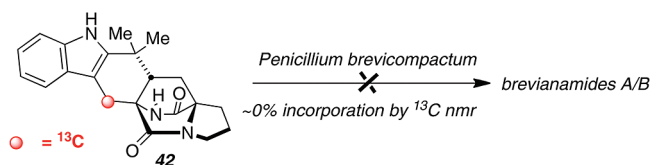
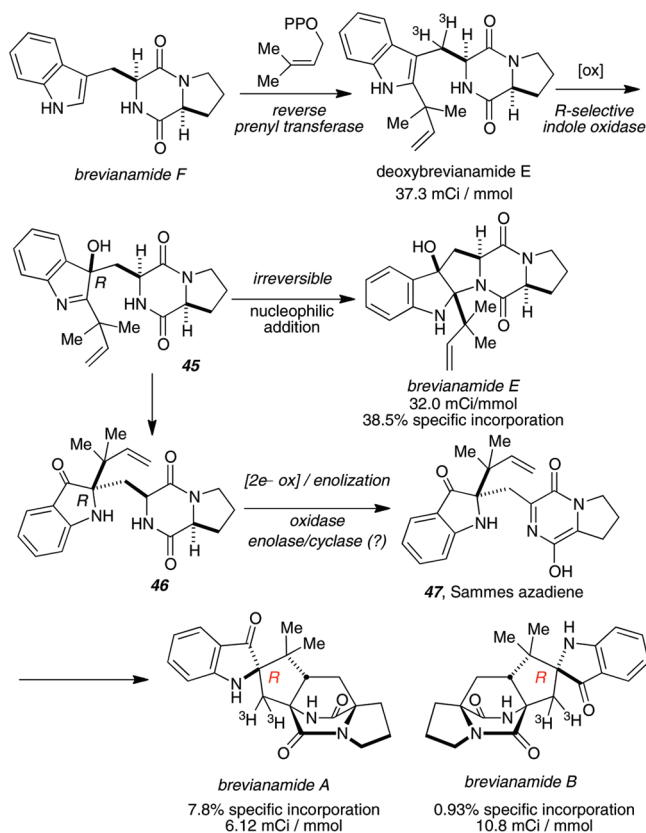


**Figure 3.** Attempted precursor incorporation experiment with racemic cycloadduct **42**.

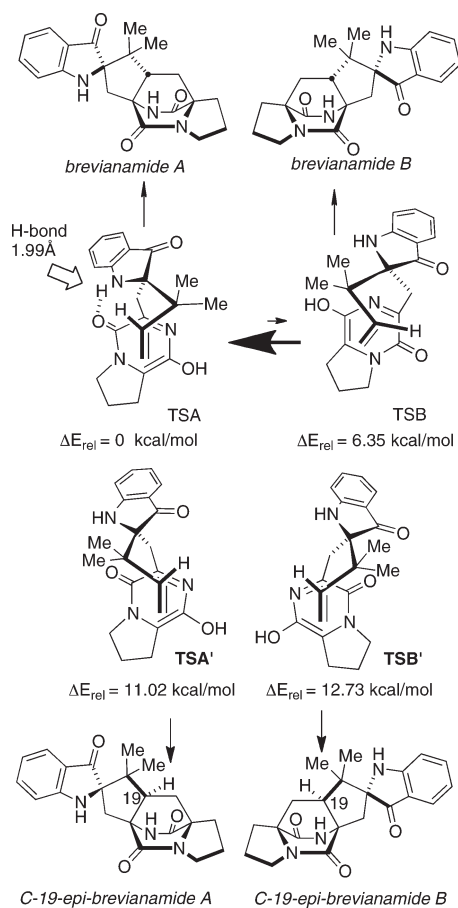
### Scheme 10. Alternative Biogenetic Pathway



these substances, this compound did not incorporate into either brevianamide A or B, and we were also unable to detect even a trace of this substance as a natural metabolite (Figure 3).

If hexacycle **42** was not on the pathway to the brevianamides, then what alternative structure was? We then turned our attention to preparing an earlier intermediate, first suggested by Birch,<sup>17</sup> namely deoxybrevianamide E, in radiolabeled form in order to determine if this was indeed the second stage after brevianamide F. We found that synthetic, tritium-labeled deoxybrevianamide E was incorporated in significant radiochemical yield into brevianamide A, B, and E in cultures of *P. brevicompactum* (Scheme 10).<sup>18</sup> The presence of brevianamide E suggested that the oxidation of the indole to either the incipient 3-hydroxyindolenine or the spiro-indoxyl, might precede the formation of the bicyclo[2.2.2]diazaoctane ring system. We found that tritium-labeled brevianamide E, when fed to cultures of *P. brevicompactum*, did not incorporate into either brevianamide A or B, revealing that this was a shunt (dead-end) metabolite. We speculated that deoxybrevianamide E was stereoselectively oxidized to the 3*R*-hydroxyindolenine that could

**Scheme 11.** Ab Initio Calculations on the Putative Diels–Alder Cycloadditions by Domingo et al.<sup>19</sup>



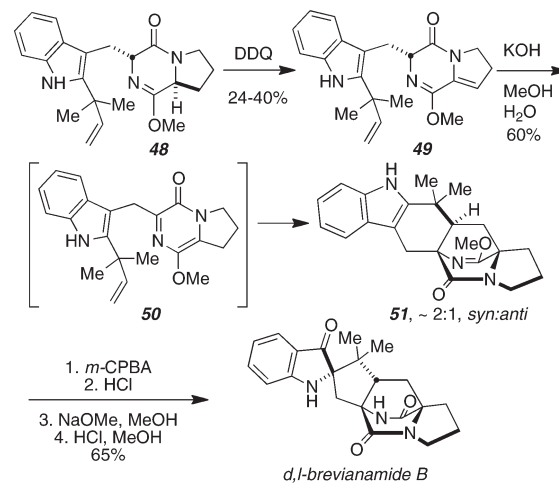
suffer three fates: (1) irreversible ring closure to brevianamide E; (2) Pinacol-type rearrangement to indoxyl **46**; and (3) a second oxidation to an azadiene species followed by IMDA to form the core bicyclo[2.2.2]ring system and final Pinacol-type rearrangement to produce the brevianamides. This alternative biogenetic hypothesis could also account for the observed relative and absolute stereochemistries of brevianamides A and B and assumed that after setting the *R*-stereogenic center at the stage of hydroxyindolenine **45** they would suffer IMDA cyclization from two of the four possible diastereomeric transition states.

This new biogenetic hypothesis has proven very elusive to secure additional experimental corroboration. We tried in earnest to prepare the indoxyl **46**, but this compound appears to be unstable, spontaneously suffering a retro-Michael reaction to give the dehydroalanine piperazinedione and the prenylated indoxyl. Some insight into this process was obtained from our collaborator, Prof. Domingo at the University of Valencia, where he performed ab initio calculations on the four diastereomeric transition-state structures for the putative IMDA reaction of azadiene **47** (Scheme 11).<sup>19</sup> This IMDA reaction was found to be controlled by frontier molecular orbitals HOMO<sub>(dieneophile)</sub>/LUMO<sub>(azadiene)</sub>. All four diastereomeric transition structures were examined, and it was found that the lowest<sub>(rel)</sub> energy transition structure is TSA, which leads to brevianamide A (see Table 1). The next highest energy transition structure is TSB, which lies approximately 6–7 kcal/mol above TSA and leads to brevianamide B. An intramolecular H-bond was found in TSA

**Table 1.** Calculated Potential Energy Barriers and Relative Energies (kcal/mol) for TSA, TSB, TSA', and TSB'<sup>19</sup>

	3-21G/3-21G		6-31G*/3-21G	
	$\Delta E_a$	$\Delta E_{rel}$	$\Delta E_a$	$\Delta E_{rel}$
TSA	31.81	0.00	38.68	0.00
TSB	39.42	7.61	45.03	6.35
TSA'	44.17	12.36	49.71	11.02
TSB'	47.07	15.26	51.41	12.73

**Scheme 12.** Biomimetic Synthesis of *d,l*-Brevianamide B

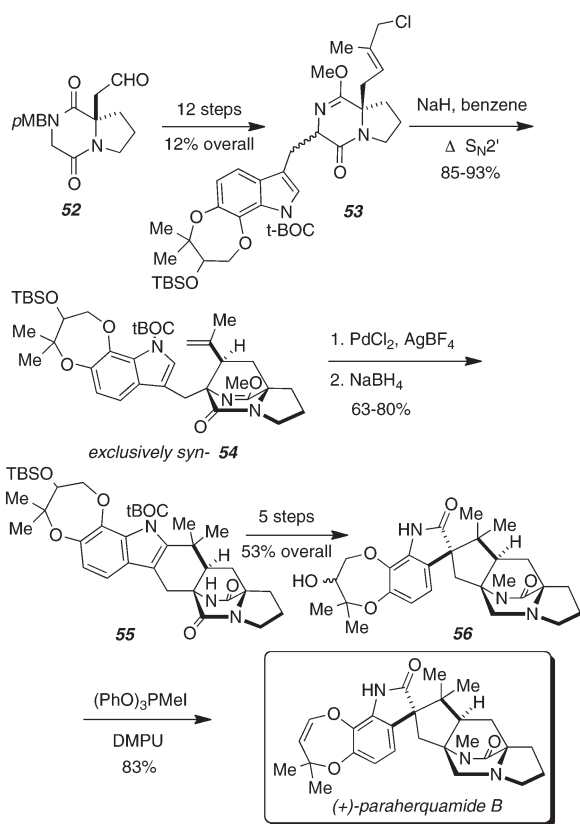


between the indoxyl N–H and the tryptophyl carbonyl group accounting for a large fraction of the relative stabilization energy. After TSB, the next highest energy transition structures are TSA' and TSB', which would lead to *C*-19-*epi*-brevianamide A and *C*-19-*epi*-brevianamide B, respectively. Our laboratory previously described the total synthesis of *C*-19-*epi*-brevianamide A, and using this authentic specimen, we were unable to detect this substance as a metabolite of *Penicillium brevicompactum*.

This theoretical study therefore predicts that the relative distribution of brevianamides A and B from *Penicillium brevicompactum* is a direct manifestation of the relative energies of the four diastereomeric transition structures: brevianamide A is the major metabolite, brevianamide B is a minor metabolite, and neither of the *C*-19-*epi* structures are found. While this provided some indirect and possibly provocative evidence for biosynthetic events following the hydroxylation of deoxybrevianamide E, it has been less than satisfying in terms of providing insight into the proposed biosynthetic IMDA reaction. We then turned our attention to attempting to validate the azadiene–IMDA construction in the laboratory.<sup>20</sup>

As shown in Scheme 12, we enjoyed early success in generating a protected, yet functional, analogue of a putative azadiene by DDQ oxidation of **48** in modest yield. Tautomerization of **49** to azadiene **50** could be followed easily by NMR, with the IMDA cyclization occurring at or below room temperature to provide a ~2:1 ratio of *syn/anti* diastereomers. These were readily separated and were converted into *d,l*-brevianamide B and the corresponding *C*-19-*epi*-brevianamide B in a few steps.

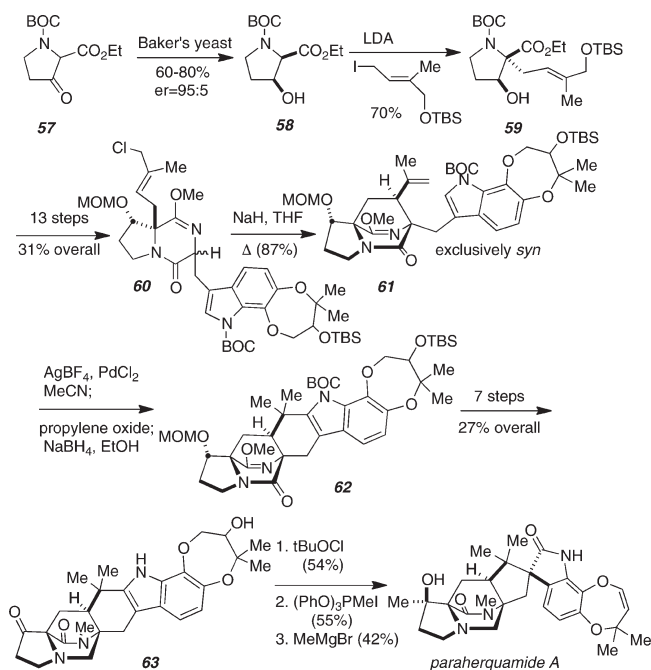
This study demonstrated that the core bicyclo[2.2.2]diazaoctane ring system common to this family might indeed arise by an

Scheme 13. Asymmetric Synthesis of (+)-Paraherquamide B<sup>21</sup>

intramolecular Diels–Alder cyclization from a preformed dioxepiperazine that subsequently undergoes oxidation to an azadiene species. It is significant that the diastereofacial bias of the Diels–Alder cyclization was not strongly affected by solvent. The same ratio of *syn/anti* diastereomers (~2:1) was obtained in THF as in aqueous methanol. As will be seen below, improved versions of this IMDA reaction were later developed in the context of preparing more complex members of this family of prenylated indole alkaloids.

Before moving to our very recent work on the biomimetic total synthesis and biosynthesis of these substances, the diastereofacially selective intramolecular S<sub>N</sub>2' reaction first developed for the synthesis of brevianamide B (Scheme 7) was successfully applied to the asymmetric total syntheses of (+)-paraherquamide B,<sup>21</sup> (–)-paraherquamide A,<sup>22</sup> and stephacidin A.<sup>23</sup> A few key elements of the paraherquamide B and A syntheses are illustrated in Schemes 13 and 14, respectively. A fortuitous feature of the closed transition-state manifold for the intramolecular S<sub>N</sub>2' reaction was the predilection for the *syn*-diastereomer, which is the natural relative stereochemistry for virtually all of the metabolites discovered after the brevianamides. This powerful methodology allowed for the stereocontrolled asymmetric synthesis of three representative members of this family.

Both the paraherquamide A and B syntheses required the construction of the dioxepin ring system, in which the final enol ether alkene was installed in the very last stage of the synthesis. In both instances, the dehydration of the hindered neopentyl-like alcohol was dehydrated with (PhO)<sub>3</sub>PMeI, and all other dehydrating reagents examined failed.

Scheme 14. Asymmetric Synthesis of (–)-Paraherquamide A<sup>22</sup>

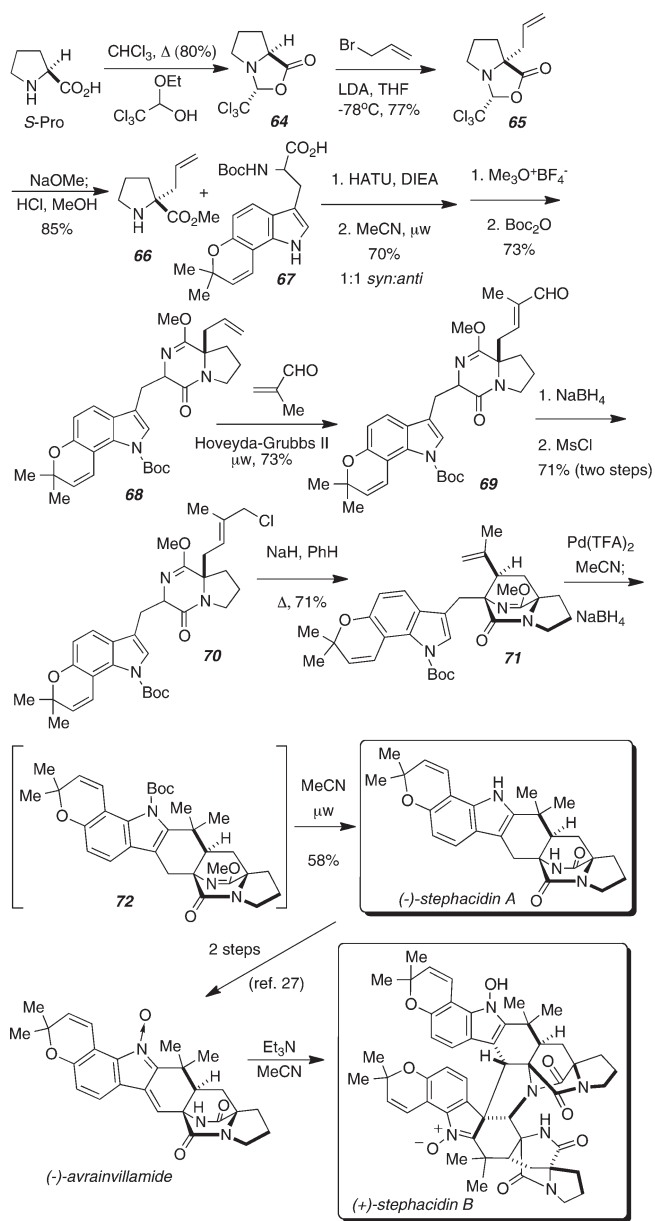
The most modern application of the intramolecular S<sub>N</sub>2' cyclization strategy was to the asymmetric total synthesis of stephacidin A, as shown in Scheme 15.<sup>23</sup> For this synthesis, we also developed an improved synthesis of the Seebach<sup>24</sup> asymmetric allylation of proline by employing chloral to make the proline enolate alkylation precursor, a process that has been published as an *Org. Synth.* procedure.<sup>25</sup> This synthesis required seventeen steps overall and proceeded in 5% overall yield from *S*-proline. As in the other instances, the intramolecular S<sub>N</sub>2' cyclization was completely diastereoselective for the desired *syn*-isomer. Employing modern cross-methathesis methodology<sup>26</sup> to install the enal and several microwave-mediated steps resulted in a highly efficient synthesis of (–)-stephacidin A following the Wacker-type cyclization of the intramolecular S<sub>N</sub>2' cyclization product.

We also endeavored to transform our totally synthetic (–)-stephacidin A into synthetic (+)-stephacidin B following the elegant path described by Baran for the conversion of stephacidin A into (–)-avrainvillamide<sup>27</sup> and the subsequent efficient dimerization of (–)-avrainvillamide to (+)-stephacidin B, first proposed by Qian-Cutrone<sup>28</sup> and then elegantly validated by Myers.<sup>29</sup>

At the same time that we were investigating the asymmetric synthesis of (–)-stephacidin A, we had devised a new and very effective method to generate the azadiene species implicated in the IMDA construction of the stephacidins and the more recently discovered notoamides.<sup>30</sup> As shown in Scheme 16, we discovered that  $\beta$ -hydroxyproline derivatives could be readily dehydrated under Mitsunobu conditions to install the unsaturation in the proline residue required for the IMDA process.<sup>31</sup>

Significantly, treatment of 74 under Mitsunobu conditions in warm dichloromethane resulted in the direct production of D, L-stephacidin A in a ~2.4:1 ratio with C-6-*epi*-stephacidin A. This was our first success at generating the free (OH) *achiral* azadiene

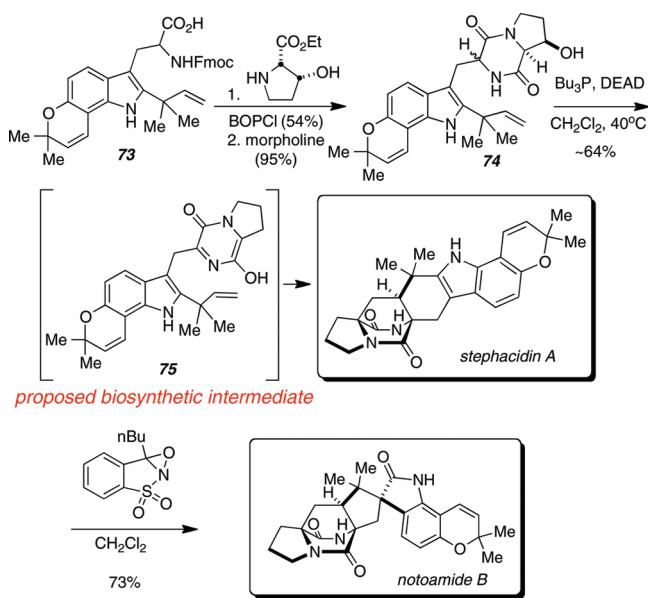
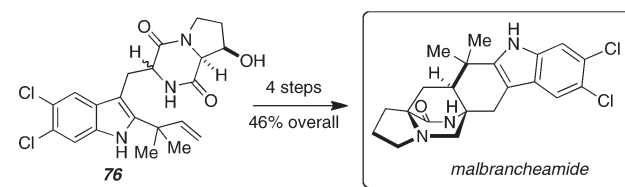
Scheme 15. Asymmetric Total Synthesis of (–)-Stephacidin A and (+)-Notoamide B



species **75** that we have implicated as a possible biosynthetic intermediate to stephacidin A. Like other IMDA reactions similar to this one, a preponderance of the desired *syn*-isomer was produced in about a 2.4:1 ratio. We also found that a Davis oxaziridine-based oxidation of stephacidin A directly produced the spiro-oxindole natural product notoamide B. This conversion experimentally validates our proposal that stephacidin A serves as the immediate biosynthetic precursor to notoamide B. The biomimetic synthesis of stephacidin A, as shown in Scheme 16, has provided us with the tools to prepare double  $^{13}\text{C}$ -labeled stephacidin A that we have recently used to further validate the bioconversion of stephacidin A into notoamide B when this synthetic, racemic, labeled precursor was fed to cultures of *Aspergillus versicolor*.<sup>32</sup>

This efficient IMDA strategy has been recently applied in our laboratory to concise, biomimetic total syntheses of D, L-malbrancheamide and D, L-malbrancheamide B (Scheme 17),<sup>33</sup>

Scheme 16. Biomimetic Total Synthesis of D,L-Stephacidin A and D,L-Notoamide B

Scheme 17. Biomimetic Total Synthesis of Malbrancheamide<sup>33</sup>

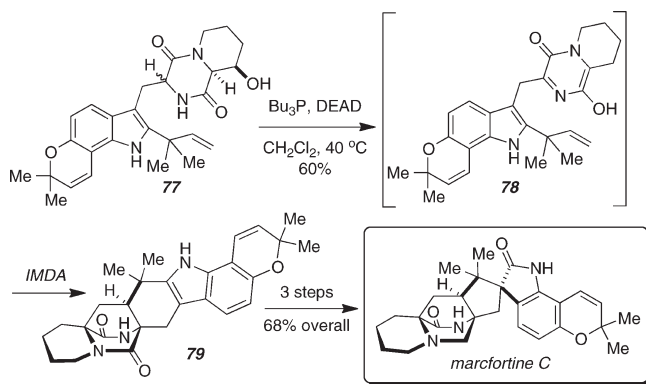
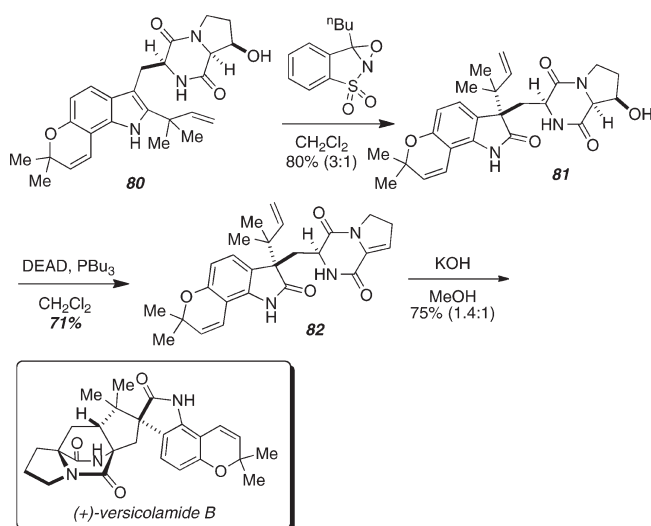
D,L-marcfortine C (Scheme 18),<sup>34</sup> D,L-brevianamide B,<sup>31b</sup> D,L-versicolamide B,<sup>30c</sup> and both (+)- and (–)-versicolamide B (Scheme 19).<sup>35</sup> The marcfortine C synthesis required fifteen steps from commercially available 6-hydroxyindole and proceeded in 3.7% overall yield.

In the case of the versicolamide synthesis, the optically pure oxindole species **81** (plus a minor diastereomer) was generated through oxaziridine oxidation. With that quaternary stereogenic center set, the Mitsunobu-based dehydration, followed by base-mediated tautomerization and IMDA cyclization furnished (+)-versicolamide B (and a diastereomer in a 1.4:1 ratio). In this instance, the IMDA cyclization reaction was entirely antiselective, a situation that was predicted based on theory by Domingo and co-workers.<sup>19b</sup>

The ab initio calculations performed by Domingo et al. revealed that for the spiro-6 ring formation, similar to that deployed in the biomimetic stephacidin A synthesis (Scheme 20, top), the *syn*-transition state is slightly favored by a little over 1 kcal/mol.<sup>19b</sup> Our experimental results on many different substrates validate this prediction.

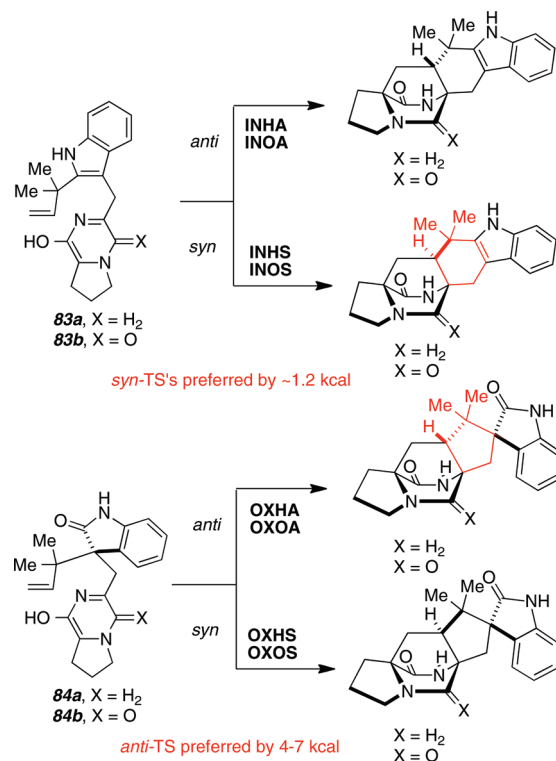
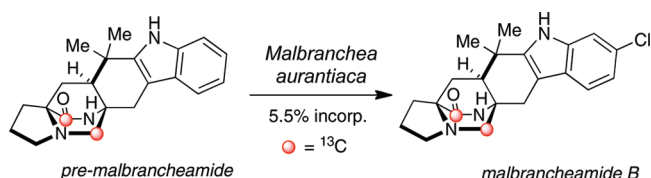
On the other hand, the corresponding spiro-5 mode of IMDA cyclization, such as that deployed in the versicolamide B synthesis (Scheme 19), was predicted to be favored by 4–7 kcal/mol. Again, our experimental observations fully support these theoretical predictions.



Scheme 18. Biomimetic Total Synthesis of Marcfortine C<sup>34</sup>Scheme 19. Synthesis of (+)-Versicolamide B<sup>35</sup>

Many of these total synthesis platforms have been extensively utilized by our laboratory to prepare isotopically labeled probe molecules to interrogate individual biosynthetic steps. For instance, the malbrancheamide synthesis was “put to work” through the preparation of double <sup>13</sup>C-labeled premalbrancheamide and was used to demonstrate that the halogenation of the indole ring occurs stepwise after the formation of the bicyclo[2.2.2]diazocane core (Scheme 21).<sup>33b</sup> We observed that double <sup>13</sup>C-labeled premalbrancheamide was converted into malbrancheamide B with 5.5% isotopic incorporation. This result established that the dioxopiperazine is reduced to the mono-oxopiperazine of premalbrancheamide before the halogenase steps and, further, that the initial site of halogenation is at the electronically preferred 6-position of the indole.

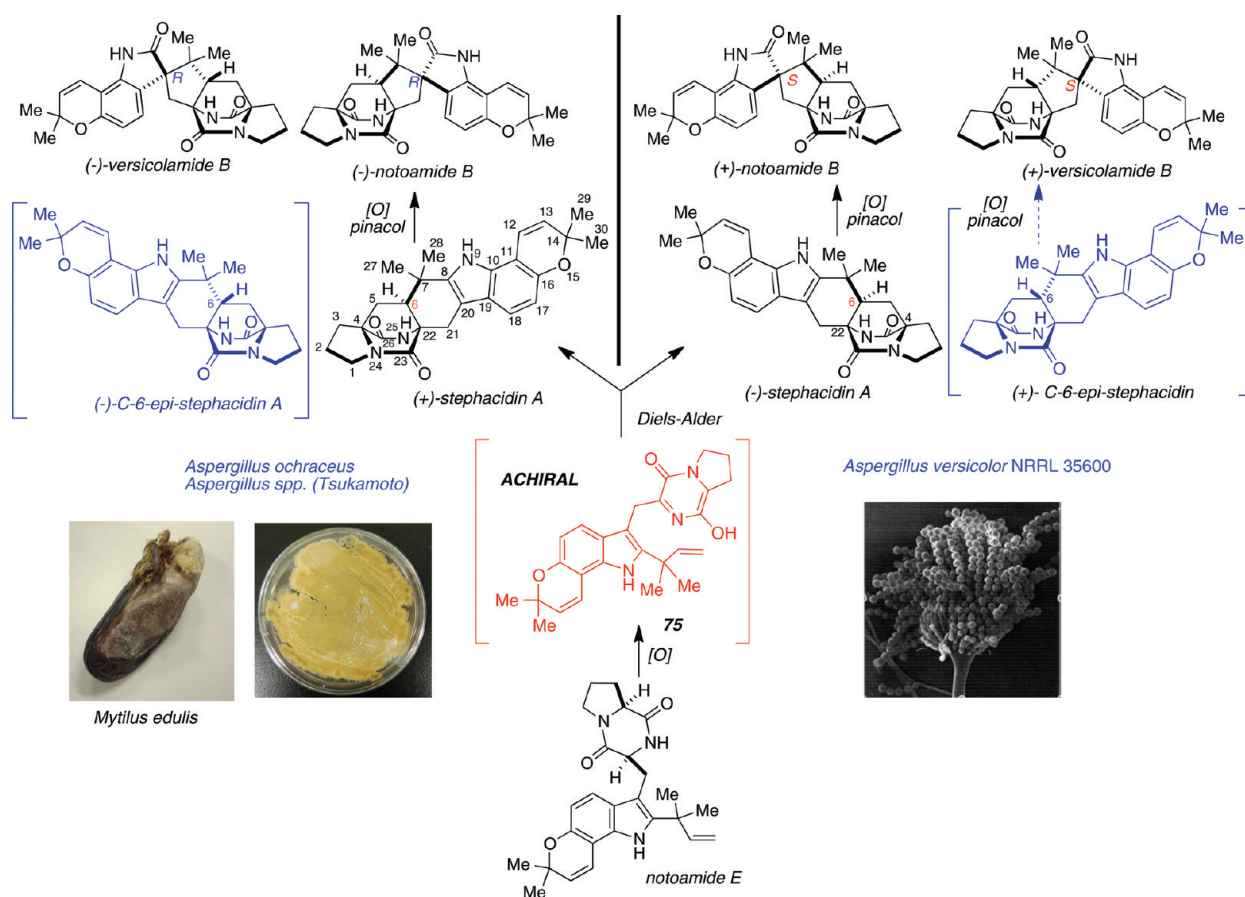
A particularly exciting discovery occurred in 2008 when Prof. James Gloer at the University of Iowa isolated (+)-versicolamide B from cultures of *Aspergillus versicolor* NRRL 35600.<sup>30c</sup> He had also isolated (–)-stephacidin A and (+)-notoamide B from the same organism. It was immediately recognized that the (–)-stephacidin A produced by this organism was the *antipode* of the same substance originally isolated by Qian-Cutrone et al. at Bristol-Myers Squibb from *Aspergillus ochraceus* WC76466.<sup>28a,36</sup> Later, Tsukamoto and co-workers isolated (+)-stephacidin A

Scheme 20. Theoretical Studies by Domingo et al.<sup>19b</sup>Scheme 21. Biosynthetic Incorporation of Pre-malbrancheamide into Malbrancheamide B<sup>33b</sup>

and (–)-notoamide B from cultures of a marine-derived *Aspergillus* sp. obtained from the common mussel *Mytilus edulis*, which was collected off Noto Peninsula in the Sea of Japan (and thus the name “notoamides”).<sup>30</sup> Very interestingly, Tsukamoto and co-workers then isolated the antipodal (–)-notoamide B from the marine-derived *Aspergillus* sp.<sup>30e</sup> Based on this, we proposed a “unified” biogenesis of the two distinct antipodal families as shown in Scheme 22. We speculated that the possible key precursor was notoamide E, a metabolite we had inadvertently synthesized before Prof. Tsukamoto was able to identify this substance as a natural metabolite in her marine-derived *Aspergillus* sp.<sup>30d</sup>

In this biogenetic scheme, we envisioned that notoamide E would be oxidized by two electrons and tautomerized to the *achiral* azadiene species **75**. Please note that this is the *same* azadiene species we generated in Scheme 16, in the context of the biomimetic synthesis of D,L-stephacidin A. Each organism, then, would have an enzyme (that we speculate is the oxidase) that would preferentially bind this species in one of four possible transition-state conformers, mediating the face-selective IMDA reaction to give the respective (+)- or (–)-stephacidin A enantiomers.

Scheme 22. Initial Biogenetic Hypothesis to Accommodate Enantio-divergent Production of Stephacidin A, Notoamide B, and Versicolamide B



We have already validated the laboratory as well as the biosynthetic transformation of double  $^{13}\text{C}$ -labeled stephacidin A into notoamide B, as mentioned above.<sup>32</sup> The remaining mystery, then, was the origin of versicolamide B, which has the rare *anti*-stereochemistry at C-6 (stephacidin numbering). Does this come from the as yet undetected minor IMDA product C-6-*epi*-stephacidin A? Or does versicolamide B arise from a distinct channel that would have to be stereochemically parallel, in an antipodal sense, in the separate species of the *Aspergillus* fungi that produce the observed natural (+)- and (-)-enantiomers?

We were in an excellent position to test this biogenetic hypothesis through the synthesis of double  $^{13}\text{C}$ -labeled notoamide E. Much to our chagrin, doubly labeled notoamide E was found to incorporate into notoamides C, 3-*epi*-C, and D (Scheme 23) in both *Aspergillus versicolor* and the marine-derived *Aspergillus* sp., but not into stephacidin A or notoamide B (nor for that matter, any metabolite possessing the bicyclo[2.2.2]diazaoctane ring system that we could detect).<sup>30d</sup> This result forced us to consider that the timing of the oxidative cyclization of the indolopyranyl ring system might occur after the putative IMDA construction of the bicyclo[2.2.2]diazaoctane core.

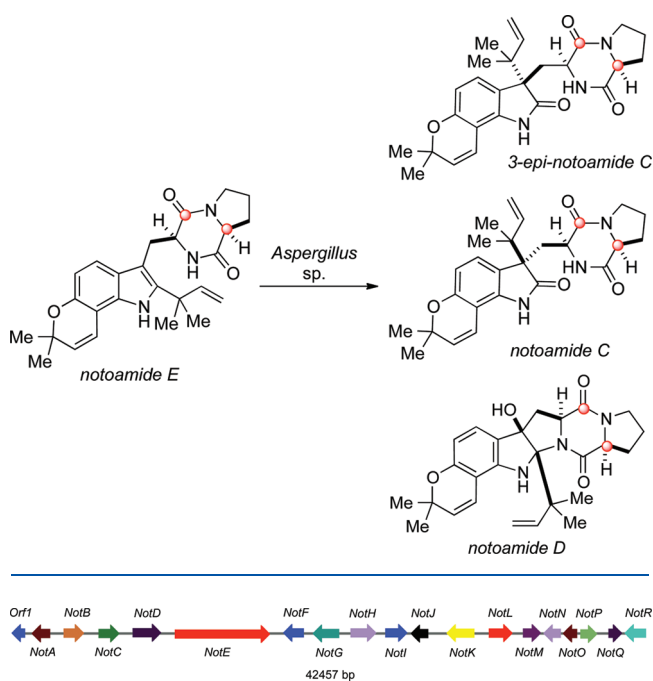
At this point we were fortunate to engage Professor David H. Sherman, at the University of Michigan, to take on the task of whole genome sequencing of *Aspergillus versicolor* and Tsukamoto's marine-derived *Aspergillus* sp. with the objective of using genome mining and proteomics technologies to characterize the biosynthetic gene clusters. From this work, which included some

additional  $^{13}\text{C}$ -labeled metabolite synthesis and precursor incorporation experiments, the biosynthetic gene clusters for the production of the notoamides and stephacidin A have very recently been characterized.<sup>37</sup>

An open reading frame (*orf*) named *notE* (Figure 4) was identified from the genome sequence using the known fumitremorgin gene *ftmA* to probe for homologous genes. Eighteen genes *notA-R* were identified and biochemical functions assigned to many of these based on bioinformatics analysis (Figure 4). Two aromatic prenyltransferases, *notC* and *notF*, were functionally expressed in *E. coli* and were biochemically characterized as a normal prenyltransferase (*NotC*) and a reverse-prenyltransferase (*NotF*). Based on the finding that *NotC* catalyzes the conversion of 6-hydroxydeoxybrevianamide E into a substance, which we have since identified as the 7-prenylation product notoamide S, we very recently proposed a revised stephacidin–notoamide biogenetic pathway (Scheme 24).

*NotE* is a presumed bimodular NRPS (Scheme 24) with adenylation (A)-thiolation (T)-condensation (C)-A-T-C domain organization and was found to share 47% amino acid sequence identity with *FtmA*. We determined that brevianamide F is efficiently transformed to deoxybrevianamide E by *NotF*, a reverse-prenyl transferase that catalyzes the alkylation at the 2-position of the indole ring with DMAPP.

In a normal prenylation reaction, such as that mediated by *NotC*, DMAPP alkylates an aromatic substrate through its C1' atom via an  $\text{S}_{\text{N}}2$  displacement, while the C3' position is involved

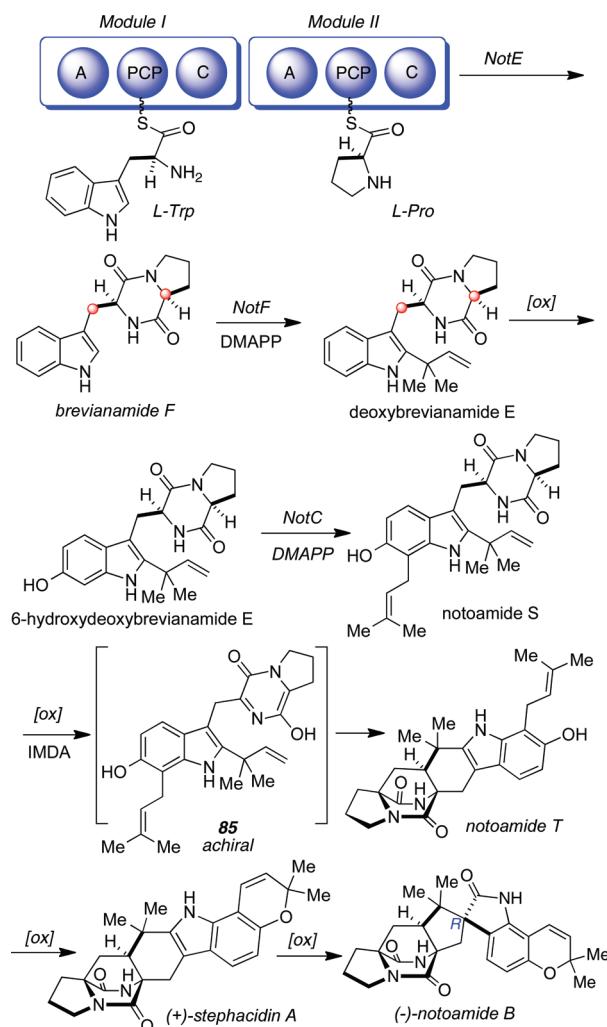
Scheme 23. Biosynthetic Transformation of Notoamide E into Notoamides C and D and 3-*epi*-Notoamide CFigure 4. Notoamide (*not*) biosynthetic gene cluster.

in the reverse prenyltransfer reaction via an  $S_N2'$  displacement. This reverse-prenylation was previously shown by our laboratory to occur with lack of facial selectivity with respect to the C–C bond-forming step on the DMAPP in paraherquamide-, austamide-, and brevianamide-producing fungi.<sup>38,39</sup> Recent access to the recombinant and functionally expressed enzyme NotE should facilitate future studies to elucidate the mechanism of the reverse-prenylation reaction.

Following the formation of notoamide S, we have hypothesized that oxidation of notoamide S occurs to give an alternative *achiral* azadiene species that suffers enantiospecific IMDA cyclization in each of the respective *Aspergillus* sp. providing notoamide T. We have recently prepared *D,L*-notoamide T by the same biomimetic IMDA strategy used to make stephacidin A (Scheme 16) and are currently preparing the isotopically labeled material for precursor incorporation experiments.

We have also very recently sequenced the genome of *Aspergillus versicolor* NRRL 35600 and have identified a biosynthetic gene cluster that is highly homologous to the one from Tsukamoto's marine-derived *Aspergillus* sp.<sup>37b</sup> Genome mining, bioinformatics analysis, and functional expression of select genes are currently in progress. It is anticipated that the mystery to the key enantio-divergent step, currently suspected to be at the stage of the notoamide S to notoamide T construction, will soon be solved.

Another surprising discovery in this program, which also relied heavily on the development of a total synthesis platform, concerned the elucidation of the absolute stereochemistry of the minor metabolite, VM55599, isolated from the paraherquamide-producing organism *Penicillium* sp. IMI32995. Everett and co-workers at Pfizer reported the isolation, structure determination, and relative stereochemical assignment of VM55599 and further suggested that this substance might be a biosynthetic precursor

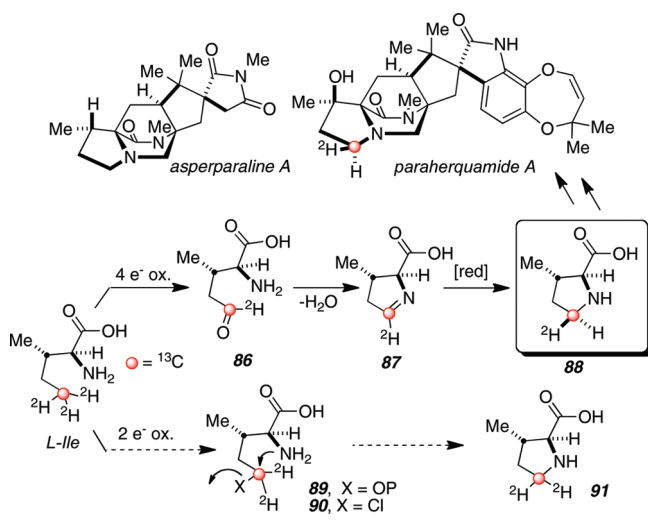
Scheme 24. Current Biogenetic Proposal for Stephacidin A (Marine-Derived *Aspergillus* sp.)

to paraherquamide.<sup>14d</sup> We discovered that the  $\beta$ -methylproline ring of paraherquamide A was derived from the oxidative cyclization of isoleucine and was not derived from the methylation of proline via *S*-adenosylmethionine.<sup>40,41</sup>

We were able to determine that the mechanism for the oxidative cyclization of isoleucine to  $\beta$ -methylproline proceeded through a net four-electron oxidation of the *D*-methyl residue of isoleucine to an aldehyde or aldehyde equivalent. Cyclization to the imine **87**, followed by a stereospecific reduction, provided  $\beta$ -methylproline, which incorporates into both asperparaline A and paraherquamide A (Scheme 25). This was made possible through the synthesis of 1-[5-<sup>13</sup>C,5-<sup>2</sup>H<sub>3</sub>] isoleucine isotopomer. Precursor incorporation experiments with this amino acid in *Penicillium fellutanum*, followed by isolation and purification of the paraherquamide A produced, revealed 0.32% incorporation of the labeled amino acid. Detailed NMR spectroscopic analysis revealed that H-16a (3.21 ppm) is the deuteron, H-16b (2.22 ppm) is the proton, and the *pro-S* hydrogen is retained in the oxidative cyclization. *This result mandates that reduction occurs on the same face of the proline ring as the methyl group, C-17.*

The take-away lessons from these experiments revealed that (1)  $\beta$ -methylproline in the paraherquamide-producing *Penicillium* sp. is biosynthetically derived from *S*-isoleucine; (2) a net



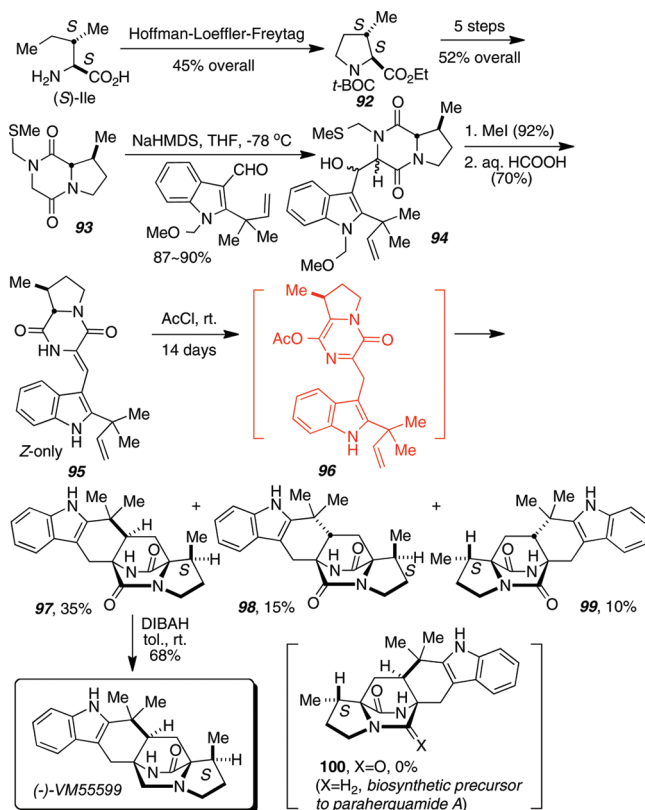
Scheme 25. Origin of the  $\beta$ -Methylproline Ring in Paraherquamide and Asperparaline Biosynthesis

four-electron oxidation followed by a two-electron reductive amination fashions the pyrrolidine ring of  $\beta$ -methylproline; (3) hydroxylation of the C-14 position in paraherquamide biosynthesis occurs with net retention of stereochemistry; and (4) most significantly, the absolute configuration of VM55599 should be pseudo-enantiomeric to that in paraherquamide A, precluding the possibility (suggested by Everett et al.) that VM55599 was a biosynthetic precursor to paraherquamide A. VM55599 is therefore a shunt (dead-end) metabolite. If this substance was not a biosynthetic precursor to paraherquamide A, then what species was?

We were able to rigorously establish the absolute configuration of VM55599 through an asymmetric, biomimetic total synthesis as shown in Scheme 26.<sup>42</sup> In this synthesis, *S*-isoleucine served as the optically pure starting material that was subjected to a Hoffman–Loeffler–Freitag conversion to optically pure  $\beta$ -methylproline. Dioxopiperazine formation and aldol condensation/dehydration afforded the unsaturated substrate **95** that was subjected to the IMDA cyclization conditions first reported by Liebscher et al. to give three of the four possible diastereomeric Diels–Alder products. Significantly, none of the “pre-paraherquamide” diastereomer was formed, which reveals that the intrinsic facial bias of this IMDA cyclization favors the rare VM55599 relative stereochemistry and not that of paraherquamide.

Based on these results, we speculated that compound **102** (where X = H<sub>2</sub>) with the  $\beta$ -methyl residue in the proline ring on the  $\alpha$ -face and having the correct absolute configuration was a plausible hexacyclic precursor to paraherquamide. We endeavored to prepare a racemic, double <sup>13</sup>C-labeled isotopomer of **102**, which was accomplished using a biomimetic IMDA construction. This synthesis produced all four possible IMDA diastereomers, the major isomer corresponding to VM55599. We performed precursor incorporation experiments with both the dioxopiperazine and monooxopiperazine forms of VM55599 and **102** and found that only **102** incorporated into paraherquamide A. Soon thereafter, we were able to isolate trace amounts of this new metabolite (**102**), which we have named “pre-paraherquamide” from the paraherquamide-producing fungi *Penicillium fellutanum* as well as from the asperparaline-producing fungi *Aspergillus japonicus* (Scheme 27).

Scheme 26. Asymmetric Synthesis of (–)-VM55599



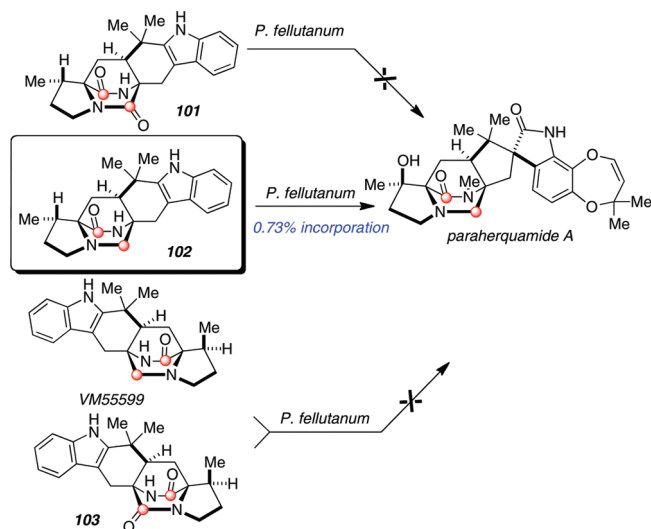
An interesting and puzzling observation from these experiments centered around the lack of incorporation of the dioxopiperazine congener to preparaherquamide, namely compound **101**. This suggests that the tryptophan-derived carboxyl residue is reduced at some point in the biosynthesis *prior* to the formation of the bicyclo[2.2.2]diazaoctane ring system or that the oxidation state of the putative azadiene in this family of metabolites proceeds through the reduced oxidation state directly providing preparaherquamide in the IMDA cyclization. Efforts to resolve this apparent anomaly, particularly when contrasted to the oxidation level apparent in the biosynthesis of the stephacidins, notoamides, and breviranamides, are an area of current focus.

On the basis of all of the available experimental data, we have proposed a “unified” biogenesis of the paraherquamides and asperparalines<sup>43</sup> as shown in Scheme 28. It appears as though preparaherquamide serves as the possible branch-point in the biogenesis of these two families where, in paraherquamide biosynthesis, the indole-derived benzenoid ring is further hydroxylated to a phenol and catechol, and prenylation steps fashion the dioxepin (such as in paraherquamide A) and pyranil ring systems (such as in paraherquamide F) extant in within this family. In the asperparaline-producing fungi, such as *Aspergillus japonicus*, the indole-derived benzenoid ring is oxidatively cleaved, removing four carbon atoms followed by further oxidative remodeling to form the novel spiro-succinimide ring system that is unique among known natural products to the asperparalines.

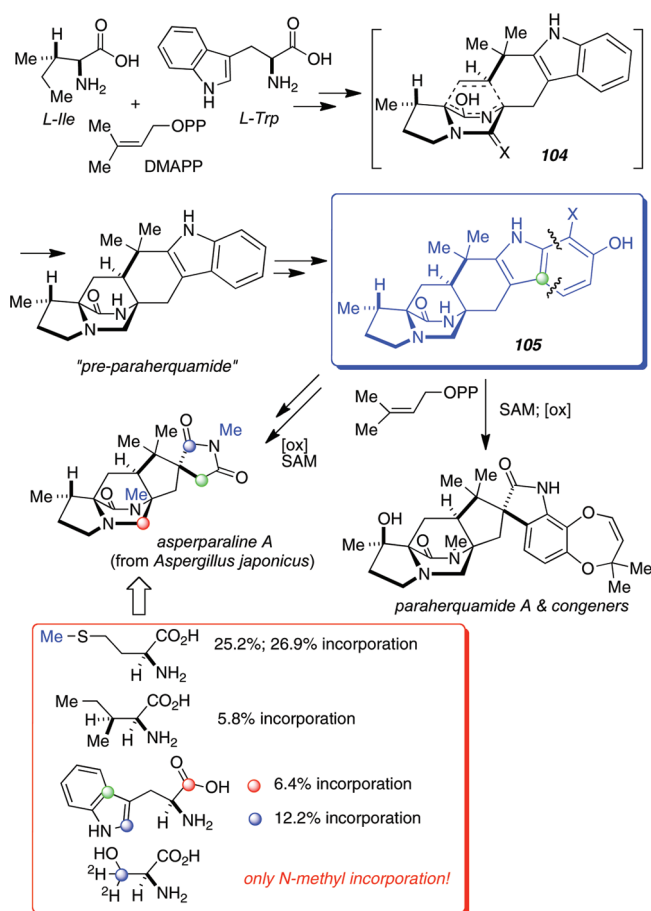
Labeled precursor incorporation experiments in *A. japonicus* revealed that the spiro-succinimide ring of asperparaline is derived from tryptophan; the  $\beta$ -methylproline residue is derived from *S*-isoleucine (as expected); and serine only labels the two *N*-methyl residues (via conversion to SAM). The lack of



Scheme 27. Discovery and Incorporation of “Pre-paraherquamide”



Scheme 28. “Unified” Biogenetic Hypothesis for the Paraherquamides and Asperparalines



incorporation of the labeled serine into the tryptophan-derived methylene residue was quite unexpected and suggests that tryptophan biosynthesis in these fungi may proceed through an

as yet undetermined mechanism. Efforts to resolve this anomaly are also underway.

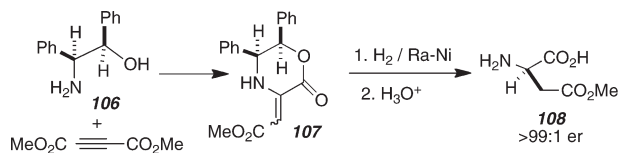
This program has benefited from a dynamic combination of total synthesis technologies that have advanced to a stage where we are confident that we can prepare, in isotopically labeled form, as either a racemate (which has become necessary to probe potential enantio-divergent steps) or in optically pure form, the substrate and product of every single putative biosynthetic transformation. The whole genome sequencing, genome mining, and proteomics technologies have provided powerful new tools that are being deployed to clone and functionally express the biological catalysts that Nature has evolved to construct this structurally stunning family of indole alkaloids.<sup>44</sup> It remains to be established if the core bicyclo[2.2.2]diazaoctane ring system is indeed fashioned by a biosynthetic intramolecular hetero-Diels–Alder reaction, as the current evidence on this provocative key point is circumstantial and indirect.<sup>45</sup> We have extensively demonstrated the chemical feasibility of this construction, and we are very anxious to learn if Nature has stumbled onto this reaction inadvertently through the oxidative processing of these nonribosomally generated dipeptides. The existence of the discrete enantiomers of stephacidin A, notoamide B, and versicolamide B constitutes the most intriguing hint and puzzle surrounding this fascinating, and pedagogically controversial question.<sup>45</sup> This project is currently at the most exciting state, and we are poised to delve more deeply into Nature’s treasure chest of closely guarded biosynthetic secrets.

### III. ASYMMETRIC SYNTHESIS OF $\alpha$ -AMINO ACIDS

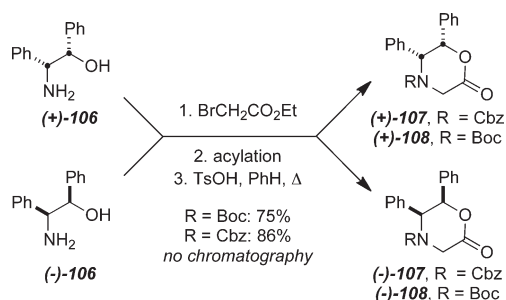
Returning to the bicyclomycin synthesis, we developed an electrophilic glycine equivalent (**1**, Scheme 1) to tackle the synthesis of the  $\beta,\beta$ -disubstituted isoleucine moiety. At the time, in the early 1980s) there were many laboratories engaged in developing asymmetric glycine enolate equivalents,<sup>46</sup> and we capitalized on this opportunity to design a chiral, nonracemic chiral auxiliary-based electrophilic glycine equivalent based on the successful C–C coupling reactivity of the bis-thiopyridyl dioxipiperazine species **1**. The molecular design of one such heterocyclic species was already present in the literature through a landmark paper by Kagan, who in 1968 published the asymmetric synthesis of aspartic acid in very high enantiomeric ratio through catalytic hydrogenation of diphenyloxazinone **107**, as shown in Scheme 29.<sup>47</sup>

Based on the obvious extension of this heterocyclic system to a glycine template, we prepared the *N*-CBz and *N*-*t*-Boc diphenyloxazinones (**107** and **108**, Scheme 30)<sup>48,49</sup> from the same optically active diphenylamino alcohol (**106**) employed by Kagan. The preparation of the optically pure amino alcohols follows from a classical diastereomeric aspartate salt resolution published by Tishler in 1951.<sup>50–53</sup> The preparation of both enantiomers of the diphenyloxazinones, as either their *N*-CBz or *N*-*t*-Boc derivatives, is shown in Scheme 30 and has been published as an *Organic Syntheses* procedure.<sup>49</sup> In addition, these compounds have been commercially available from Aldrich Chemical since the late 1980s. This methodology therefore provides unambiguous and convenient access to either *D*-(*R*)- or *L*-(*S*)-configured  $\alpha$ -amino acids in a high degree of chemical and optical purity.

We have previously extensively reviewed the chemistry of these highly versatile amino acid templates, and only a few highlights of the application of this methodology to more complex natural products synthesis will be briefly touched on here.<sup>54</sup>

Scheme 29. Kagan's Aspartic Acid Synthesis<sup>47</sup>

## Scheme 30. Preparation of the Diphenyloxazinones



It must be stated clearly here that these reagents are members of the “chiral auxiliary pool” for asymmetric synthesis; the 1,2-diphenylamino alcohol moiety is destroyed in the final deblocking step to access the new, optically active  $\alpha$ -amino acid and cannot be recycled. This might be considered to be a disadvantage of this methodology. These substances are therefore not readily applicable for large scale (>10 kg) industrial manufacturing of amino acids but are, rather, ideally suited to the preparation of research and preclinical quantities of amino acids where speed, flexibility, and reliability are the major discerning criteria. On the other hand, the destruction of the chiral auxiliary in the setting for which this methodology is ideally suited, namely medicinal chemistry and other high-throughput applications, turns out to be a *major advantage* of this system. As described in a number of publications from our laboratory, as well as many other laboratories, the diphenyl amino alcohol moiety is typically reduced to give a water-insoluble byproduct, bibenzyl, which can be conveniently extracted away from the polar, water-soluble zwitterionic amino acid or *N*-*t*-Boc amino acid. This obviates, in most cases, chromatographic or ion-exchange purification of the final amino acid.

For the electrophilic reaction manifold, the oxazinone (e.g., (–)-**107** or **108**) is treated with *N*-bromosuccinimide in a nonpolar solvent delivering the *anti*-bromide **109** in essentially quantitative yield; reaction of **109** with a variety of carbon-based nucleophiles in the presence of mild Lewis acids furnishes the  $\alpha$ -substituted oxazinones (**111**) in good yield and with generally excellent diastereoselectivities (Scheme 31). The key C–C bond-forming reaction is believed to proceed through the agency of a highly reactive *N*-acyl imminium ion species (**110**) that is attacked from the least-hindered face of the oxazinone, *anti*- to the two phenyl substituents. After purification of the derivatized oxazinone, the chiral auxiliary was cleaved in most cases via catalytic hydrogenation over a heterogeneous palladium catalyst, typically in excellent yields to give the free amino acids. Dissolving metal conditions were also successfully employed to produce the amino acid derivatives and, in the case of unsaturated side chains, obviated saturation of olefinic residues.

The scope of reactive intermediates that can be generated from these oxazinone heterocycles for participation in

## Scheme 31. Electrophilic Glycinate Methodology

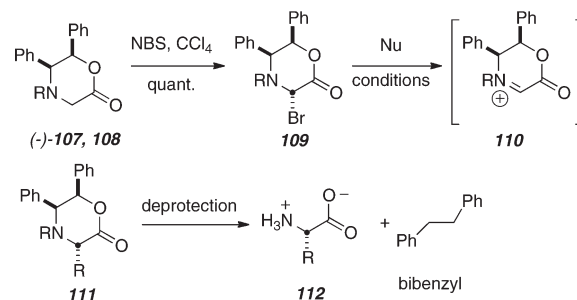


Table 2. Modes of Reactivity and Classes of Amino Acids

Mode of Reactivity	Classes of Amino Acids
electrophilic glycinate	simple aliphatic $\alpha$ -amino acids $\gamma,\delta$ -unsaturated $\alpha$ -amino acids <i>E</i> - $\beta,\gamma$ -unsaturated $\alpha$ -amino acids arylglycines biarylglycines
glycine enolate	simple aliphatic $\alpha$ -amino acids $\alpha,\alpha$ -disubstituted $\alpha$ -amino acids $\gamma,\gamma$ -unsaturated $\alpha$ -amino acids 2,6-diaminopimelic acids cyclic amino acids <i>anti</i> - $\beta$ -hydroxy $\alpha$ -amino acids <i>syn</i> - $\beta$ -amino $\alpha$ -amino acids
azomethine ylide	di- and trisubstituted pyrrolidine carboxylic acids
$\alpha,\beta$ -dehydro/phosphonate $\alpha,\beta$ -dehydro	<i>E</i> -1-aminocyclopropanecarboxylic acids pyrrolidine-2-amino-2-carboxylic acids cyclohexenyl-4-amino-4-carboxylic acids
C-1 oxocarbenium ion	peptide isosteres

diastereoselective C–C bond-forming reactions, has been significantly expanded to include *N*-acyl imminium ions (glycine electrophile), enolate, radical, azomethine ylide,  $\alpha,\beta$ -dehydro functionalization, and most recently, manipulation of the lactone carbonyl residue gaining access to peptide isosteres (Table 2 and Figure 5).

We have utilized the chiral glycine methodology to synthesize a variety of natural products, including  $\beta$ -carboxyaspartic acid,<sup>55</sup> (+)-6-hydroxymethyl-2,6-diaminopimelic acid,<sup>56</sup> (–)-cucurbitine,<sup>57</sup> norcoronamic acid,<sup>58</sup> coronamic acid,<sup>58</sup> 2,6-diaminopimelic acid,<sup>59</sup> statine,<sup>60</sup>  $\gamma$ -D(L)-glutamyl-L-*meso*-diaminopimelic acid dipeptide,<sup>61</sup> (–)-spirotryprostatin B,<sup>62</sup> (–)-spirotryprostatin A,<sup>63</sup> (–)-tetrazomine,<sup>64</sup> (2*S*,3*R*)-capreomycinide,<sup>65</sup> capreomycin IB,<sup>66</sup> (S)-(-)-carnitine,<sup>67</sup> (R)-(-)-carnitine,<sup>68</sup> hypusine,<sup>69</sup> negamycin,<sup>70</sup> renieramycin G,<sup>71</sup> jourumycin,<sup>71</sup> cylindrospermopsin,<sup>72</sup> 7-*epi*-cylindrospermopsin,<sup>73</sup> and 7-deoxycylindrospermopsin.<sup>74</sup>

Cylindrospermopsin (CY) was isolated as the principal hepatotoxin from *Cylindrospermopsis raciborskii* in 1992 after suspicion of its involvement in an outbreak of hepatoenteritis that hospitalized 150 people on Palm Island, Australia.<sup>75</sup> It has since been isolated in Japan from *Umezakia natans*<sup>76</sup> and in Israel from *Aphazinomenon ovalisporum*.<sup>77a</sup> Following the discovery of the

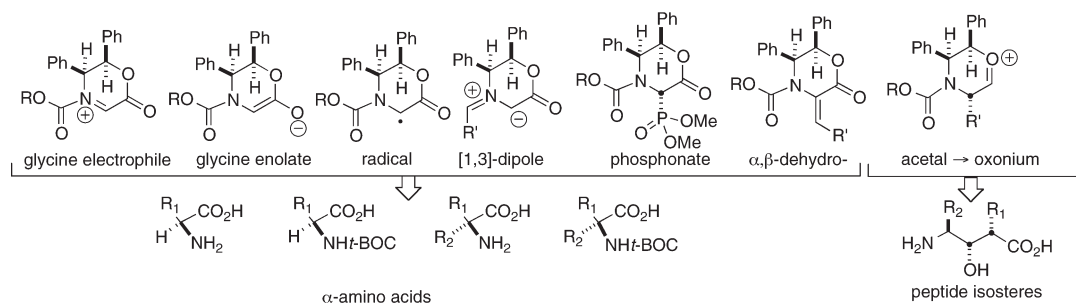


Figure 5. Various modes of reactivity accessible to the diphenyloxazinones.

parent compound, 7-*epi*-cylindrospermopsin was isolated from *A. ovalisporum* as a toxic minor metabolite.<sup>77b</sup> 7-Deoxycylindrospermopsin was initially isolated from *C. raciborskii* and has recently been coisolated with CY in China from *Raphidiopsis curvata*.<sup>78</sup> Cylindrospermopsin has been shown to be a potent hepatotoxin ( $LD_{50} = 0.2 \mu\text{g}/\text{kg}$  in mice);<sup>79</sup> 7-*epi*CY is equipotent with CY,<sup>24</sup> while 2-deoxyCY was thought to be nontoxic.<sup>75c</sup> Unlike the peptidyl hepatotoxic microcystins and nodularins, the cylindrospermopsins do not inhibit PP1 or PP2A. Their toxicity appears to result at least in part from the inhibition of protein synthesis.<sup>75,80</sup> The translation step of protein synthesis is inhibited by the cylindrospermopsins, but the mechanism of this inhibition is not yet known. Cylindrospermopsin has also been shown, *in vitro*, to be a noncompetitive inhibitor ( $K_i = 10 \mu\text{M}$ ) of the uridine monophosphate (UMP) synthase complex, although *in vivo* assays do not support a general inhibition of UMP synthesis.<sup>81</sup> Terau et al. were able to show that one of the first symptoms of poisoning with CY was the detachment of ribosomes from the membrane of the endoplasmic reticulum.<sup>80a</sup> It was also shown that in mammalian cell cultures, cell death was accompanied by a marked decrease in glutathione (GSH), an essential endogenous reductant to the antioxidative capabilities of hepatocytes.<sup>82</sup>

At the onset of this project little was known about the mechanism of action of this family of hepatotoxins. This encouraged us to develop an efficient and flexible synthesis of these alkaloids. We were intrigued by the observations that CY and 7-*epi*CY are toxic and 7-deoxyCY reportedly was not (although our work later showed this to be incorrect). Cytochrome P450 oxidation had been purported to mediate their toxicity.<sup>80</sup> We thought that an oxidation event at C7 or C8 may produce the enol-guanidine **113** (Figure 6); alternatively, C15 oxidation may generate the guanidinimine **114**. Both of these intermediates are potentially redundant through extensive tautomerization, and both are electrophilic intermediates, perhaps responsible for the observation that oxidized metabolites of CY may alkylate DNA.<sup>80,83</sup> These considerations helped guide our synthetic investigations.

In addition, Shaw et al. proposed the unusual uracil tautomer (**115**, Figure 6) for 7-deoxyCY<sup>75c</sup> that we were suspicious was incorrect. We also sought to develop the first synthesis of 7-deoxyCY and interrogate both the structural proposal and the claim that this metabolite was nontoxic.<sup>75c</sup> Cylindrospermopsin has attracted considerable synthetic attention and has been synthesized in racemic form by Snider<sup>84</sup> and Weinreb<sup>85</sup> and in optically active form by White,<sup>86</sup> who was also the first to establish the absolute stereochemistry.

The glycine enolate reactivity was deployed for concise, asymmetric syntheses of all three natural cylindrospermopsin

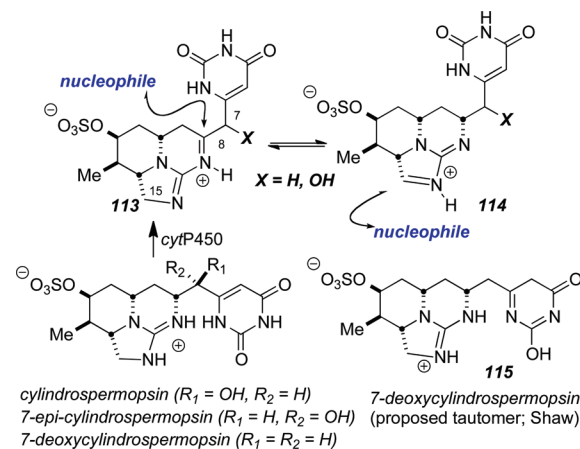


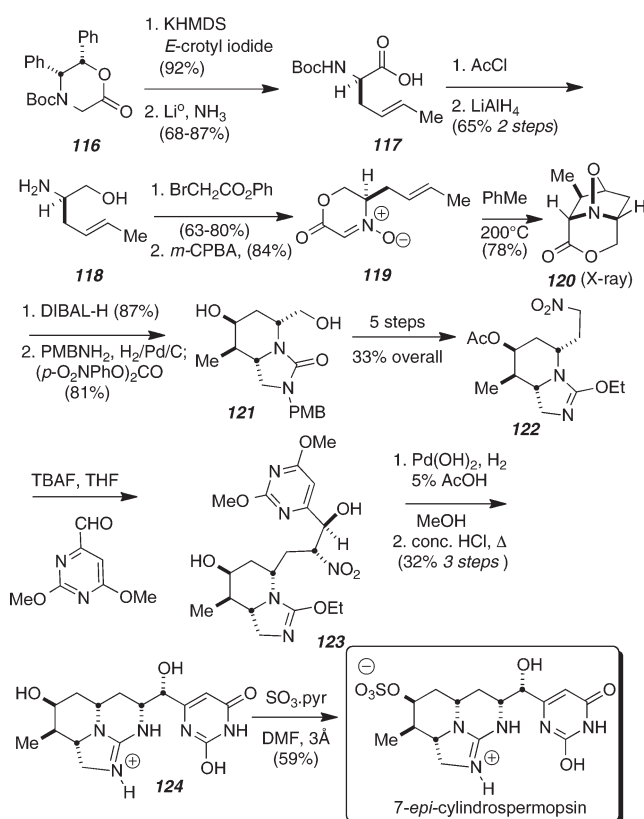
Figure 6. Biomechanistic queries on the cylindrospermopsins.

alkaloids via a key intramolecular nitron [1,3]-dipolar cycloaddition reaction on the crotylglycine-derived species **119** (Scheme 32).<sup>72–74</sup> The desired regiochemistry of the dipolar cycloaddition (**119** to **120**) proceeded to the extent of 10:1 in hot toluene but  $\text{Sc}(\text{OTf})_3$  at 25 °C gave **120** in 78–84% yield (12:1 regioselectivity); X-ray analysis of **120** secured the assigned structure. Reductive processing of **120** provided the functionalized A-ring of the cylindrospermopsins which was then homologated to the nitroalkane (**122**) and coupled to the pyrimidine moiety. Reductive guanidinylation gave the tetracycle (**124**) that was sulfated to give 7-*epi*CY.

The same overall strategy was deployed to prepare cylindrospermopsin and 7-deoxyCY. Our synthesis of 7-deoxyCY corrected the structural mis-assignment made by Shaw et al. and provided the first pure sample of this substance for biochemical and biological evaluation. Having completed the total syntheses of all the cylindrospermopsin alkaloids, we were able to examine the feasibility of our biomechanistic hypothesis for the intermediacy of **113** or **114** (Figure 6). This work was done through a collaboration with Prof. Maria Runnegar. While synthetic CY was a potent inhibitor of protein synthesis in hepatocytes (4% of control at 3.3  $\mu\text{M}$ ), the C8 diastereomer required a concentration of 320  $\mu\text{M}$  to achieve the same level of inhibition. Two orders of magnitude less toxic, this suggests that they are not processed through a common metabolic intermediate. Most significantly, our synthetic (racemic) 2-deoxyCY also proved to be a potent inhibitor of protein synthesis, contrary to the initial report by Shaw et al.<sup>75c</sup>

Protein synthesis was completely inhibited at 12  $\mu\text{M}$ , *in vitro*, and at 10  $\mu\text{M}$  in whole cells, displaying potency within an order

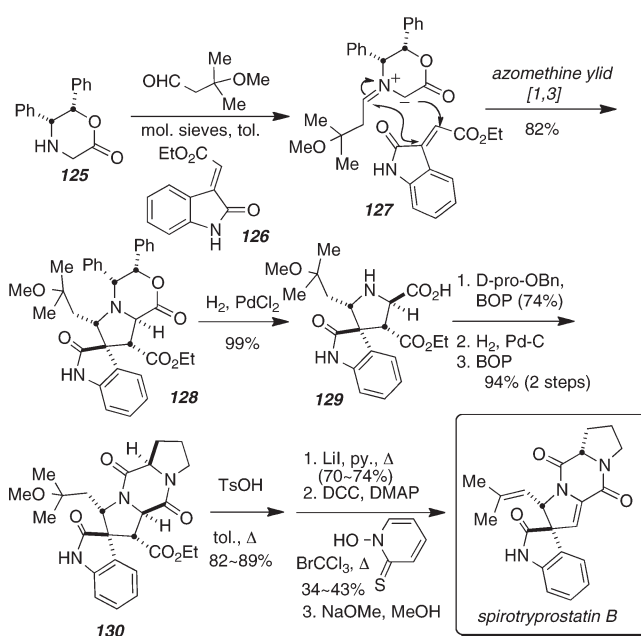


Scheme 32. Asymmetric Synthesis of Natural 7-*epi*-Cylindrospermopsin

of magnitude of CY. Resembling intoxication by CY, synthetic 2-deoxyCY also inhibits the synthesis of glutathione (GSH).<sup>82</sup> The deoxygenated C8 diastereomer also required a 100-fold increase in concentration to elicit these effects. These results suggest that (1) substitution at C7 is not requisite for the toxicity of these alkaloids; (2) a common oxidized metabolite at C8 is not involved; and (3) in agreement with previous studies, intermediates lacking the uracil showed greatly diminished toxicity. Our synthetic work on the cylindrospermopsins has thus served to reveal several fundamentally new and important insights about the stereochemistry at C-7 and C-8, provided the correct structure of 7-deoxyCY, and significantly revealed that C-7 oxygenation is not required for the expression of toxicity.

A more recent mode of reactivity that we and others have exploited via the diphenyloxazinones, is the generation of azomethine ylides for both intermolecular and intramolecular [1,3]-dipolar cycloaddition reactions. Three examples from our laboratory highlight this powerful pyrrolidine construction. As shown in Scheme 33, the asymmetric total synthesis of spirotryprostatin B, a structurally novel microtubule inhibitor isolated by Osada et al. from *Aspergillus fumigatus*,<sup>87</sup> was accomplished. This molecule and the closely related spirotryprostatin A have attracted extensive synthetic attention.<sup>88,89</sup> The key three-component dipolar cycloaddition reaction was accomplished through the reaction of the oxazinone **125** with the isatin-derived dipolarophile **126** and 3-methoxy-3-methylbutanal, which provided the desired cycloadduct **127**, whose structure was confirmed by X-ray analysis.<sup>62</sup> Hydrogenation to the amino acid, coupling to *D*-proline benzyl ester and cyclization then fashioned the pentacycle (**130**), which was subjected to a Barton-modified

## Scheme 33. Asymmetric Synthesis of Spirotryprostatin B via an Azomethine Ylide Cycloaddition



Hunsdiecker oxidative decarboxylation and final thermodynamic epimerization of the proline residue to deliver spirotryprostatin B.

We deployed similar methodology to achieve a very concise five-step asymmetric synthesis of spirotryprostatin A.<sup>63,91</sup> This synthesis platform enabled us to prepare several derivatives of the spirotryprostatins, and in particular, we prepared the enantiomer of the natural metabolite of spirotryprostatin B isolated from *Aspergillus fumigatus*; we also prepared C-12-*epi*-spirotryprostatin B and the corresponding dehydrospirotryprostatin B. These three substances represent incremental geometrical changes at the proline  $\alpha$ -methine residue, with the  $\alpha,\beta$ -dehydro(prolyl) analogue possessing a geometry in-between that of natural spirotryprostatin B and the 12-*epi*-diastereomer (Figure 7).<sup>90</sup> All three of these substances, along with several other synthetic analogues, were tested for cytotoxic activity and the capacity to disrupt microtubule formation by our collaborator and discoverer of the spirotryprostatins, Dr. Hiroyuke Osada at RIKEN, Japan. Surprisingly, C-12-*epi*-spirotryprostatin B proved cytotoxic to tSF210 cells at about 10-fold higher concentrations than that for the natural product, but was not a microtubule inhibitor. Even more astonishing was the observation that the dehydro analogue was devoid of cytotoxic activity. This reveals that the proline residue in the spirotryprostatin structural framework must make very intimate contact with its' receptor protein (as yet undetermined) as the subtle changes in geometry at the proline residue strongly impact biological activity.

In a second foray utilizing the dipolar cycloaddition methodology, we have recently constructed the cyclopentane core of palau'amine and congeners (Figure 8) as shown in Scheme 34.<sup>92</sup>

Palau'amine, a dauntingly complex hexacyclic bis-guanidine antibiotic isolated from the sponge *Stylotella agminata*,<sup>93</sup> is a biologically intriguing substance whose structure, stereochemistry, biosynthesis, and total synthesis have attracted considerable attention.<sup>94</sup> Palau'amine displays potent cytotoxic and immunosuppressive activities,<sup>93</sup> and a recent, brilliant total synthesis of racemic palau'amine by the Baran laboratory is particularly



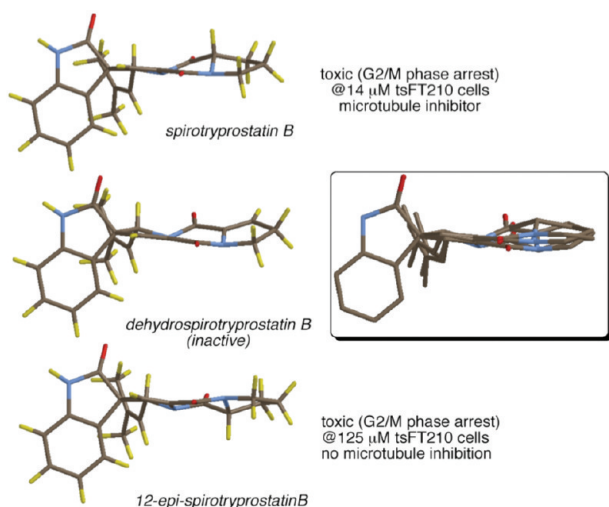


**Figure 7.** Overlay of spirotryprostatin B, C-12-*epi*-spirotryprostatin B, and dehydrospirotryprostatin B.

noteworthy.<sup>95</sup> The relative stereochemistry of palau'amine was recently revised independently by Quinn<sup>96a</sup> and Köck<sup>96b</sup> to the stereostructure depicted in Figure 8 and turned out to be a fortuitous stereochemical array for our approach based on an intramolecular [1,3]-dipolar cycloaddition reaction that sets up the fully substituted C-16 stereogenic center.

Our synthesis commences with the enolate acylation of commercially available oxazinone **108** to provide **131** (relative stereochemistry unassigned and inconsequential). Removal of the *t*-Boc group furnishes aminoketone **132**, which was condensed with formaldehyde to generate the incipient azomethine ylide (**A**) that produced tricyclic intramolecular cycloaddition product **133** as a single diastereomer in 63% overall yield for the three steps. The intrinsic facial bias of this intramolecular cycloaddition remains unclear and constitutes the subject of ongoing studies.

Reductive processing of **133** led to **135** in 61% overall yield. Ruthenium-mediated oxidation to ketoamide **136** was next converted into the unsaturated ketone by IBX oxidation to enone **137** in 80% yield. Stereoselective installation of the two one-carbon arms to enone **137** was accomplished in two stages beginning with a Morita–Baylis–Hillman type of hydroxymethylation and a subsequent nitromethane addition to give exclusively the desired 1,2-*anti* product. The relative stereochemistry of the vicinal hydroxymethyl and nitromethyl substituents in **140** are set with the correct relative stereochemistry as per the newly reassigned stereochemistry of palau'amine. Studies to apply this asymmetric approach to construct palau'amine are currently under investigation.

A third, also unfinished, foray into complex alkaloid synthesis is an asymmetric approach to nakdomarin and the manzamine alkaloids.<sup>97</sup> As shown in Scheme 35, three-component condensation of the diphenyloxazinone **125** with aldehyde **141** and the unstable *exo*-methylene piperidinone **142** gave the desired cycloadduct **143**. This substance has been transformed into the spiro-tricyclic species **144** that was subsequently reduced and converted into the alkynone substrate **146** that is currently being investigated for furan formation and final modeling to nakdomarin. The three-component azomethine ylide condensation reaction has proven particularly powerful, as three or more stereogenic centers can be generated in a single step and the tolerance of other functional groups has proven broad.

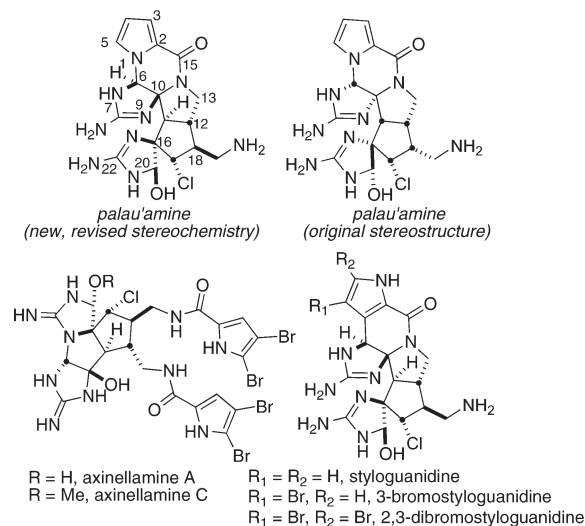
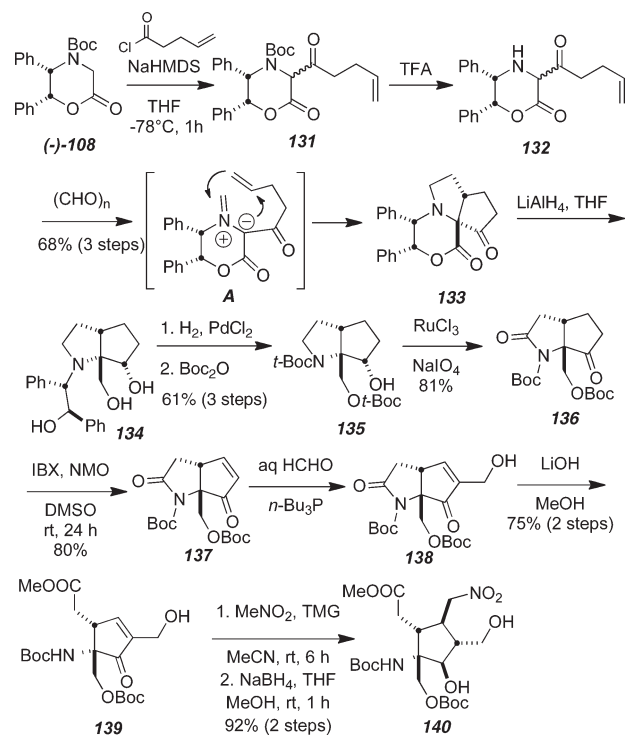


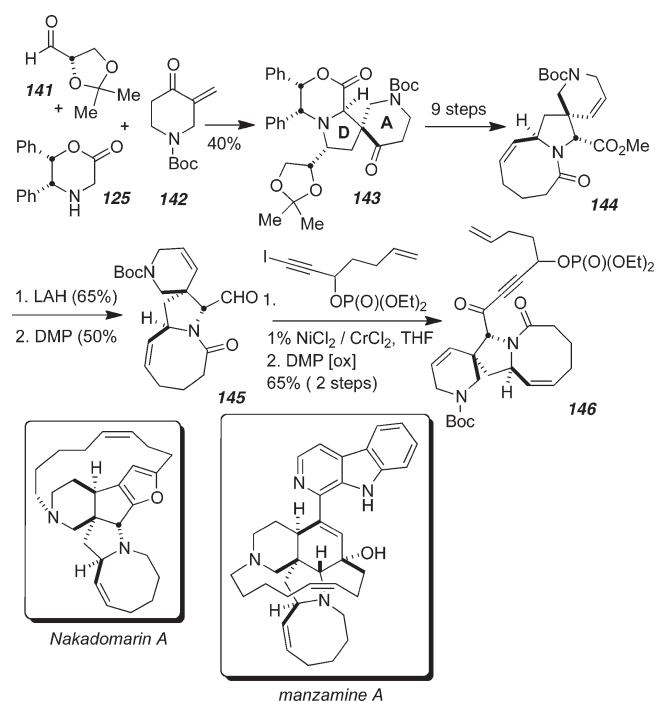
**Figure 8.** Structures of palau'amine and congeners.

### Scheme 34. Asymmetric Synthesis of the Cyclopentane Core of Palau'amine (**140**)<sup>92a</sup>



The azomethine ylide dipolar cycloaddition methodology has been recently utilized by the Schreiber laboratory to generate a focused, diversity-oriented synthesis library of spiro-oxindoles (Figure 9),<sup>98</sup> some of which proved active with the diphenyloxazinone template still intact.

The asymmetric amino acid methodology continues to be refined and extended by our laboratory, as well as many others, to access both simple as well as complex nitrogenous substances of biomedical significance. Our current focus has been to utilize this system where appropriate to other programs in alkaloid chemistry, some of which will be briefly touched on here.

Scheme 35. Dipolar Cycloaddition Approach to Nakadomarin<sup>97</sup>

## IV. TETRAHYDROISOQUINOLINE ALKALOIDS

We initially became interested in the family of tetrahydroisoquinoline alkaloids when the structure and preliminary mode of action of quinocarcin was disclosed by the Kyowa Hakko Kogyo Co. in Japan.<sup>99</sup> We were struck by the reported observation that quinocarcin damaged DNA in an oxygen-dependent manner independent of added metal salts such as iron or copper. We investigated the chemistry of this natural product and discovered that quinocarcin spontaneously disproportionates into the known, inactive cometabolites quinocarcinol and the newly identified oxidation product quinocarcinamide.<sup>100a</sup> We subsequently demonstrated that this spontaneous redox disproportionation reaction is general for the fused oxazolidine-containing antitumor alkaloids, including quinocarcin, tetrazomine, and bioxalomycin.<sup>100c</sup> In the presence of molecular oxygen, either the reduction radical species **150** or the oxidation radical **149** can react with dioxygen ultimately forming superoxide. In this scenario, these drugs serve as their own reductant. Given the presence of an exogenous one-electron reducing agent (such as DTT, GSH, ascorbate, or other reducing agents), quinocarcin, tetrazomine, and bioxalomycin (the natural members of this class that contain the fused oxazolidine), can *catalytically* mediate the reduction of molecular oxygen to superoxide, ultimately resulting in the production of reactive oxygen radical species that can damage DNA and other cellular macromolecules.

During the course of our studies on the mechanism of the redox disproportionation of the oxazolidine, we discovered an important stereoelectronic control element necessary for this process to occur.<sup>100</sup> As shown in Figure 10, we have ascertained through the chemical synthesis of configurationally defined analogues that the fused oxazolidine ring must be capable of adopting a *trans*-antiperiplanar geometry of the oxazolidine nitrogen lone pair and the adjacent methine hydrogen that participates in the redox disproportionation; the corresponding

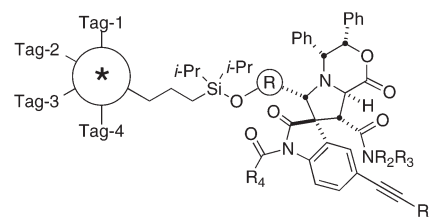


Figure 9. Schreiber's spirooxindole library.

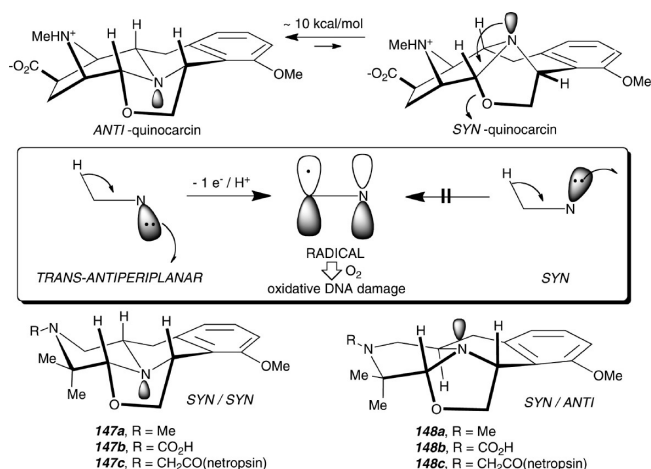


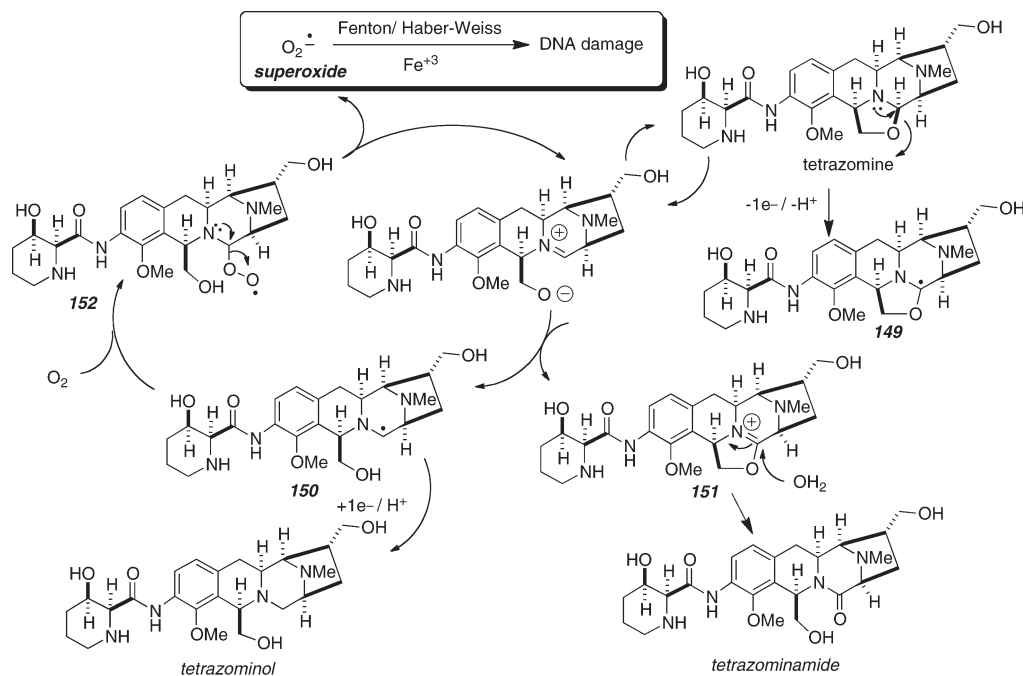
Figure 10. Stereoelectronic control of redox disproportionation.

*syn*-periplanar arrangement renders such oxazolidines inert to redox cycling and is inactive with respect to mediating damage to DNA (Figure 10).<sup>100,101</sup>

The significant conclusion from these studies, which relied heavily on the synthesis of configurationally defined stereoisomers (**147** and **148**), can be summarized as follows: (1) an intact oxazolidine is required for the redox disproportionation culminating in superoxide production and subsequently for inflicting oxidative damage to DNA, and (2) there is an obligatory stereoelectronic requirement for a *trans*-antiperiplanar arrangement of the nitrogen lone pair and adjacent methine of the oxazolidine for redox cycling and (unexpectedly) for DNA alkylation. The synthetic technology platforms we have developed during the course of this program have enabled the total syntheses of quinocarcinamide, quinocarcin (a formal total synthesis),<sup>102</sup> tetrazomine (including assignment of the relative and absolute configuration),<sup>64</sup> jorumycin,<sup>71</sup> reneiramycin G,<sup>71</sup> cribrastain 4,<sup>103</sup> and Et-743 (a formal total synthesis).<sup>104</sup> Several synthetic strategies were examined over the course of this program to construct the bicyclo[3.2.1]core of quinocarcin, tetrazomine, and bioxalomycin, as well as the bicyclo[3.3.1]core of Et-743, saframycin, jorumycin, cribrastatin, and congeners (Scheme 36).

For the asymmetric syntheses of (–)-jorumycin and (–)-reneiramycin G, we developed an asymmetric synthesis of the “left-half” tetrahydroisoquinoline (THIQ) deploying the oxazolidine-based amino acid enolate chemistry discussed above. The initial Pictet–Spengler reaction with ethyl glyoxylate (Scheme 37, **156** to **157**) provided only the undesired *anti*-THIQ, which was readily epimerized to give the requisite *syn*-THIQ that was set up for connection to the second tyrosine-derived amino acid (Scheme 38).

Scheme 36. Autoredox Disproportionation of Tetrazomine

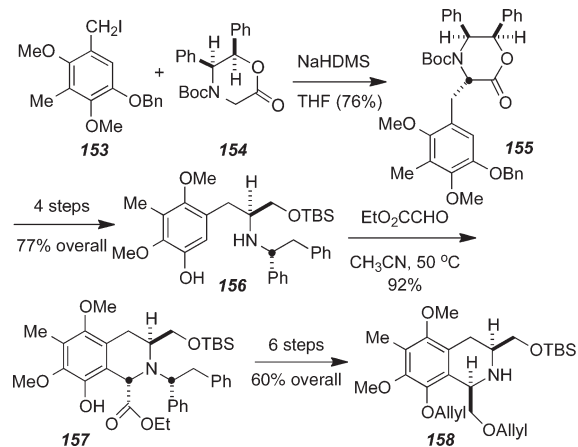


Condensation of **158** with **159** was made possible through the acid chloride, followed by processing to the key carbinolamine **162**. It was found that acid-mediated removal of the *N*-*t*-Boc residue concomitant with the second Pictet–Spengler cyclization delivered the desired pentacycle **163** that was used for the synthesis of both (–)-jorumycin and (–)-renieramycin G. During the course of these studies, it was found that, if the final Pictet–Spengler reaction were conducted on the corresponding *N*-methylamine (as opposed to the *N*-*t*-Boc derivative), the initial *syn*-stereochemistry of THIQ **164** suffered quantitative epimerization to the unnatural *anti*-stereochemistry shown for **165** (Scheme 39).

Undaunted by such unexpected, and undesired, stereochemical behavior, we capitalized on this opportunity to evaluate the effect of this somewhat subtle change in geometry of the rather rigid pentacyclic framework of these alkaloids, which had heretofore never been examined. We thus endeavored to convert the crystalline pentacycle **165** into 3-*epi*-jorumycin and 3-*epi*-renieramycin G, and these agents were tested side by side with synthetic samples of (–)-jorumycin and (–)-renieramycin G for antiproliferative activity against two human cancer cell lines (human colon A549 and human lung HCT-116, Table 3). (–)-Jorumycin displayed potent growth inhibition with GI<sub>50</sub> values in the low nanomolar range (1.9–19.2 nM), while the other compounds were found to be substantially less cytotoxic. Comparing the results of (–)-renieramycin G and its 3-*epi*-counterpart, it appears that these amide-containing substrates may be capable of exerting cytotoxic effects through alternative mechanisms, such as quinone-mediated redox cycling, which remain fully intact irrespective of the C3 stereochemical configuration.

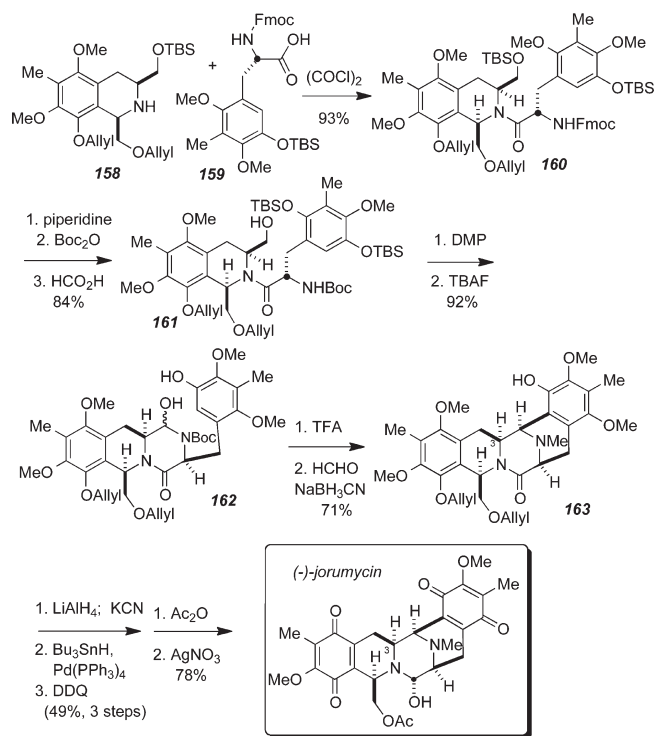
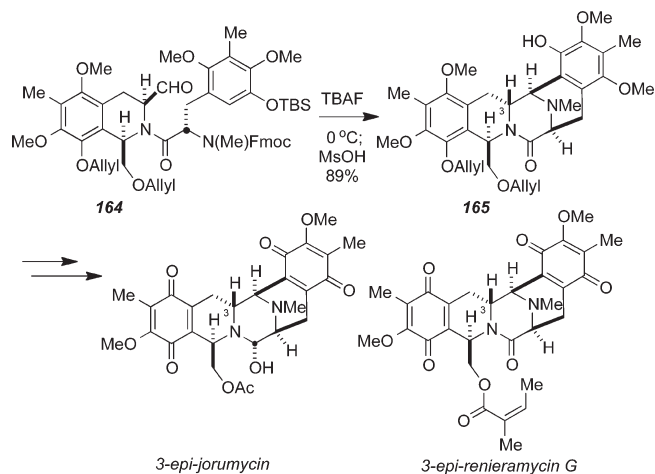
A somewhat distinct conceptual approach was developed for the asymmetric synthesis of (–)-cribrostatin 4 (renieramycin H) that deployed a tricyclic β-lactam as the synthetic precursor to

Scheme 37. Synthesis of a Versatile THIQ



the second Pictet–Spengler sequence (Scheme 40).<sup>103</sup> The tricyclic THIQ containing the fused β-lactam was prepared through the agency of an asymmetric Staudinger reaction. Despite the extensive chemistry of β-lactams in the literature spanning more than fifty years, very little has been published on methods to chemoselectively reduce β-lactams to β-amino aldehydes and β-amino alcohols. We found that L-Selectride proved to be a useful reagent for the mild reduction of the β-lactam ring in **168** to afford an incipient β-amino aldehyde that spontaneously suffered β-elimination, followed by intramolecular iminium ion formation and Pictet–Spengler closure to pentacycle **169** in 62% yield. The final stages of the synthesis proved straightforward and benefited from the known selenium dioxide oxidation of the benzylic position reported by Danishefsky and co-workers in their earlier and independent accomplishment of the cribrostatin 4 synthesis.<sup>105</sup>

## Scheme 38. Asymmetric Synthesis of (–)-Jorumycin

Scheme 39. Preparation of 3-*epi*-Jorumycin and 3-*epi*-Renieramycin G

Turning to the more complex problem of Et-743, we decided to solve a nagging stereochemical issue that came up in our total syntheses of quinocarcin, tetrazomine, jorumycin, and renieramycin G: namely, the difficulty we encountered in setting the two arms of the left-half THIQ with the requisite *syn*-relative stereochemistry. Direct Pictet–Spengler cyclizations (such as 156 to 157, Scheme 37) gave predominantly, or in some instances, exclusively, the undesired *anti*-THIQ that required thermodynamic epimerizations to set the correct relative stereochemistry.

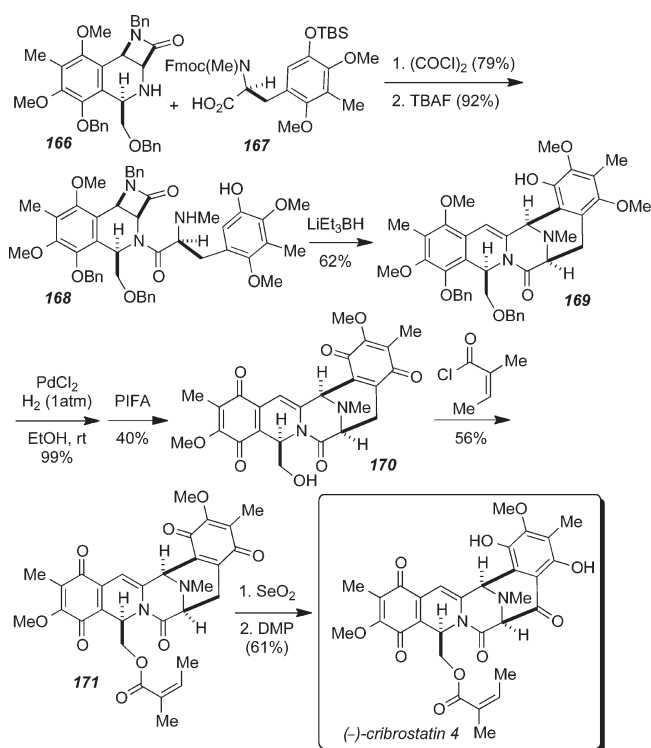
We devised a radical-based cyclization to fashion the desired *syn*-THIQ core, as shown in Scheme 41, on a glyoxalimine-based

## Table 3. Antiproliferative Activities

compd	cell line	
	AS49	HCT-116
3- <i>epi</i> -jorumycin	4.64	0.61
(–)-jorumycin	0.02	0.002
3- <i>epi</i> -renieramycin G	10.1	1.4
(–)-renieramycin G	12.9	3.87

<sup>a</sup> Values reported are  $\text{GI}_{50}$  in  $\mu\text{M}$ .

## Scheme 40. Asymmetric Synthesis of (–)-Cribrostatin 4



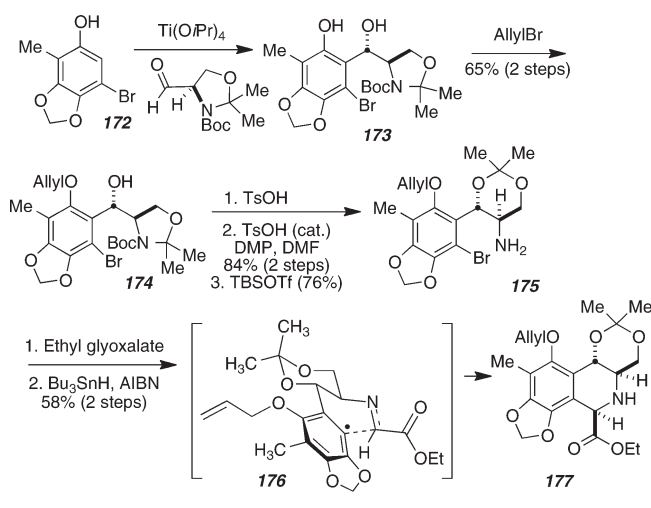
substrate.<sup>104</sup> The use of Garner's aldehyde, in a Friedel–Crafts alkylation on aryl bromide 172, provided the requisite amino alcohol substrate 173 that was condensed with ethylglyoxylate to form the corresponding imine. Aryl radical generation and cyclization proceeded through the chair–chair transition-state species (176) that disposed the carboethoxy residue equatorial, resulting in the desired *syn*-THIQ 177.

With the correct relative and absolute stereochemistry now efficiently addressed, tricycle 177 was converted through to pentacycles 182 and 183 (Scheme 42). This posed a regiochemistry problem we expected to encounter with the unsymmetrical tyrosine residue that we deliberately installed with the aim of economizing on the fashioning of the upper-right aryl residue that is unique to the ecteinascidins. While a solution to this regioselectivity issue has been recently devised, pentacycle 182 was transformed into a pentacyclic intermediate (184) prepared by Danishefsky and co-workers in their formal total synthesis of Et-743.<sup>106,107</sup>

We are also currently seeking to apply the methodologies we have developed for the total syntheses of several members of the tetrahydroisoquinoline family of antitumor agents, as described



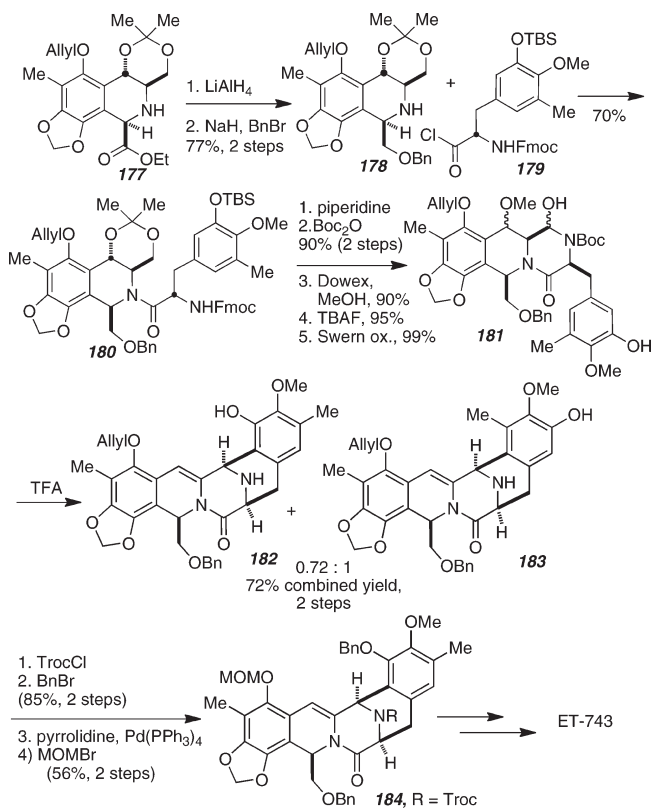
## Scheme 41. Diastereoselective Tetrahydroisoquinoline Construction for Et-743



above, to the asymmetric synthesis of the bioxalomycins. While these ongoing studies will not be summarized here, we did discover another unique mechanism of action of bioxalomycin during the course of working with this agent in the oxazolidine redox disproportionation studies briefly described above. We discovered that bioxalomycin  $\alpha_2$  is capable of covalent inter-strand cross-linking duplex DNA in the minor groove, in a highly site-specific manner at 5'-CpG steps.<sup>108</sup> We further demonstrated that this reaction occurs through alkylation of the exocyclic amine residues of the opposing deoxyguanosine residues. While the detailed structure of this lesion has not been completely elucidated, an accruing mass of indirect experimental evidence points to the mechanism and structure depicted in Figure 11. We have suggested that the cross-link occurs between C7 and C13b, wherein an *o*-quinonemethide species (**186**, Figure 11) is the *bis*-electrophile.

Remers and co-workers published a computational study<sup>109</sup> on this subject, wherein the presumed sites for cross-linking were C7 and C3a. Remers concluded that DNA cross-linking for this agent would not be possible. The optimal N2 to N2 distance in a 5'-CpG<sup>3'</sup> step is between 3.1 and 3.6 Å for B-form DNA. We have carried out preliminary molecular mechanics calculations on bioxalomycin noncovalently bound to DNA in an effort to determine likely modes of DNA interstrand cross-linking. We have found that there is excellent presentation of the putative electrophilic sites at C7 and C13b for **186** if the aromatic portion of the drug partially intercalates into the DNA helix. The modeling exercise on the positioning of the C7/C13b presentation that would result in cross-linked species (**187**) places both C7 and C13b within  $\sim 4.5$  Å of the proximal N2 of the opposing 2'-deoxyguanosine residues. Carrying out a similar modeling exercise on the presentation of the C7 and C3a sites (**185**, bottom Figure 12) also provides a feasible presentation of these electrophilic sites to the opposing 2'-deoxyguanosine residues, although the distances are somewhat greater ( $\sim 5$ – $6$  Å) than that for **186**. Modeling of two other possible electrophilic site combinations, C9/C13b and C3a/C9, gave a badly distorted DNA fragment that was not capable of maintaining Watson–Crick base-pairing; these sites are therefore thought to be highly unlikely.

We have also performed corroborating DNA cross-linking studies with cyanocycline (Scheme 43). In the absence of the

Scheme 42. Formal Total Synthesis of Et-743<sup>104</sup>

reducing agent DTT, there is no cross-linked product formed. However, in the presence of 0.1 mM DTT, a cross-linked product with properties identical to those obtained with bioxalomycin  $\alpha_2$  was obtained, albeit in somewhat lower yield. We attribute the lower yield to the inefficient reduction of the quinone to the dihydroquinone under the reaction conditions. The fact that cyanocycline, in the absence of a reducing agent, does not lead to cross-linking provides additional, indirect, yet provocative support for our contention that the *o*-quinone methide species **186** is a plausible species generated (via reduction of the quinone to the dihydroquinone) yielding the cross-linked adduct. These data are consistent with the molecular modeling picture we have of the most likely cross-linked species **187**.

This mode of reactivity reveals the dense complexity of molecular reactivity that Nature has installed in this beautiful alkaloid and includes DNA monoalkylation, interstrand cross-linking, redox disproportionation, and redox cycling of reactive oxygen radical species. Our laboratory is continuing to apply our synthetic technology around this family of alkaloids to further explore and exploit the multiple modes of chemical and biochemical reactivity that these fascinating alkaloids display.

**Biosynthesis of Et-743.** Trabectedin (Et-743 or Yondelis) has received authorization for commercialization from the European Commission for advanced soft tissue sarcoma, after failure of anthracyclines and ifosfamide, for patients who are unsuited to receive these agents. Et-743 is also in phase III clinical trials for ovarian cancer and phase II clinical trials for prostate, breast, and pediatric cancers.<sup>110</sup> Zalypsis (PM00104/50) is a related analogue that has begun phase I clinical trials for the treatment of solid tumors. Clinical supplies of Et-743 have become a major challenge, as the sea whip that houses the producing organism is

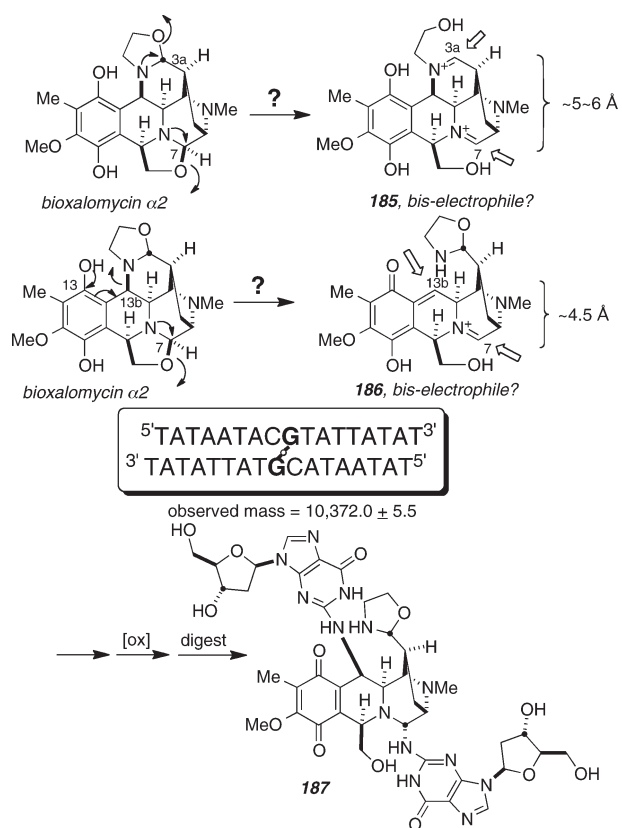


**Figure 11.** Proposed mechanism and structure of the bioxalomycin-induced covalent interstrand DNA cross-link.

difficult to collect and has proven recalcitrant to culture. The current manufacturing process to make clinical supplies of Et-743 relies on the large-scale fermentation of cyanosauracin B, followed by a multistep semisynthesis.<sup>111</sup> As this drug becomes more widely adopted, pressure on the price of this drug, which is very expensive to manufacture, will increase. A key challenge in natural product biosynthesis involves isolation, characterization, and analysis of pathways from marine invertebrate (e.g., sponges, tunicates, ascidians, octacorals) symbionts. Although significant progress has been made toward identification and analysis of the biosynthetic gene clusters of several marine-derived natural products, such as bryostatin and onnamide,<sup>112</sup> the study of these systems has so far been limited to gene cluster sequencing and bioinformatic analysis. Et-743, on the other hand, brings together a number of key elements to drive the search for an effective solution to this urgent source problem using a cross-disciplinary chemical biology approach. Although the natural product can be isolated directly from the marine tunicate *Ecteinascidia turbinata*, the yield is poor (1 mg of natural product/kg of marine tunicate). However, the high promise of this compound suggests that source restrictions will ultimately limit the scope of development and clinical use for treatment of a wider range of malignancies.

In collaboration with the Sherman laboratory at the University of Michigan, we have endeavored to elucidate the biosynthesis of Et-743 using a combination of metagenomics, proteomics, metabolomics, and chemical synthesis of probe substrates and putative biosynthetic intermediates. While this work is currently at a preliminary stage, we have used synthetic technologies developed in our laboratory to prepare probe substrates for the proteomics phase of this work and modern whole-genome

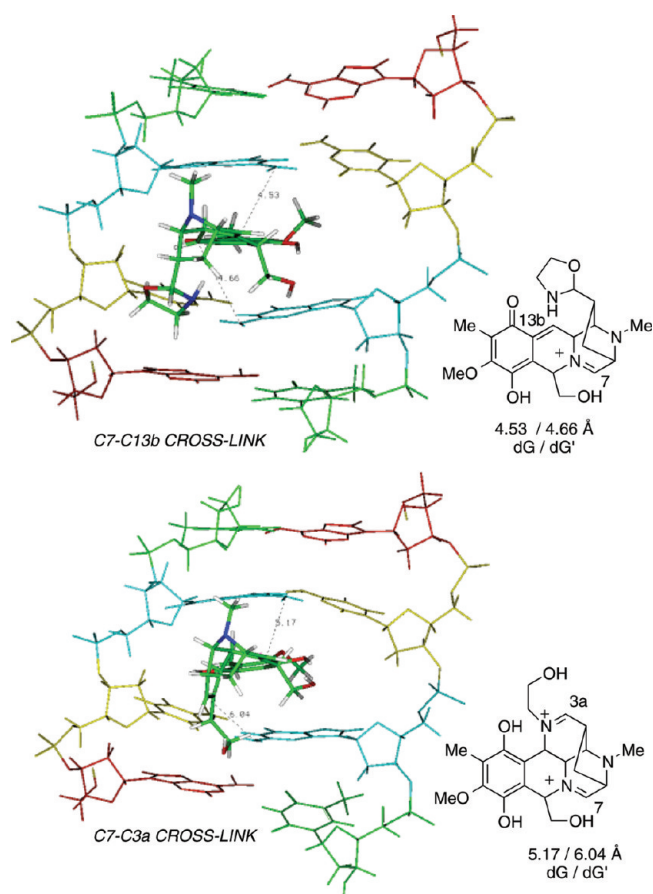
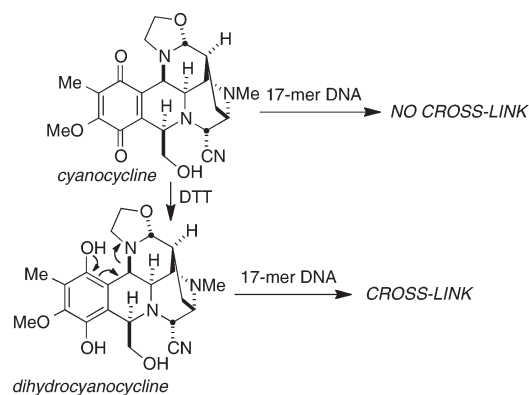


**Figure 12.** Molecular modeling of the two most reasonable modes for interstrand cross-link formation by bioxalomycin  $\alpha 2$ .

### Scheme 43. Cyanocycline Requires Reduction to Dihydrocyanocycline to Cross-Link DNA



sequencing technologies for genome mining. Results of this exciting phase of our work on the tetrahydroisoquinoline natural products will soon be made available and constitute a major new thrust in direction for our work in this field.

## V. TAXOL BIOSYNTHESIS

Chemists and biologists alike have been drawn to Taxol (paclitaxel) because of its promising spectrum of antineoplastic activity, its unique mechanism of action, and the synthetic

challenge that the complex and densely functionalized ring system poses.<sup>113</sup> Taxol was first isolated from the bark of the Pacific Yew, *Taxus brevifolia*.<sup>114</sup> Unfortunately, the Yew is slow-growing and is primarily found in environmentally sensitive areas of the Pacific Northwest, and stripping the tree of its bark kills the Yew. It takes three trees to obtain ~10 kg of bark from which 1 g of Taxol can be isolated.<sup>113c</sup> FDA approval of Taxol for the treatment of advanced ovarian cancer<sup>113a</sup> has created a severe supply and demand problem. Collection of renewable *Taxus* sp. needles and clippings has attenuated this problem somewhat, but as the drug has become more widely adopted, particularly for use earlier in the course of cancer intervention and for new therapeutic applications, pressure on the Yew population has continued to increase worldwide. Alternative means of Taxol production are therefore being vigorously pursued since cost and availability will continue to be significant issues.

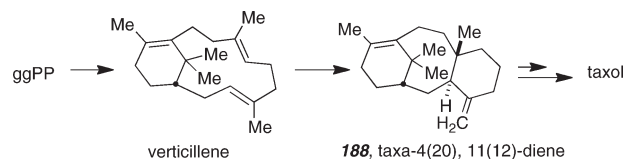
To date, totally synthetic methods have fallen short as an alternative source for Taxol production<sup>115</sup> because of the complex structure of Taxol that mandates lengthy and expensive synthetic routes. A method that has proven viable is the semisynthesis of Taxol from 10-deacetylbaccatin III that can be isolated from the needles, a renewable source, of the European Yew, *Taxus baccata*.<sup>113b,c</sup> The commercial supply of Taxol and semisynthetic precursors will have to increasingly rely on biological methods of production. This can be reasonably achieved by (1) extraction from intact *Taxus* plants, (2) *Taxus* cell culture,<sup>116</sup> or (3) microbial systems.<sup>117</sup> In order to produce large quantities of Taxol or a pharmacophoric equivalent by semisynthetic or, perhaps, by genetically engineered biosynthetic methods, it is essential to gain a better understanding of the detailed biosynthetic pathways<sup>116–118</sup> in *Taxus* sp.

In 1966, Lythgoe and co-workers proposed a biosynthetic pathway in which the tricyclic carbon framework of the taxoids was envisioned to arise by the sequential intramolecular cyclizations of the double bonds of geranylgeranyl pyrophosphate (ggPP) to 1(*S*)-verticillene and then to taxa-4(20),11(12)-diene (Scheme 44).<sup>119</sup>

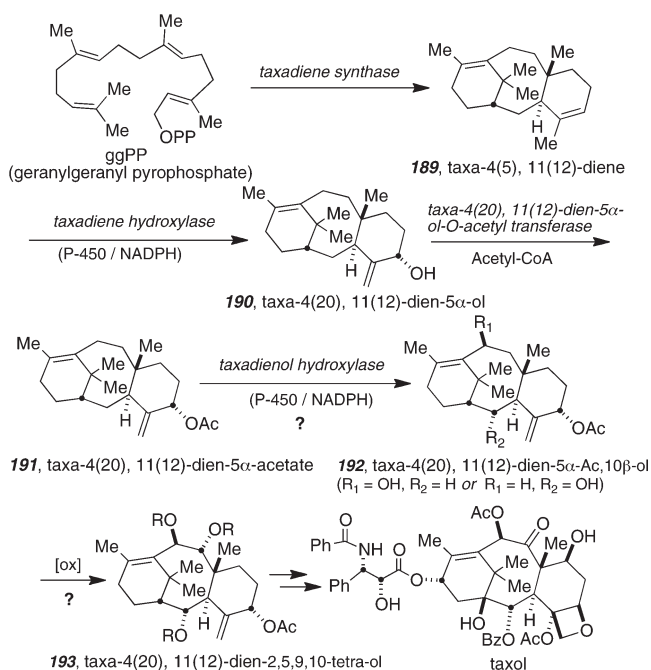
Our group, in collaboration with the Croteau laboratory (Washington State University), have demonstrated that the “Lythgoe taxadiene” is not the first committed intermediate on the taxoid biosynthetic pathway, but rather that taxa-4(5),11(12)-diene (**189**, Scheme 45) is the major metabolite.<sup>120–122</sup> This was demonstrated by a total synthesis<sup>122</sup> of both isomeric taxadienes and administration of synthetic <sup>13</sup>C-labeled taxa-4(20),11(12)-diene (**188**) to cell-free microsomes of *Taxus canadensis*.<sup>120c</sup> Crossover experiments and the lack of biotransformation of the Lythgoe diene (**188**) in *Taxus* microsomes had initially cast considerable doubt on the intermediacy of this substance in taxoid biosynthesis.<sup>121</sup> On the other hand, using ggPP as a substrate, taxa-4(5),11(12)-diene (**189**) has been shown to be the primary product of taxadiene synthase, an enzyme recently characterized, cloned, and functionally expressed by the Croteau laboratory.<sup>120</sup> However, we have since demonstrated that recombinant taxadiene synthase indeed produces ~5% of the Lythgoe diene (**188**) plus <1% percent of the corresponding 3,4-diene isomer.<sup>121</sup>

Mechanistic work completed in our laboratories on taxadiene synthase revealed a very unique mode of terpenoid cyclization (Scheme 46). Croteau has reported that the taxadiene synthase step is slow and possibly limiting in the net metabolic carbon flux to Taxol.<sup>120</sup> We have further established that the first hydroxylation product in the Taxol pathway is taxa-4(20),11(12)-dien-5 $\alpha$ -ol (**190**) through total synthesis and biosynthetic incorporation

#### Scheme 44. Early Biosynthetic Proposal from ggPP to Taxol



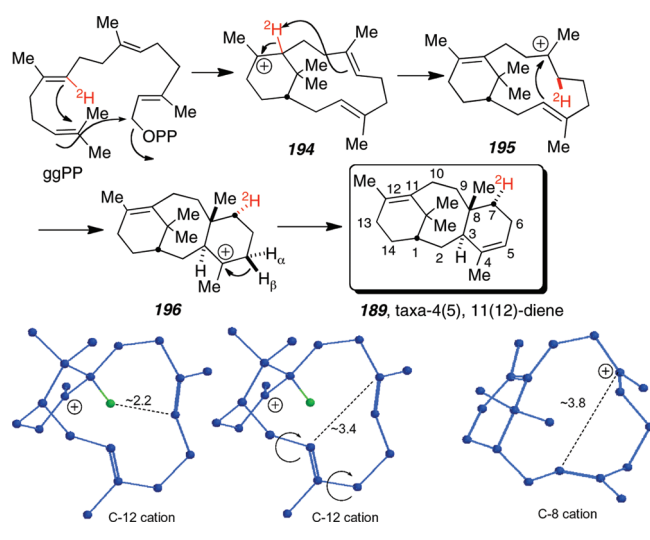
#### Scheme 45. Croteau–Williams Biogenesis of Taxol<sup>120–123</sup>



into Taxol, 10-deacetylbaccatin III, and cephalomannine in vivo in *Taxus brevifolia*.<sup>123</sup> Furthermore, a synthetic sample of taxa-4(20),11(12)-dien-5 $\alpha$ -acetate (**191**) has been used to establish that, following hydroxylation of **189** to **190**, the next step in the pathway appears to be acetylation of **190** to acetate **191**.<sup>124</sup> The Croteau laboratory has cloned and expressed taxa-4(20),11(12)-dien-5 $\alpha$ -ol-O-acetyl transferase from *Taxus canadensis* in *E. coli*.<sup>124</sup> Thus, the first three biosynthetic steps have now been established as shown in Scheme 45, and we have devoted considerable effort to elucidate the subsequent sequence of hydroxylations to the fully oxygenated Taxol core.

Because of the very low yield of natural taxadiene obtainable from biological sources (an extract from 750 kg of *Taxus brevifolia* bark powder yielded<sup>120a</sup> ~1 mg of 85% pure **189**) and the remaining uncertainty as to the sequence of hydroxylation reactions to taxoids,<sup>120,123</sup> synthetic access to these isotopically labeled tricyclic diterpenes proved to be essential for several reasons: (1) synthesis provides access to stable- and/or radio-labeled substrates from which pathway metabolites can be made by microsomal and/or recombinant enzyme biotransformation, and (2) the synthetic metabolites facilitate the identification, isolation, and structure elucidation of new pathway metabolites that are produced biosynthetically in very tiny amounts. The second point was amply demonstrated by our synthesis of taxa-4(20),11(12)-dien-5 $\alpha$ -ol (**190**), which preceded the identification and isolation of this substance from *Taxus brevifolia*.<sup>123</sup>



Scheme 46. Mechanism of Taxadiene Synthase<sup>120,121</sup>

Indeed, the identification of this substance as a biosynthetic intermediate would have proven far more difficult if the synthetic reference sample were not available. The first point has also been amply demonstrated, as described below, since synthetic, tritium-labeled **190** and the corresponding acetate **191** have served as the *exclusive* substrates from which the intermediate hydroxylation products (diol, triol, tetraol, and pentaol) have been produced biosynthetically. It should also be noted that Taxol has now been identified in several strains of microorganisms,<sup>117</sup> and our laboratory has provided samples of stable- and radioisotopically labeled taxadienes to numerous other laboratories interested in identifying pathway intermediates to taxoids.

Since ggPP serves as a starting material for many other biosynthetic pathways,<sup>125</sup> any number of the steps may be rate-limiting in the secondary metabolic flux to Taxol. Total synthesis as well as semisynthesis technologies have enabled us to prepare many probe substrates, as well as numerous putative biosynthetic intermediates that are produced in either cell culture or in *Taxus* sp. stems in amounts too small to isolate and determine the structure of such substances. Access to synthetic, authentic materials has proven absolutely key to penetrating the complex biosynthetic matrix of taxoid metabolism. We have used these synthetic probe substrates to elucidate several fundamentally novel enzymatic reactions, such as the taxadiene synthase-catalyzed cyclization of ggPP to taxadiene (**189**) and the cytochrome P450-mediated oxidation of taxadiene (**189**) to taxadienol (**190**).<sup>123</sup> While much remains unknown, detailed here is a synopsis of the most exciting findings.

**Mechanism of Taxadiene Synthase.** In collaboration with the Croteau laboratory, the Coates laboratory (University of Illinois), and the Floss laboratory (University of Washington), we have determined the fascinating mechanism of the “one-step” cyclization of ggPP to taxa-4(5),11(12)-diene (**189**) as shown in Scheme 46.<sup>120</sup>

Our group has focused on the stereochemistry and mechanistic implications of the unprecedented migration of the C11 hydrogen atom to C7.<sup>121</sup> The Floss laboratory synthesized the requisite deuterated ggPP substrate (shown, Scheme 46), and this substrate was converted into taxadiene via soluble recombinant synthase from *Taxus cuspidata*. We observed >90% retention of deuterium at C7. Our laboratory elucidated the

stereochemistry of the deuterium migration by 2D NMR and 1D TOCSY and unambiguously established that the deuterium atom migrates to the  $\alpha$ -face of C-7. The observation that the deuterium transfer from C11 to C7 occurs with such a high degree of isotopic retention, coupled with the exclusive transfer to the  $\alpha$ -face of C7, suggests that the mechanism for the transfer of the deuterium from C11 to C7 occurs *intramolecularly*. We are aware of no precedent for such an intramolecular proton transfer during an olefin-cation cyclization reaction, and thus the mechanism of taxadiene synthase is strikingly unique in this regard.<sup>121</sup>

Of further interest is the facial bias of the final C8/C3 olefin-cation cyclization. Considering the known relative stereochemistry of the taxoid B/C ring juncture, the C3/C4  $\pi$ -system *must* attack the putative C8 cation formed immediately following the C11/C7 proton migration from the *same face* to which the newly installed proton at C7 migrated. Molecular modeling of this process, which formally involves a criss-cross of bond formation across the C7/C8  $\pi$ -system, proved quite insightful. The molecular model of the C8 cation suggests that, upon pyramidalization at C7 and fashioning of the C11/C12 olefin, the conformation of the 12-membered ring twists, relative to that of the C12 cation, rocking the C3/C4  $\pi$ -system into the correct facial orientation for capture of the C8 cation establishing the *trans*-fused B/C ring juncture.

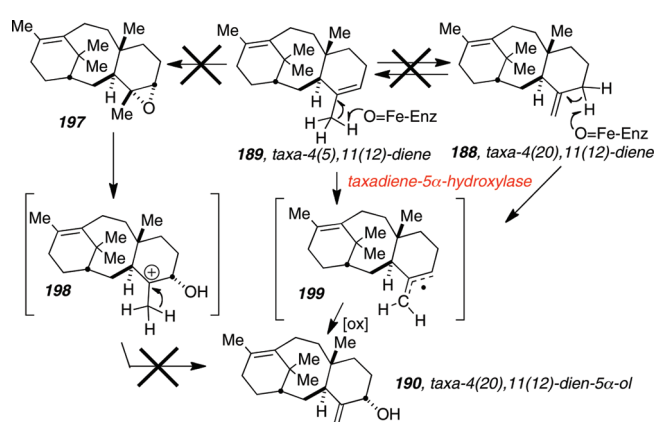
#### Elucidation of the Mechanism of Taxadiene Hydroxylase.

This experiment was designed to discern if the cytochrome P450 hydroxylation of taxa-4(5),11(12)-diene (**189**) to taxa-4(20),11(12)-dien-5 $\alpha$ -ol (**190**) proceeds through an epoxide intermediate or an allylic radical species. We have examined the interesting mechanistic question regarding the cytochrome P450 conversion of taxa-4(5),11(12)-diene into taxa-4(20),11(12)-dien-5 $\alpha$ -ol with allylic transposition.<sup>126</sup> No isomerization of taxa-4(5),11(12)-diene (**189**) to the 4(20),11(12)-diene isomer (**188**) (or vice versa) was observed in *Taxus* sp. microsomes (or *Spodoptera* microsomes enriched in the recombinant 5 $\alpha$ -hydroxylase) under standard assay conditions. Similarly, no interconversion of either positional isomer was observed in the presence of Mg<sup>2+</sup>, NAD<sup>+</sup>, NADH, NADP<sup>+</sup>, or flavin cofactors at pH values from 4 to 10. From these studies, we concluded that taxa-4(5),11(12)-diene (**189**) is not appreciably isomerized to taxa-4(20),11(12)-diene (**188**) under physiological conditions and that the migration of the double bond from the 4(5)- to the 4(20)-position in the process of taxadienol formation is an inherent feature of the cytochrome P450 oxygenase reaction with taxa-4(5),11(12)-diene (**189**) as substrate. It follows that taxa-4(20),11(12)-diene (**188**) is but a minor natural product of *Taxus* sp. formed by taxadiene synthase that is an adventitious, yet efficient, substrate for the 5 $\alpha$ -hydroxylase.

Previous efforts to evaluate the 5 $\alpha$ -hydroxylation reaction by the native enzyme, by a search for an epoxide intermediate and through the use of [20-<sup>2</sup>H<sub>3</sub>]taxa-4(5),11(2)-diene to examine a kinetic isotope effect (KIE) on the deprotonation step, failed to distinguish between two reasonable mechanistic possibilities.<sup>123a</sup>

The two mechanistic manifolds that were considered involve (1) preliminary conversion of the 4(5)-double bond of taxa-4(5),11(12)-diene (**189**) to the corresponding 4(5)-epoxide (**197**), followed by ring-opening to carbenium ion species **198** and elimination of a proton from the C20 methyl group to yield the allylic alcohol product (**190**), and (2) an alternate route involving cytochrome P450-mediated abstraction of hydrogen from the C20 methyl of the substrate (**189**) to yield the allylic radical (**199**), to which oxygen is added at C5 yielding **190** (Scheme 47).



Scheme 47. Mechanism of Taxadiene Hydroxylase<sup>126</sup>

The utilization of the isomeric taxa-4(20),11(12)-diene (**188**) by the hydroxylase, with efficiency comparable to that of the natural epoxide (**197**) in the reaction cycle. These results instead suggest a mechanism involving abstraction of a hydrogen radical from C20 for **189** (or from C5 in the case of the 4(20)-isomer **188**), leading to the common intermediate, allylic radical **199**, followed by oxygen insertion selectively from the 5 $\alpha$ -face of this radical intermediate to accomplish the net oxidative rearrangement. It also appears that the somewhat tighter binding of the 4(20)-isomer substrate (**188**) may be a reflection that this isomer more closely mimics the allylic radical intermediate.<sup>126</sup>

The synthesis of the lightly oxygenated taxoids has proven much more difficult than initially anticipated, and we have deployed both total synthesis technologies,<sup>122</sup> as well as semi-synthesis, from two major taxoid shunt metabolites: taxusin, which is oxygenated at C5, C9, C10, and C13, and a related taxoid, obtained from the Japanese Yew, that is oxygenated at C5, C9, C10, and C14 (Figure 13).<sup>127</sup> A few highlights of our initial total synthesis of taxadiene are shown in Scheme 48.<sup>122</sup> Access to these lightly oxygenated substrates has been extensively exploited in the selective removal and addition of oxygenation to the taxoid core. In several instances, the synthetic, authentic samples proved indispensable for the identification of these trace natural metabolites in Yew.

In collaboration with the Croteau laboratory, recent progress has included most notably the construction of transgenic *Taxus* cell lines, which are enabling an understanding of late pathway steps (C13-side chain assembly) and early pathway steps leading to taxane tetraol intermediates. Current work has focused on the functional characterization of taxoid oxygenases (all appear to be P450s), acyl transferases, and on the synthesis of labeled substrates for elucidating the remaining pathway steps. Of the nine presumptive taxane core oxygenases, the Croteau laboratory has cloned and characterized six of these P450s: the 2 $\alpha$ -<sup>128</sup> 5 $\alpha$ -<sup>126</sup> 7 $\beta$ -<sup>129</sup> 9 $\alpha$ -<sup>130</sup> 10 $\beta$ -<sup>131</sup> and 13 $\alpha$ -hydroxylases,<sup>132</sup> primarily by functional expression in yeast.<sup>133</sup> The remaining fourteen, functionally undefined cytochrome P450 clones from an induced *Taxus* cell cDNA library have been transferred to the baculovirus/insect cell expression system because of the instability of these recombinant enzymes in yeast microsomes, and eight of these were satisfactorily coexpressed with the *Taxus* P450 reductase for subsequent evaluation, which is an ongoing work.

What has become clear from these studies is that the midsection of the Taxol biosynthesis pathway is, in fact, not a "path" way at all.<sup>134</sup> Rather, there is a softening of substrate specificity among the P450 enzymes that are each designed to oxygenate the taxoid core at a specific position. The net result is that each oxygenated product can function as a substrate of altering efficiency for each P450, resulting in a complex matrix of oxygenated polyols, many of which find their way to baccatin III and Taxol. We believe that this may prove to be a general phenomenon among secondary metabolite biogenetic oxygenations, particularly where there are multiple oxygenases, such as exists in the Taxol system. We have further observed that metabolites which accumulate, such as taxusin, often turn out to be shunt metabolites, as they are not processed further by downstream modeling enzymes. It is easy to be fooled into looking at metabolite co-occurrence as a potential blueprint for a putative biosynthetic pathway. The real intermediate biosynthetic substrates are often produced in trace or undetectable amounts (and thus do not accumulate), requiring the engagement of synthetic chemistry to prepare and then test these substances for bioconversion. This project, as well as the prenylated indole alkaloid project discussed above, have firmly underscored the importance of total synthesis to access biosynthetic substrates which are, after all, natural products in their own right.

## VI. FR900482 AND MITOMYCIN C

Another natural product family in which we have become deeply interested is the FR900482-mitomycin family of antitumor drugs. FR900482 and FR66979 are natural products obtained from the fermentation harvest of *Streptomyces sandaensis* no. 6897 at the Fujisawa Pharmaceutical Co. in Japan.<sup>135–137</sup> FR900482, along with its derived triacetate FK973 and the O-methylated analog FK317, have been advanced into human clinical trials as potential chemotherapeutic agents for the treatment of a variety of solid malignancies. In preliminary mode of action studies carried out at Fujisawa Co., FK973 was demonstrated to effect the formation of DNA interstrand cross-links and DNA–protein cross-links in L1210 cells.<sup>136</sup> In contrast to MMC,<sup>138</sup> FK973 does not cause oxidative single strand scission of DNA. Furthermore, FK973 was found to be significantly less toxic than mitomycin C and is approximately threefold more potent.<sup>139</sup> Of significant interest is the finding that both FK973 and FR900482 are active against multidrug-resistant P388 cells.<sup>136a,c</sup> In initial phase I clinical trials, patients treated with FK-973 exhibited vascular leak syndrome (VLS), and this substance was subsequently withdrawn from clinical development.<sup>137</sup> VLS is characterized by an increase in vascular permeability that leads to increased leakage of fluids into interstitial spaces, resulting in peripheral edema and ultimately organ failure.<sup>140</sup> Additional VLS symptoms include weight gain, hypoalbuminemia, pleural, and pericardial infusion and pulmonary and cardiovascular failure. VLS has been linked to exposure to immunotoxins such as ricin A and to treatment with high concentrations of cytokines such as interleukin-2 (IL-2), as well as to various pathological conditions such as T-cell lymphoma, sepsis, trauma, and burns.<sup>140</sup>

On the other hand, FK-317 has shown considerable promise to become a clinically important therapeutic alongside the structurally related and widely used antitumor drug mitomycin C (MMC).<sup>138</sup> Significantly, FK-317 was found not to induce vascular leak syndrome in patients and recently advanced from a very successful phase I trial to phase II human clinical trials.

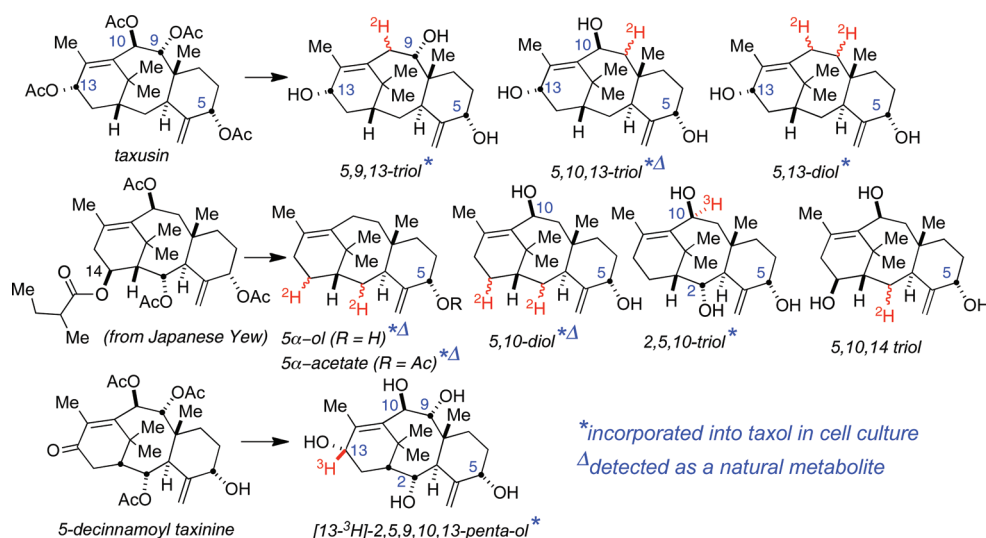
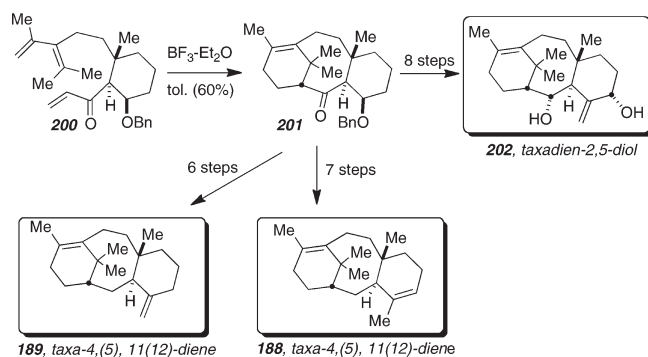


Figure 13. Semisynthesis of lightly oxygenated taxoids.

#### Scheme 48. IMDA-Based Synthesis of Taxadienes<sup>122</sup>



The structurally and mechanistically related antitumor drug MMC has been in clinical use for over thirty years, and as will be discussed, considerable overlap between the two families of drugs exists with some critical differences. It is well-established<sup>138,139</sup> that MMC is reductively activated by either a one-electron or two-electron pathway to provide the electrophilic mitosene (204) via the semiquinone radical anion (203, Scheme 49). MMC cross-links DNA (structure 206) preferentially at 5' CpG<sup>3'</sup> sites<sup>4</sup> and also mediates oxidative cleavage of DNA. The oxidative cleavage reaction is a manifestation of superoxide production by MMC resulting from the adventitious reduction of molecular oxygen by the semiquinone radical anion intermediates (203, 204 or 205); subsequent Haber–Weiss/Fenton cycling produces hydroxyl radical and related reactive oxidants capable of causing nonselective tissue damage. The relatively low host toxicity of FR900482, FK973, and FK317 in human clinical trials relative to MMC may be correlated to the incapacity of these (formerly Fujisawa or “FR”) drugs to cause indiscriminate oxidative damage to DNA and other healthy cellular constituents.

Like MMC, the FR drugs also require reductive activation both in vivo and in vitro. The FR drugs do not produce random single strand breaks in DNA, which is typically associated with redox cycling of reactive oxygen radical species. The low toxicity of the Fujisawa drugs relative to MMC may thus be a manifestation of differences in the chemical means by which the drugs are

activated. The Fujisawa drugs and MMC both share the ability to cross-link DNA (with the same 5' CpG<sup>3'</sup> sequence selectivity)<sup>138</sup> through the agency of a bioreductively generated mitosene. The major structural difference between MMC and FR900482 and congeners is the presence of the quinone moiety in MMC and the hydroxylamine hemiketal of the Fujisawa drugs.

In MMC, the quinone functionality is an obligate functional array for the reductive unmasking of the potent, bis-electrophilic mitosene (204). In the Fujisawa drugs, it has been unambiguously established that the reductively labile functionality is the N–O bond of the unique hydroxylamine hemiketal.<sup>141</sup> Given the potential clinical promise of the Fujisawa drugs, coupled with both their unusual structures and relationship to MMC, a great deal of effort has been directed toward the synthesis of these natural products.<sup>142</sup>

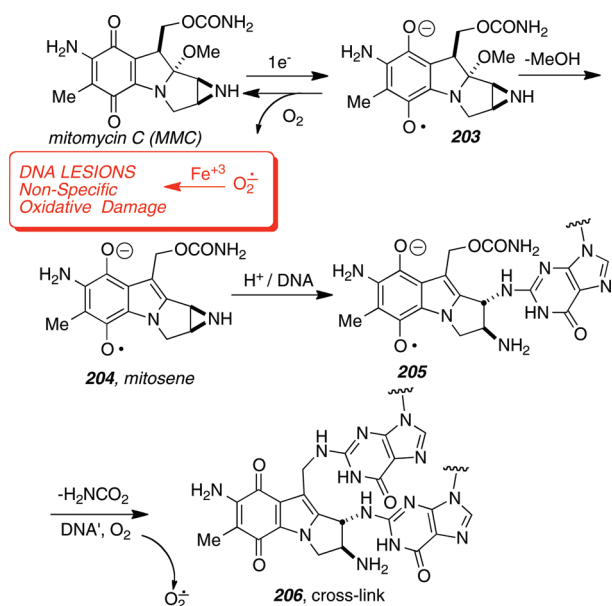
It has been demonstrated that FR900482 (and by analogy, FR66979, FK317, and FK973) undergo reductive activation in vitro to form the reactive mitosene derivative 209 (Scheme 50), which preferentially cross-links duplex DNA at 5' CpG<sup>3'</sup> steps.<sup>141</sup>

The mechanism of reductive activation, which has been examined by both our laboratory and the Hopkins laboratory, has been established to involve the thiol-mediated two-electron reduction of the N–O bond<sup>141</sup> in the presence of trace Fe(II) salts<sup>141</sup> generating the transient ketone 207, which rapidly cyclizes to the carbinolamines 208. Expulsion of water has been inferred as the rate-determining step en route to the electrophilic mitosene 209.<sup>141</sup>

It can thus be seen that FR900482, and MMC are actually naturally occurring clever “pro-drugs” that must be reductively activated in vivo to expose the highly reactive bis-electrophilic mitosene derivatives that are responsible for the biological activity displayed by these substances. We have sought to exploit the concept of latent triggering of mitosenes through the design and synthesis of new antitumor agents with improved selectivity and therapeutic potential based on the FR900482 structural array.

We have completed the asymmetric total synthesis of (+)-FR900482 and (+)-FR66979, as shown in Scheme 51.<sup>143</sup> This highly convergent synthesis has been accomplished in thirty-three steps from commercially available materials and constitutes one of the shortest syntheses of these drugs on record.

Scheme 49. Mechanism of Activation and DNA Interstrand Cross-Linking by Mitomycin C



We developed a novel, one-step method to construct the unique hydroxylamine hemiketal of these agents involving a dimethyl-dioxirane (DMDO)-mediated removal of the *N-p*-methoxybenzyl protecting group concomitant with hydroxylation of the aniline nitrogen atom, as shown in the conversion of **216** → **218**.

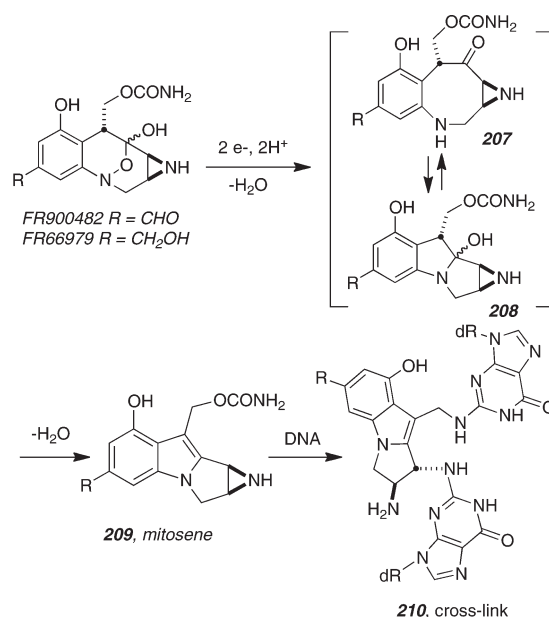
The aldol condensation of **215**, which yields a 1:1 mixture of diastereomers, fortuitously allowed epimerization of the undesired epimer to **216** without attendant dehydration. Synthetic (+)-FR66979 was obtained from **218** after protecting group removals and installation of the carbamoyl residues and LiBH<sub>4</sub> reduction; a final Swern oxidation reaction converts FR66979 into FR900482.

We have exploited the synthetic technology developed for FR900482 to construct the first biochemically functional mitosene progenitor that can be activated photochemically.<sup>64,65</sup> As shown in Scheme 52, acetylation of **214** (from Scheme 51) with the photolabile 6-nitroveratryl chloroformate (NVOC-Cl) (75%), followed by a similar series of steps to that used in the total synthesis of FR900482, gave the crystalline mitosene progenitor **219** (X-ray).

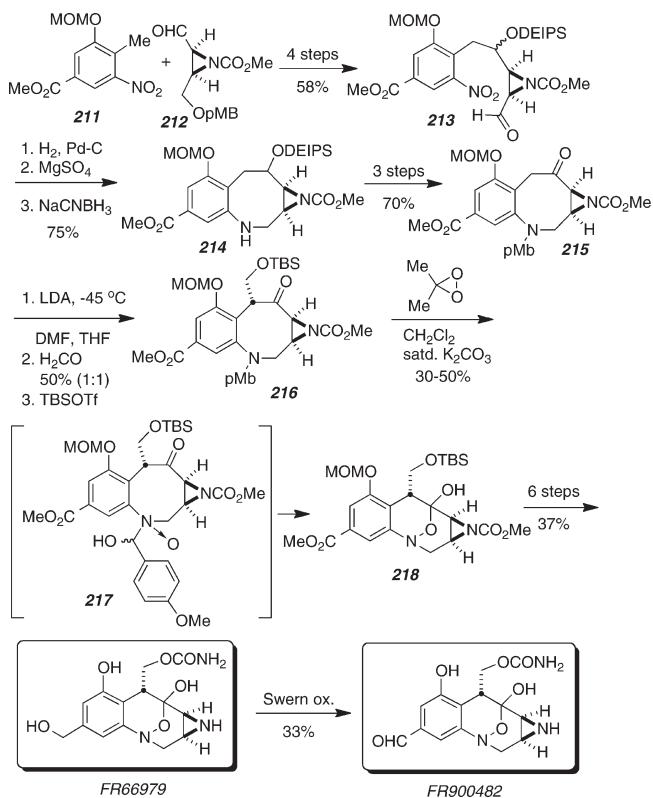
The capacity of **219** to cross-link DNA was initially evaluated using linearized pBR322 plasmid DNA by denaturing alkaline agarose gel electrophoresis and then, at high resolution, using a 5'-<sup>32</sup>P-labeled 33 bp oligonucleotide substrate. Footprint analysis of the cross-linked product revealed that **219** cross-links a synthetic DNA duplex at the identical 5' CpG<sup>3'</sup> step as that observed for FR900482. Corroboration of the footprinting data was secured by substitution of the 2'-deoxyguanosine base with 2'-deoxyinosine at the 5' CpG<sup>3'</sup> steps. Reactions with the 2'-deoxyinosine modified duplex resulted in no observable cross-link, while the use of the 2'-deoxy-7-deazaguanosine showed cross-links in the same manner as the unmodified 2'-deoxyguanosine-containing duplex. These results strongly implicate the N-2 exocyclic amine of 2'-deoxyguanosine as the site of alkylation in the same manner as the natural products.

Another manner in which we have exploited the creative invention that Nature has designed into FR900482 was through

Scheme 50. Mechanism of Reductive Activation of FR900482 and FR66979

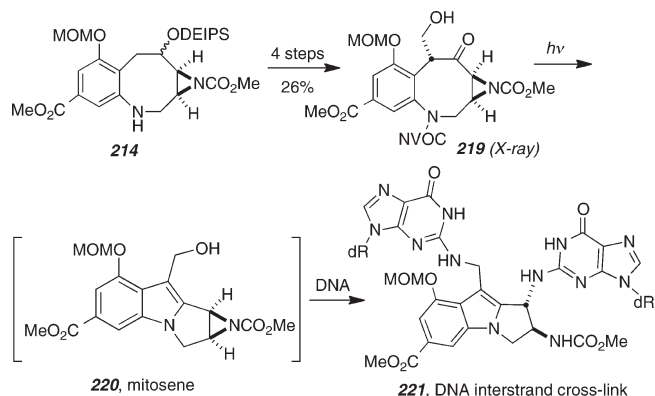


Scheme 51. Asymmetric Synthesis of FR66979 and FR900482



the semisynthetic installation of the hydroxylamine hemiketal functionality, which is unique to FR900482 and congeners, into a pyrrolizidine alkaloid framework. The pyrrolizidine alkaloids are a large family of primarily plant alkaloids that are typically



Scheme 52. Synthesis of a Photoactivated Pro-mitotense<sup>144</sup>

rendered toxic by oxidation via liver cytochrome P450 enzymes. We wondered if we could “borrow” the reductively activated hydroxylamine hemiketal from FR900482 and “insert” this into the pyrrolizidine alkaloid structural framework to create a hitherto unknown reductively activated pyrrolizidine alkaloid (Scheme 53).<sup>145</sup>

This was accomplished by the vonBraun-type ring-opening of commercially available monocrotaline, oxidation to the aldehyde, acetal protection, and oxidation of the secondary amine to the hydroxylamine with *m*-CPBA (Scheme 54).<sup>145</sup>

Removal of the acetal gave the tricyclic hydroxylamine hemiketal **228**, which constitutes the first reductively activated pyrrolizidine alkaloid. Treatment of this species with Fe(II)-EDTA resulted in the generation of the highly reactive and toxic species dehydromonocrotaline that mediated covalent cross-linking of DNA.

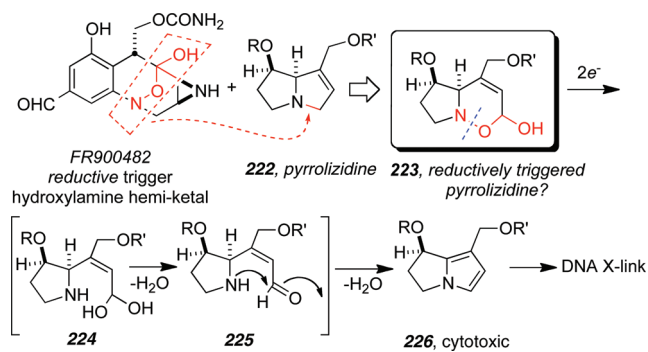
This same strategy was also deployed to make the first phototriggered dehydromonocrotaline progenitor (**230**, Scheme 55) by simply installing an *N*-VOC residue on the same ring-opened intermediate **227** used in Scheme 54. Photolytic removal of the *N*-VOC residue in the presence of duplex DNA resulted in multiple covalent cross-links.<sup>146</sup>

The synthetic chemistry developed for the total synthesis of FR900482 has borne multiple fruits and still holds vast untapped potential for further exploiting the fascinating chemical and biochemical reactivities packed into this small, heterocyclic natural product. We are continuing to refine and develop this chemistry for the preparation of biochemical and biological tools to study the interactions of these drugs in the context of chromatin.

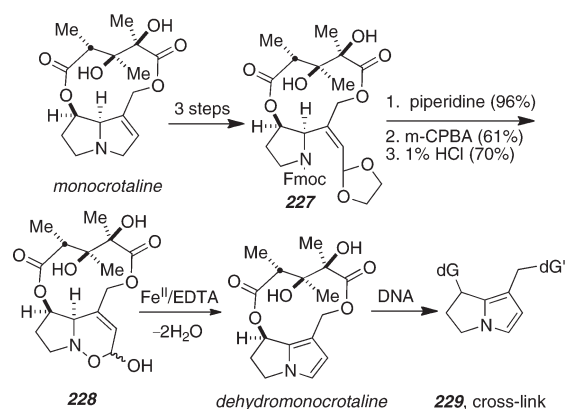
In collaboration with Karolin Luger’s laboratory, we used the synthetic photochemically activated derivative of FR400482 (compound **219**) to investigate the molecular mechanism of this class of drugs in a biologically relevant context.<sup>147</sup> We found that the organization of DNA into nucleosomes effectively protects the DNA against drug-mediated interstrand cross-linking while permitting monoalkylation. This monoalkylated, nucleosomal DNA has the potential to form covalent cross-links between chromatin and nuclear proteins. Using *in vitro* techniques, we observed that interstrand cross-linking of free DNA results in a significant decrease in basal and activated transcription. In addition, we found that covalently cross-linked plasmid DNA by the photoactivated FR900482 analog is inefficiently assembled into chromatin.

**Cross-Linking of FR900482 to HMG-A1.** In collaboration with Prof. Raymond Reeves’ laboratory at Washington State

## Scheme 53. Design of a “Chimeric” FR900482-Pyrrolizidine Alkaloid Hybrid



## Scheme 54. Synthesis and Activation of a Reductively Activated Pyrrolizidine Alkaloid



University, we have discovered that FR900482 covalently cross-links the high-mobility group-A1 (HMG-A1) oncoproteins to chromosomal DNA in Jurkat cells.<sup>148</sup> The basic strategy we have deployed is shown in Figure 14 and involved treatment of Jurkat cells that overexpress the HMG-A1 oncoproteins with sublethal concentrations of FR900482 (typically  $<1 \mu\text{M}$ ). Using a modified chromatin immunoprecipitation (ChIP) procedure, fragments of DNA that have been covalently cross-linked by FR900482 to HMG-A1 proteins *in vivo* were PCR-amplified, isolated, and characterized. The nuclear samples from control cells were devoid of DNA fragments, whereas the nuclear samples from cells treated with FR900482 contained DNA fragments which were cross-linked by the drug to the minor groove-binding HMG-A1 proteins *in vivo*.

Additional control experiments established that the drug also cross-linked other nononcogenic minor groove-binding proteins (HMG-B1 and HMG-B2) but does not cross-link major groove-binding proteins (i.e., Elf-1 and NFkB) *in vivo*. These results constituted the first demonstration that FR900482 cross-links a number of minor groove-binding proteins *in vivo* and suggests that the cross-linking of the HMG-A1 oncoproteins to chromosomal DNA may significantly participate in the mode of efficacy of FR900482 as a chemotherapeutic agent. *The ability of this class of compounds to cross-link the HMG-A1 proteins in the minor groove of DNA represents the first demonstration of drug-induced cross-linking of a specific cancer-related protein to DNA in living cells.* The capacity of FR900482 to cross-link the HMG-A1 oncoprotein with nuclear DNA *in vivo* potentially represents a significant



## Scheme 55. First Photolabile Progenitor of Dehydromonocrotaline

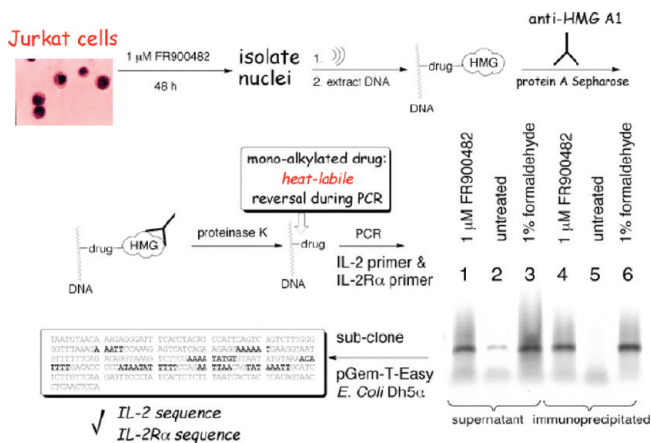
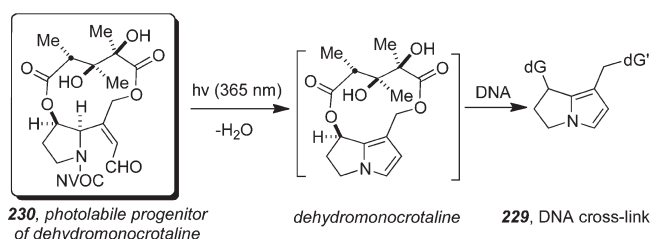


Figure 14. ChIP assay used to demonstrate the cross-linking of FR900482 to HMG-A1 bound to chromosomal DNA in Jurkat cells.

elucidation of the antitumor efficacy of this family of anticancer agents.

**Elucidation of the Mechanistic Basis for the Induction of Vascular Leak Syndrome by FR900482.** In a second study, we have obtained chromatin immunoprecipitation (ChIP) data showing that the two drugs FK317 and FR900482 differ markedly in the manner in which they induce cell death.<sup>148</sup> Four different diagnostic procedures, including flow cytometric analyses employing Annexin-V staining and caspase activation assays, demonstrated that *whereas FR900482 induces necrosis, FK317 induces an unusual necrosis-to-apoptosis switch that is drug concentration dependent*: at low doses FK317 induces necrosis and at higher concentrations it induces apoptosis (Figure 15). Northern blot analyses of drug-treated cells suggest that this “switch” is mediated, at least in part, by modulation of the expression levels of the gene coding for the antiapoptosis protein Bcl-2. Additional support for this idea comes from the observation that FR900482, in contrast to FK317, induces the expression of proteins such as IL-2 and IL-2R $\alpha$  which are known elicitors of both Bcl-2 gene expression and VLS.

**FK317 versus FR900482: Mode of Cell Death.** We have thus discovered very significant differences in the mode of cell death induced by the two closely related antitumor agents FR900482 and FK317. There seemed to be a mysterious paradox with respect to why FR900482 led to the expression of vascular leak syndrome (VLS) in patients, whereas FK317 treatments are devoid of this seriously deleterious side effect. Indeed, the termination of human clinical trials for FR900482 was a direct consequence of VLS. *Very surprisingly, FK317 does not induce VLS, and as a consequence, FK317 advanced from phase I to*

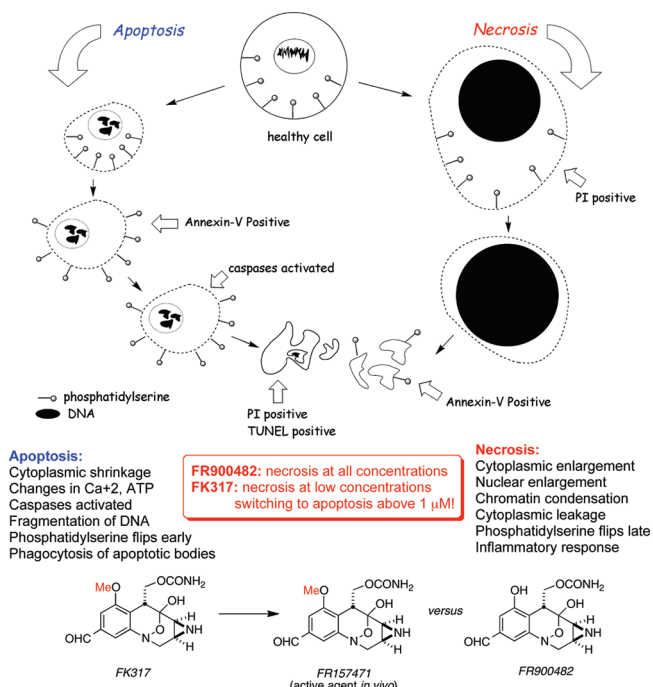
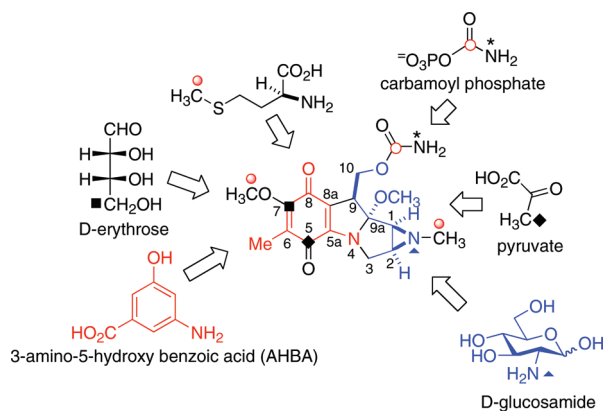


Figure 15. Apoptotic versus necrotic cell death mediated by FR900482 and FK317.

phase II human clinical trials. In an effort to elucidate the underlying cellular mechanisms of FR900482 and FK317 with respect to VLS, we have examined the differential expression of IL-2, a cytokine well-known to be a causative agent in VLS, in cells treated with FK317 and FR900482. Our findings are summarized below:

- (1) Both IL-2 and IL-2R $\alpha$  are overexpressed in cells, as evidenced by Northern blot and Western blot analysis. Overexpression of IL-2 is known to be the causative agent in the induction of VLS.
- (2) The antiapoptosis gene Bcl-2 is overexpressed in cells treated with FR900482 at all concentrations tested (Northern Blot analysis). This succinctly explains why FR900482-treated cells die by necrosis instead of apoptosis.
- (3) Cells treated with FR900482 display cellular characteristics of necrotic cell death at all concentrations tested.
- (4) Cells treated with FK317 display IL-2 and IL-2R $\alpha$  expression at levels of healthy, untreated cells (Northern and Western blot analysis). This clearly explains why patients treated with FK317 do not display VLS. We believe that this is a very significant finding that should be of general use in the preclinical evaluation of all antitumor drugs and should provide a simple preclinical expression profile of antitumor drugs headed for clinical trials that could potentially save enormous amounts of money on drugs doomed for failure through induction of VLS.
- (5) Cells treated with FK317 display Bcl-2 expression levels that are slightly upregulated at  $\sim 1$  mM, but Bcl-2 expression is significantly down-regulated at concentrations greater than 1 mM (Northern blot analysis). *This exciting finding reveals that FK317 is capable of inducing a rare concentration-dependent necrosis to apoptotic switch.*

The molecular and mechanistic bases of these striking differences between FR900482 and FK317 are at present unknown



**Figure 16.** Radiolabeled precursor incorporation studies on the mitomycins.

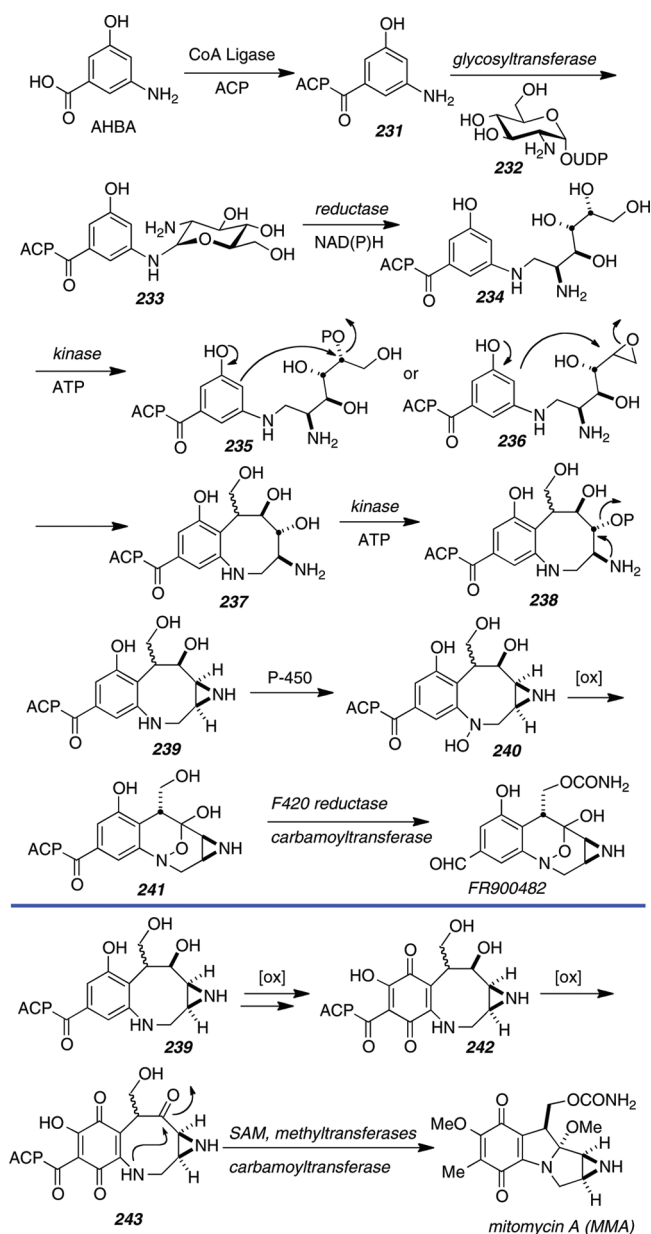
and rendered all the more puzzling by the fact that both drugs mediate covalent adduction of the HMG-A1 protein on the *same* IL-2 and IL-2R $\alpha$  genes. It has been established that FK317 is metabolized *in vivo* to give the active agent FR157471. Therefore, the only structural difference between FR900482 and FK317 is the phenolic *O*-methyl residue in FK317 versus the hydroxyl residue in FR900482. The fact that such a small difference in structure can have such profound effects on the cell biology of these agents remains striking and demands an explanation. Elucidation of the structural and mechanistic reasons for these highly unexpected observations will be fascinating to unravel.

**Biosynthesis of FR900482 and MMC.** In a new direction for this program, we have established a collaboration with Prof. David Sherman's laboratory at the University of Michigan to elucidate the biosynthesis of FR900482 and MMC, which are close biogenetic cousins. We have also harnessed the synthetic chemistry we have developed for the total synthesis of FR900482 and MMC to prepare isotopomers of certain putative biosynthetic intermediates, thereby obtaining structural and mechanistic information on the biosynthesis of these closely structurally related antibiotics. The biosynthesis of these agents is poorly understood, and we have embarked on a multidisciplinary approach to elucidating a number of fascinating details of the respective biosynthetic pathways.

Through precursor labeling and feeding experiments done primarily in the 1970s, the basic biosynthetic constituents of MMC were elucidated and are summarized in Figure 16. The primary building blocks are erythrose, AHBA, D-glucosamine, pyruvate, carbamoyl phosphate, and methionine.

Recently, the biosynthesis of MMC and FR900482 has been more deeply investigated by the Sherman laboratory.<sup>149</sup> These studies have led to the identification, cloning, and sequencing of the biosynthetic gene cluster in *Streptomyces sandaensis* (FR900482) and *Streptomyces lavendulae* (MMC) by the Sherman laboratory.<sup>149</sup> The FR900482 biosynthetic gene cluster (the *frb/fbc* gene cluster) consists of 49 FR900482 biosynthetic genes spanning 56-kb of contiguous DNA.<sup>25</sup> The functions of the gene-encoded protein products involved in the biosynthesis of MMC (and, by homology, FR900482) include the assembly of the primary biosynthetic precursors, dihydrobenzoxazine structure formation, tailoring functionality (i.e., hydroxylation, carbamylation, and carbonyl reduction), plus resistance and export of the drugs. A unified biogenesis for the elaboration of FR900482 and MMC is shown in Scheme 56.

**Scheme 56.** Proposed Unified Biogenesis of FR900482 and MMC



Based primarily on precursor structure and metabolite co-occurrence, the biosynthetic proposal shown in Scheme 56 has been formulated by Sherman and recently modified by our group.<sup>150</sup> First, AHBA is loaded onto an acyl carrier protein via a CoA ligase (*Frbd* or *MitE*). A glycosyl transferase connects the amino group of AHBA to the anomeric center of D-glucosamine (*mitB*).

Several steps are particularly interesting to us and have implications regarding the genetic overlap between the two families of natural products. For instance, the relative stereochemistry of the aziridine ring (C1/C2) and the carbamoyl-containing hydroxymethyl residue (C9, MMC numbering) is *anti*- in FR900482 and *syn*- in MMC. Of additional note is that within the mitomycin family, MMC, MMA, MMF, and porfirmycin possess the *anti* relative stereochemistry, whereas MMB and MMD have the *syn* relative stereochemistry. Thus, formation

of the aryl C8a–C9 bond either occurs via distinct genetically encoded pathways and intermediates or the C9 stereogenic center is subject to epimerization, resulting in both diastereomeric relationships. Sherman initially suggested that this bond formation might occur through an intramolecular Friedel–Crafts type of alkylation from a phosphorylated intermediate such as **235**, and we have subsequently suggested that the corresponding epoxide species **236** may also be subject to Payne rearrangement prior to cyclization to an eight-membered ring core. The potential Payne rearrangement would thus provide a third mechanistic possibility for the divergence to the C1/C9 *syn* and *anti* stereochemistries.

A second issue of intrigue concerns the modeling of the hydroxylamine hemiketal in FR9004882 versus the quinone-containing *S/S*-carbinolamine system of the mitomycins. Is there a common, late-stage intermediate that is diverted by distinct oxidases in each biosynthetic system? Or do the two biosynthetic pathways diverge at a much earlier stage?

Finally, because of the intrinsic lability of the eight-membered ketone-containing substrates to form mitosene intermediates, this strongly suggests that oxidation of the C9a secondary alcohol to the corresponding ketone must occur *after* the formation of the quinone (for MMC, see **239** → **242** → **243**) and hydroxylamine (for FR900482, see **239** → **240** → **241**). While many other possible pathways and intermediates might be envisioned, including alternative sequencing of the transformations postulated in Scheme 56, our approach to unravel these pathways will begin with the synthesis, labeling, and incorporation studies of some reasonable early- and late-stage intermediates from which we hope to narrow and ultimately completely define the two pathways.

## VII. HDAC INHIBITORS

The most recent area that has attracted our attention concerns the relatively recent discovery of several macrocyclic natural products that potently inhibit histone deacetylase enzymes. Histone deacetylases (HDACs) are enzymes involved in the epigenetic regulation of gene expression. The discovery of the first human histone deacetylase protein derived from studies of a natural product, trapoxin, which conferred a differentiation phenotype upon cultured cancer cells. Using ligand affinity chromatography and protein biochemistry, the laboratory of Stuart Schreiber at Harvard University discovered HDAC1 and HDAC2.<sup>151</sup> Subsequent efforts in the Schreiber laboratory discovered additional related deacetylases, HDAC4, HDAC5, and HDAC6.<sup>152</sup> To date, eighteen HDACs have been identified, which are generally divided into four classes, based on sequence homology to yeast counterparts. It has been widely recognized that HDACs are promising targets for therapeutic interventions intended to reverse aberrant epigenetic states associated with cancer.<sup>153,154</sup> In addition, experimental evidence identifies a plausible therapeutic benefit for patients with nonmalignant diseases, such as inflammatory/autoimmune illness (e.g., psoriasis,<sup>155</sup> rheumatoid arthritis<sup>156</sup>), genetic conditions (e.g., sickle cell anemia,<sup>157</sup> spinal muscle atrophy<sup>158</sup>), and neurodegenerative diseases (e.g., Huntington's disease<sup>159</sup>). However, the genotoxicity of HDAC inhibitors observed in preclinical studies has limited their promise beyond cancer, highlighting the pressing need for highly selective, pharmaceutically tractable agents. Within cancer research, a number of HDAC inhibitors have progressed rapidly through clinical trials.<sup>160,161</sup> For example,

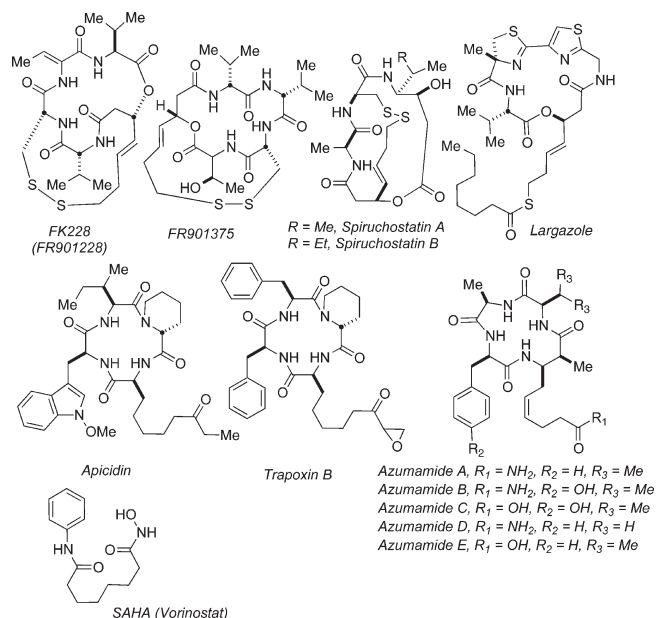


**Figure 17.** Structures of some known HDAC inhibitors.

suberoylanilide hydroxamic acid (SAHA, also known as vorinostat and marketed as Zolinza; Merck & Co., Inc.) was approved last year for the treatment of advanced cutaneous T-cell lymphoma. Approval was granted as part of the FDA orphan drug program, following a priority review. Depsipeptide (also known as FK228 or FR901228 and given the general name romidepsin; Gloucester Pharmaceuticals, Inc.) has also demonstrated potent antiproliferative effects at well-tolerated doses and has progressed well through clinical trials. However, during a phase II study, serious cardiac adverse events were observed, limiting enthusiasm for the agent and requiring a careful reconsideration of the structure–activity relationships and pharmacotoxicology.<sup>162,163</sup> Consequently, FK228 is in limited development in advanced cancers, such as relapsed, refractory multiple myeloma. A number of other cyclic peptides with structures analogous to that of FK228 have exhibited potent HDAC inhibitory activity, and some of these are also candidates in varying stages of clinical trials (Figure 17).<sup>164,165</sup>

We first became interested in the depsipeptide natural product FK228 and developed an improved synthesis of this drug, based on the pioneering work of Simon.<sup>166,167</sup> We were particularly interested if the depsipeptide played a functional role in the mode of binding to the class I HDACs, of which FK228 is a very potent and selective inhibitor.

During our work on the synthesis of a variety of FK228 analogues, Leusch et al. published the isolation and structure determination of the marine natural product largazole.<sup>168</sup> It became immediately apparent from an examination of the structure that largazole should also be an HDAC inhibitor, as it shares the same thiol-containing side chain that the known HDACi's FK228, FR901375, and spiruchostatin possess (Figure 17).

FK228 is a pro-drug that must be activated by reductive-opening of the disulfide linkage to expose the (*S*)-3-hydroxy-7-mercaptohept-4-enoate moiety, which coordinates tightly to the active site Zn<sup>2+</sup> atom of the class I HDACs (Figure 18). As this sulfhydryl residue is acylated in largazole, it seemed plausible to us that esterase or lipase-based removal of the octanoyl residue



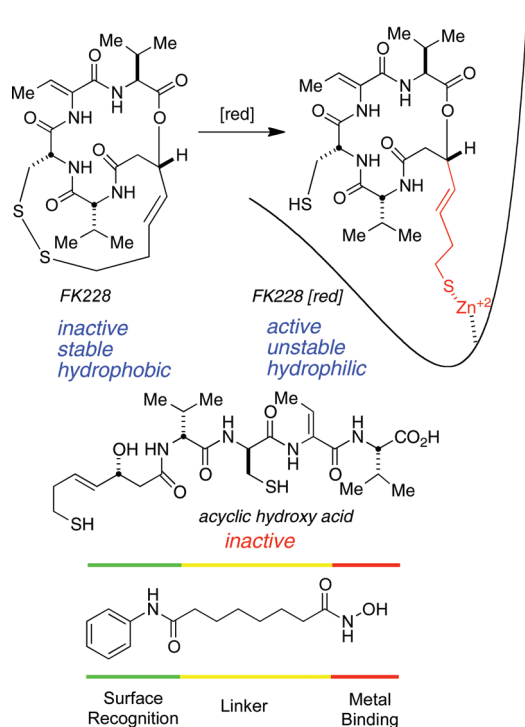
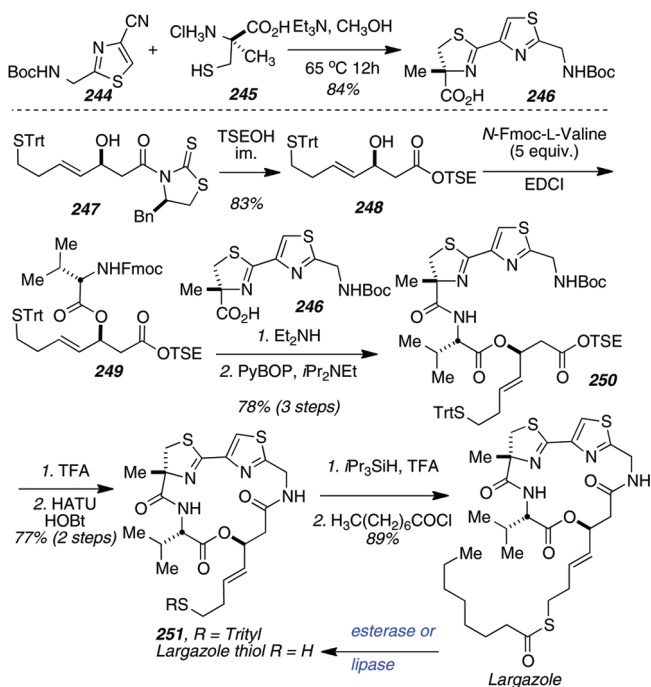


Figure 18. Mechanism of activation of FK228 and HDACi model.

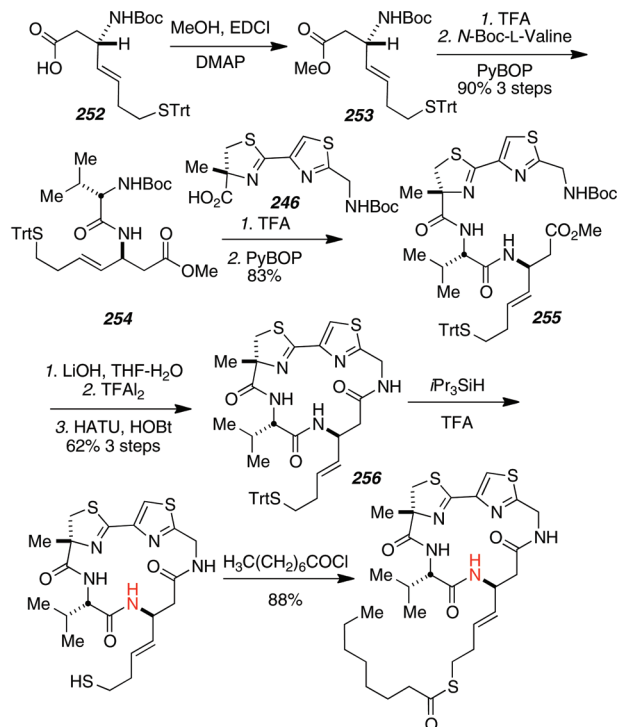
### Scheme 57. Total Synthesis of Largazole<sup>169</sup>



from largazole (a pro-drug) would give the active form of this species, the largazole thiol. This has been firmly validated by our laboratory and others.<sup>169,170</sup>

Most known HDACi's are composed of a cap group, responsible for surface recognition of the opening to the active site of the enzymes, a linker region, and a metal-binding functionality (see Figure 18 for SAHA). This three-component model

### Scheme 58. Synthesis of the Largazole Peptide Isostere



257, largazole peptide isostere thiol    258, largazole peptide isostere

renders the design and synthesis of new HDACi's an intellectually challenging and potentially highly rewarding endeavor.

Based on the rather difficult total synthesis of FK228 itself, as well as the commensurate challenges of synthesizing analogues of FK228, we turned our attention to largazole as a scaffold from which changes to the cap group, linker, and thiol-binding domain seemed more amenable. Largazole is conformationally more rigid than FK228 while also possessing a 16-membered depsipeptide macrocycle. While we recognize that the sum-total of these structural features should not be oversimplified in terms of manifestation of biochemical HDAC inhibitory activity and whole-cell biological activity, we suggest that the structural features of these natural products might be conceptualized (and chemically manipulated) as having major (but not exclusive) impacts on the following properties of these drugs:

- (1) The length (from the peptide backbone) and functionality in the zinc-binding arms are largely responsible for potency with respect to HDAC inhibition and contribute to HDAC isoform selectivity.
- (2) The specific amino acid sequences and side-chain residues in the cap region impart further HDAC isoform selectivity.
- (3) The macrocycle size and conformational display of the scaffold are intimately associated with binding affinity (biochemical potency) and should be candidates for manipulation to achieve altered potency as well as isoform selectivity.

We quickly moved to develop a total synthesis of largazole that would be amenable to making deep-seated structural changes. Our synthesis, shown in Scheme 57, proved to be rapid and scalable and also provided an authentic specimen of largazole thiol, the presumptive active form of the drug.<sup>169</sup>

It was exciting to observe the amount of synthetic attention that largazole received, as eight independent total syntheses of



**Table 4.** HDAC Inhibitory Activity ( $IC_{50}$ ; nM)

compd	HDAC1	HDAC2	HDAC3	HDAC6
FK228	0.2	1	3	200
FK228 isostere	10	80	70	>3000
largazole thiol	0.1	0.8	1	40
largazole isostere thiol	0.9	4	4	1500
largazole isostere	>3000	>3000	>3000	>3000
SAHA	10	40	30	30

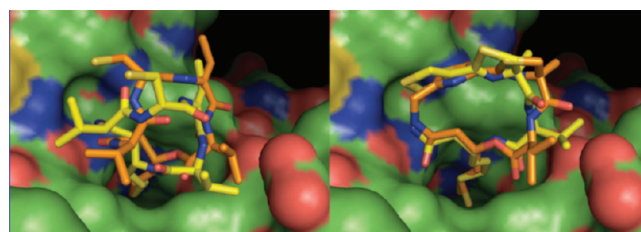
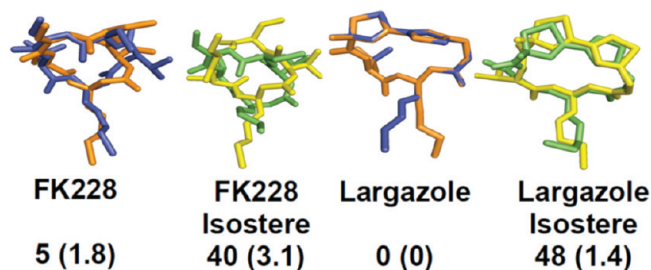
this natural product were reported in the literature within just a few months of the disclosure of the structure.<sup>169,170</sup> We next decided to prepare the peptide isostere of largazole, as it is well-known that depsipeptides are rapidly cleaved by serum esterases and might severely limit the bioavailability of the natural product as a potential drug candidate (Scheme 58). In conjunction with this study, we also endeavored to prepare the peptide isostere of FK228 by modifying our total synthesis of the depsipeptide natural product.<sup>171</sup> We were fortunate to establish a dynamic collaboration with Prof. James E. Bradner, Dana-Farber Cancer Research Institute, and Prof. Stuart L. Schreiber, Broad Institute of Harvard and MIT, to biochemically and biologically evaluate our synthetic compounds. As shown in Table 4, the HDAC inhibitory activities of synthetic FK228, the FK228 peptide isostere, largazole thiol, the largazole peptide isostere thiol, and the largazole peptide isostere were compared to SAHA.

A striking observation emerged from these experiments. Comparable potencies are observed between FK228 and largazole thiol, as expected. However, disparate potencies are observed between their respective peptide isosteres. As demonstrated in Table 4, the amide isostere of FK228 is a 50-fold less potent inhibitor of HDAC1 than is the natural product.

The peptide isostere of largazole thiol (257) is, indeed, modestly reduced in potency against HDAC1 compared to the natural product, but only by ninefold. The trend of increased potency for the largazole peptide isostere thiol versus the FK228 peptide isostere was preserved across all human class I HDACs tested (Table 4). We decided to deploy computational methods to study the effects of isostere replacement and model the disparate observed target potencies. We were fortunate to engage Prof. Olaf Wiest, of the University of Notre Dame, to analyze the lowest energy unbound and protein-bound conformations of the four thiol derivatives by employing Monte Carlo methods.

The preferred coordination modes of the four analyzed structures are shown in Figure 19. The thiol extends toward the zinc ion at the bottom of the entrance channel with a Zn–S distance of  $\sim 2.5$  Å, while the macrocycle sits on the mouth of the pocket. The hydrocarbon chain fills the hydrophobic channel lined by Phe150 and Phe205. The orientation of the macrocycle is similar in the ester and the amide isostere, maximizing lipophilic interactions with cap residues.

Analysis of the structures and energetics of the conformational space of the four compounds revealed an interesting conformation–activity relationship. Superimposed in Figure 20 are the binding conformations (orange for FK228 and largazole, yellow for amide isosteres) and the global minimum conformation (blue for depsipeptides and green for amide isosteres), as well as the relative energies (in kJ/mol) and rms values for higher energy conformations of the four compounds under study. For FK228, the optimum binding geometry is only 5 kJ/mol above the global minimum conformation, which is

**Figure 19.** Coordination mode of FK228 (left) and largazole thiol (right) to the HDAC1 active site. Depsipeptides are shown in orange, and amide isosteres are shown in yellow.**Figure 20.** Superimposed lowest and binding conformations of FK228 and largazole as well as their peptide isosteres.

within an rms of 1.8 Å and therefore structurally similar. In contrast, the amide isostere is much more rigid, and the preferred geometry for binding is not only much higher in energy (40 kJ/mol) than the lowest energy conformation, but with an rms of 3.11 Å also structurally very different. There are no conformations that are energetically accessible and that resemble the bound conformation. Binding of the amide isostere of FK228 will therefore involve a significant distortion of the protein surface and/or loss of binding interactions, leading to the experimentally observed loss of activity.

For largazole thiol, the lowest energy conformation is also the preferred binding conformation. Although the optimum binding geometry for the largazole isostere is 48 kJ/mol higher in energy than the most stable conformation, the geometries are within an rms of 1.41 Å and thus very similar, as seen on the top right of Figure 20. As a result, the conformational change of the protein required to bind the low energy conformation of the macrocycle cap is relatively small, and much of the binding interaction will be maintained even if the low-energy conformation is bound. The effect of the isostere substitution in the largazole macrocycle is predicted to be smaller than in FK228 and in agreement with the experimental results. This was exploited for the design of improved binders with predicted, and subsequently confirmed, picomolar activity.<sup>172</sup>

With Prof. Wiest's molecular modeling as our design guide, we have endeavored to begin what might prove to be a long and interesting journey of harnessing the synthetic chemistry platform originally deployed to make the natural product for the preparation of isoform-selective HDACi's. We are particularly interested in achieving isoform selectivity within the class I HDACs, as there are no known agents that currently discriminate between these enzymes. To date, we have made numerous deep-seated structural changes to the largazole framework, and a few of the many synthetic analogues we have prepared are displayed in Figure 21. We are tackling alterations to the cap group, with the objective of exploiting differences of surface amino acid residues

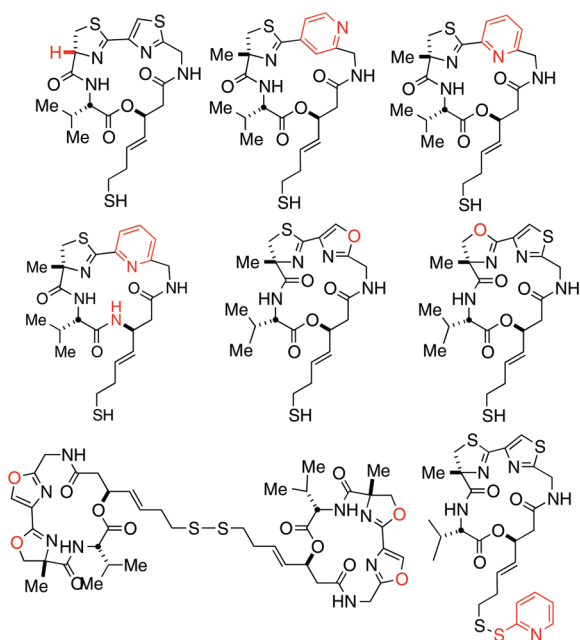


**Figure 21.** Sampling of synthetic largazole analogs that displayed potent Class I HDACi activity.

among HDACs 1–3 that might impart isoform selectivity. We are also examining alternative zinc-binding functionality, as well as making changes to the linking chain of atoms between the macrocycle and the zinc-binding residue. Finally, disulfide (activated by reduction) and other masked forms of the zinc-binding sulfhydryl residue are on our drawing board of synthetic targets.

## CONCLUSION

In this Perspective, the objective was to illustrate how the concepts, strategies, and development of practical tools for total syntheses have been extensively applied in our laboratory to interrogate interesting biomechanistic and/or biosynthetic aspects of complex, biologically relevant natural products. Our laboratory has been fortunate to have been able to accomplish the synthesis of many of the natural products described herein that attracted our interest. The synthetic strategies and ultimate solutions we have developed, in many cases, were driven by the quest for obtaining powerful and often indispensable tools for interrogating some of these very tantalizing puzzles. As a ubiquitous trait of scientific research, the more questions we asked and attempted to address with the synthetic probe molecules in hand, the more new unanswered questions emerged, irresistibly drawing us deeper and deeper into each family of metabolites. We have come to realize that total synthesis projects can very much be viewed as a true beginning of a larger program and not an abrupt conclusion once the natural target molecule has been assembled. When chemistry begins at the advanced vantage point of an established synthesis, new and often unanticipated opportunities for inquiry can be contemplated. As synthetic organic chemists continue to grapple with an ever-changing landscape of funding opportunities and justifications for our art, we do not hesitate to strongly advocate the case for exploiting natural products synthesis for connecting organic chemistry as a discipline to a broader swath of science. We have been additionally fortunate to have been able to interest and engage a wide range of

collaborators in some of these projects, and their skills and expertise have made our journeys both fruitful and intellectually satisfying.

## AUTHOR INFORMATION

### Corresponding Author

\*E-mail: [rmw@lamar.colostate.edu](mailto:rmw@lamar.colostate.edu)

## ACKNOWLEDGMENT

I am deeply indebted to all of my former and current co-workers whose names appear in the publications cited for their hard work, dedication, creativity, and scientific passion. I am especially grateful to a large number of collaborators all over the world, who have enriched our research program immeasurably. I also need to acknowledge my wife Jill and two sons Ridge and Rainier for their love and support. Our research program over the years has been generously funded by the National Institutes of Health, the National Science Foundation, The Herman Frasch Foundation, The Infectious Diseases Research Institute, the Multiple Myeloma Research Foundation, The Colorado State University Cancer Super Cluster, The Petroleum Research Fund of the American Chemical Society and several corporations, including Eli Lilly, Merck & Co., G.D. Searle, Ajinomoto Co., Japan, Fujisawa Pharmaceutical Co., Japan, Kyowa Hakko Kogyo Co., Japan, Sankyo Co., Japan, Fujisawa, The Japanese Society for the Promotion of Science, Microcide Pharmaceutical Co., HemaQuest, Xcyte Therapies, Phoenicia, and the American Chemical Society. The images in the TOC Graphic and Scheme 22 of *Aspergillus versicolor* were provided by doctorfungus.org.

## DEDICATION

<sup>†</sup>This paper is dedicated to Professor Ei-ichi Negishi, Professor Yoshito Kishi, and the late Professor R. B. Woodward for their extraordinarily high standards of scientific excellence and for invaluable mentoring.

## REFERENCES

- (1) (a) Miyoshi, T.; Miyairi, N.; Aoki, H.; Kohsaka, M.; Sakai, H.; Imanaka, H. *J. Antibiot.* **1972**, *25*, 569–575. (b) Kamiya, T.; Maeno, S.; Hashimoto, M.; Mine, Y. *J. Antibiot.* **1972**, *25*, 576–581. (c) Nishida, M.; Mine, Y.; Matsubara, T. *J. Antibiot.* **1972**, *25*, 582–593. (d) Nishida, M.; Mine, Y.; Matsubara, T.; Goto, S.; Kuwahara, S. *J. Antibiot.* **1972**, *25*, 594–601. Bicyclomycin (Aizumycin) was simultaneously isolated from *Streptomyces aizunensis* (e) Miyamura, S.; Ogasawara, N.; Otsuka, H.; Niwayama, S.; Tanka, H.; Take, T.; Uchiyama, T.; Ochiai, H.; Abe, K.; Koizumi, K.; Asao; Matsuki, K.; Hoshino, T. *J. Antibiot.* **1972**, *25*, 610–612. (f) Miyamura, S.; Ogasawara, N.; Otsuka, H.; Niwayama, S.; Tanaka, H.; Take, T.; Uchiyama, T.; Ochiai, H. *J. Antibiot.* **1973**, *26*, 479–484. (g) Miyoshi, T.; Iseki, M.; Konomi, T.; Imanaka, H. *J. Antibiot.* **1980**, *33*, 480–487. (h) Iseki, M.; Miyoshi, T.; Konomi, T.; Imanaka, H. *J. Antibiot.* **1980**, *33*, 488–493. (i) Ochi, K.; Tsurumi, Y.; Shigematsu, N.; Iwami, M.; Umehara, K.; Okuhara, M. *J. Antibiot.* **1988**, *41*, 1106–1115.
- (2) (a) Williams, R. M.; Armstrong, R. W.; Dung, J.-S. *J. Am. Chem. Soc.* **1984**, *106*, 5748–5750. (b) Williams, R. M.; Armstrong, R. W.; Dung, J.-S. *J. Am. Chem. Soc.* **1985**, *107*, 3253–3266. (c) Williams, R. M. *Tetrahedron Lett.* **1981**, *22*, 2341–2344. (d) Williams, R. M.; Dung, J.-S.; Josey, J.; Armstrong, R. W.; Meyers, H. *J. Am. Chem. Soc.* **1983**, *105*, 3214–3220.
- (3) (a) Zwiefka, A.; Kohn, H.; Widger, W. R. *Biochemistry* **1993**, *32*, 3564–3570. (b) Magyar, A.; Zhang, X.; Kohn, H.; Widger, W. R.



- J. Biol. Chem.* **1996**, *271*, 25369–25374. (c) Riba, I.; Gaskell, S. J.; Cho, H.; Widger, W. R.; a Kohn, H. *J. Biol. Chem.* **1998**, *273*, 34033–34041. (d) Magyar, A.; Zhang, X.; Abdi, F.; Kohn, H.; Widger, W. R. *J. Biol. Chem.* **1999**, *274*, 7316–7324. (e) Weber, T. P.; Widger, W. R.; Kohn, H. *Biochemistry* **2002**, *41*, 12377–12383. (f) Skordalakes, E.; Brogan, A. P.; Boon Park, S.; Kohn, H.; Berger, J. M. *Structure* **2005**, *13*, 99–109.
- (4) (a) Kohn, H.; Abuzar, S. *J. Am. Chem. Soc.* **1988**, *110*, 3661–3663. (b) Syed Abuzar, S.; Kohn, H. *J. Am. Chem. Soc.* **1990**, *112*, 3114–3121. (5) Someya, A.; Iseki, M.; Tanaka, N. *J. Antibiot.* **1979**, *32*, 402–407. (6) (a) Williams, R. M.; Tomizawa, K.; Armstrong, R. W.; Dung, J.-S. *J. Am. Chem. Soc.* **1985**, *107*, 6419–6421. (b) Williams, R. M.; Tomizawa, K.; Armstrong, R. W.; Dung, J.-S. *J. Am. Chem. Soc.* **1987**, *109*, 4028–4035. (7) Williams, R. M.; Sabol, M. R.; Kim, H.; Kwast, A. *J. Am. Chem. Soc.* **1991**, *113*, 6621–6633. (8) For reviews on the chemistry of bicyclomycin, see: (a) Williams, R. M.; Durham, C. A. *Chem. Rev.* **1988**, *88*, 511–540. (b) Williams, R. M. Stereoselective Synthetic and Mechanistic Chemistry of Bicyclomycin. In *Studies in Natural Products Chemistry*; Atta-ur-Rahman, Ed.; Elsevier: Amsterdam, 1993; Vol. 12. (9) Williams, R. M.; Armstrong, R. W.; Maruyama, L. K.; Dung, J.-S.; Anderson, O. P. *J. Am. Chem. Soc.* **1985**, *107*, 3246–3253. (10) (a) Birch, A. J.; Wright, J. J. *J. Chem. Soc., Chem. Commun.* **1969**, 644–645. (b) Birch, A. J.; Wright, J. J. *Tetrahedron* **1970**, *26*, 2329–2344. (c) Birch, A. J.; Russell, R. A. *Tetrahedron* **1972**, *28*, 2999–3008. (d) Bird, B. A.; Remaley, A. T.; Campbell, I. M. *Appl. Environ. Microbiol.* **1981**, *42*, 521–525. (e) Bird, B. A.; Campbell, I. M. *Appl. Environ. Microbiol.* **1982**, *43*, 345. (f) Robbers, J. E.; Straus, J. W. *Lloydia* **1975**, *38*, 355–356. (g) Paterson, R. R. M.; Hawksworth, D. L. *Trans. Br. Mycol. Soc.* **1985**, *85*, 95–100. (h) Wilson, B. J.; Yang, D. T. C.; Harris, T. M. *Appl. Microbiol.* **1973**, *26*, 633–635. (i) Coetzer, J. *Acta Crystallogr.* **1974**, *B30*, 2254–2256. (11) Williams, R. M.; Glinka, T. *Tetrahedron Lett.* **1986**, *27*, 3581–3584. (12) (a) Williams, R. M.; Glinka, T.; Kwast, E. *J. Am. Chem. Soc.* **1988**, *110*, 5927–5929. (b) Williams, R. M.; Glinka, T.; Kwast, E.; Coffman, H.; Stille, J. K. *J. Am. Chem. Soc.* **1990**, *112*, 808–821. (13) (a) Polonsky, J.; Merrien, M.-A.; Prange, T.; Pascard, C. *J. Chem. Soc., Chem. Commun.* **1980**, 601–602. (b) Prange, T.; Buillion, M.-A.; Vuilhorgne, M.; Pascard, C.; Polonsky, J. *Tetrahedron Lett.* **1981**, *22*, 1977–1980. (14) (a) Yamazaki, M.; Fujimoto, H.; Okuyama, E.; Ohta, Y. *Proc. Jpn. Assoc. Mycotoxicol.* **1980**, *10*, 27. (b) Yamazaki, M.; Okuyama, E. *Tetrahedron Lett.* **1981**, *22*, 135–136. (c) Blanchflower, S. E.; Banks, R. M.; Everett, J. R.; Manger, B. R.; Reading, C. *J. Antibiot.* **1991**, *44*, 492–497. (d) Blanchflower, S. E.; Banks, R. M.; Everett, J. R.; Reading, C. *J. Antibiot.* **1993**, *46*, 1355–1363. (e) Whyte, A. C.; Gloer, J. B. *J. Nat. Prod.* **1996**, *59*, 1093–1095. (15) Porter, A. E. A.; Sammes, P. G. *J. Chem. Soc., Chem. Commun.* **1970**, 1103. (16) Birch, A. J. *J. Agric. Food Chem.* **1971**, *19*, 1088–1092. (17) Baldas, J.; Birch, A. J.; Russell, R. A. *J. Chem. Soc., Perkin Trans. 1* **1974**, 50–52. (18) (a) Sanz-Cervera, J.-F.; Glinka, T.; Williams, R. M. *J. Am. Chem. Soc.* **1993**, *115*, 347–348. (b) Sanz-Cervera, J. F.; Glinka, T.; Williams, R. M. *Tetrahedron* **1993**, *49*, 8471–8482. (19) (a) Domingo, L. R.; Sanz-Cervera, J. F.; Williams, R. M.; Picher, M. T.; Marco, J. A. *J. Org. Chem.* **1997**, *62*, 1662–1667. (b) Domingo, L. R.; Zaragoza, R. J.; Williams, R. M. *J. Org. Chem.* **2003**, *68*, 2895–2902. (20) (a) Williams, R. M.; Sanz-Cervera, J. F.; Sancenón, F.; Marco, J. A.; Halligan, K. *J. Am. Chem. Soc.* **1998**, *120*, 1090–1091. (b) Williams, R. M.; Sanz-Cervera, J. F.; Sancenón, F.; Marco, J. A.; Halligan, K. *Bioorg. Med. Chem.* **1998**, *6*, 1233–1241. (c) Sanz-Cervera, J. F.; Williams, R. M.; Marco, J. A.; López-Sánchez, J. M.; González, F.; Martínez, M. E.; Sancenón, F. *Tetrahedron* **2000**, *56*, 6345–6358. (d) Adams, L. A.; Valente, M. W. N.; Williams, R. M. *Tetrahedron* **2006**, *62*, 5195–5200. (21) (a) Cushing, T. D.; Sanz-Cervera, J. F.; Williams, R. M. *J. Am. Chem. Soc.* **1993**, *115*, 9323–9324. (b) Cushing, T. D.; Sanz-Cervera, J. F.; Williams, R. M. *J. Am. Chem. Soc.* **1996**, *118*, 557–579. (22) (a) Williams, R. M.; Cao, J.; Tsujishima, H. *Angew. Chem., Int. Ed.* **2000**, *39*, 2540–2544. (b) Williams, R. M.; Cao, J.; Tsujishima, H. *J. Am. Chem. Soc.* **2003**, *125*, 12172–12178. (23) Artman, G. D.; Grubbs, A. W.; Williams, R. M. *J. Am. Chem. Soc.* **2007**, *129*, 6336–6342. (24) Artman, G. D.; Williams, R. M. *Org. Synth.* **2009**, *86*, 262–273. (25) (a) Seebach, D.; Boes, M.; Naef, R.; Schweizer, W. B. *J. Am. Chem. Soc.* **1983**, *105*, 5390–5398. (b) Beck, A. K.; Blank, S.; Job, K.; Seebach, D.; Sommerfeld, T. *Org. Synth.* **1995**, *72*, 62–73. (26) Chatterjee, A. K.; Choi, T.-L.; Sanders, D. P.; Grubbs, R. H. *J. Am. Chem. Soc.* **2003**, *125*, 11360–11370. (27) (a) Baran, P. S.; Guerrero, C. A.; Ambhaikar, N. B.; Hafenstein, B. J. *Angew. Chem., Int. Ed.* **2005**, *44*, 606–609. (b) Baran, P. S.; Guerrero, C. A.; Ambhaikar, N. B.; Hafenstein, B. J. *Angew. Chem., Int. Ed.* **2005**, *44*, 3892–3895. (c) Baran, P. S.; Hafenstein, B. D.; Ambhaikar, N. B.; Guerrero, C. A.; Gallagher, J. D. *J. Am. Chem. Soc.* **2006**, *128*, 8678–8693. (28) (a) Qian-Cutrone, J.; Haung, S.; Shu, Y.-Z.; Vyas, D.; Fairchild, C.; Menendez, A.; Krampitz, K.; Dalterio, R.; Kloor, S. E.; Gao, Q. *J. Am. Chem. Soc.* **2002**, *124*, 14556–14557. (b) Qian-Cutrone, J.; Krampitz, K. D.; Shu, Y.-Z.; Chang, L. P. U.S. Patent 6,291,461, 2001. (c) Nussbaum, F. *Angew. Chem., Int. Ed.* **2003**, *42*, 2068–2071. (d) Fenical, W.; Jensen, P. R.; Cheng, X. C. U.S. Patent 6,066,635, 2000. (e) Sugie, Y.; Hirai, H.; Inagaki, T.; Ishiguro, M.; Kim, Y.-J.; Kojima, Y.; Sakakibara, T.; Sakemi, S.; Sugiura, A.; Suzuki, Y.; Brennan, L.; Duignan, J.; Huang, L. H.; Sutcliffe, J.; Kojima, N. *J. Antibiot.* **2001**, *54*, 911–916. (29) (a) Herzon, S. B.; Myers, A. G. *J. Am. Chem. Soc.* **2005**, *127*, 5342–5344. (b) Myers, A. G.; Herzon, S. B. *J. Am. Chem. Soc.* **2003**, *125*, 12080–12081. (30) (a) Kato, H.; Yoshida, T.; Tokue, T.; Nojiri, Y.; Hirota, H.; Ohta, T.; Williams, R. M.; Tsukamoto, S. *Angew. Chem., Int. Ed.* **2007**, *46*, 2254–2256. (b) Tsukamoto, S.; Kato, H.; Samizo, M.; Nojiri, Y.; Onuki, H.; Hirota, H.; Ohta, T. *J. Nat. Prod.* **2008**, *71*, 2064–2067. (c) Greshock, T. J.; Grubbs, A. W.; Jiao, P.; Wicklow, D. T.; Gloer, J. B.; Williams, R. M. *Angew. Chem., Int. Ed.* **2008**, *47*, 3573–3577. (d) Tsukamoto, S.; Kato, H.; Greshock, T. J.; Hirota, H.; Ohta, T.; Williams, R. M. *J. Am. Chem. Soc.* **2009**, *131*, 3834–3835. (e) Tsukamoto, S.; Kawabata, T.; Kato, H.; Greshock, T. J.; Hirota, H.; Ohta, T.; Williams, R. M. *Org. Lett.* **2009**, *11*, 1297–1300. (31) (a) Greshock, T. J.; Grubbs, A. W.; Tsukamoto, S.; Williams, R. M. *Angew. Chem., Int. Ed.* **2007**, *46*, 2262–2265. (b) Greshock, T. J.; Williams, R. M. *Org. Lett.* **2007**, *9*, 4255–4258. (32) Finefield, J. M.; Greshock, T. J.; Sherman, D. H.; Tsukamoto, S.; Williams, R. M. Unpublished results. (33) (a) Miller, K. A.; Welch, T. R.; Greshock, T. J.; Ding, Y.; Sherman, D. H.; Williams, R. M. *J. Org. Chem.* **2008**, *73*, 3116–3119. (b) Ding, Y.; Greshock, T. J.; Miller, K.; Sherman, D. H.; Williams, R. M. *Org. Lett.* **2008**, *10*, 4863–4866. (34) Greshock, T. J.; Grubbs, A. W.; Williams, R. M. *Tetrahedron* **2007**, *63*, 6124–6130. (35) Miller, K. A.; Tsukamoto, S.; Williams, R. M. *Nature Chem.* **2009**, *1*, 63–68. (36) Phil Baran and co-workers were the first to corroborate the absolute configuration of the (+)-stephacidin A produced by *Aspergillus ochraceus* through their elegant total synthesis of both antipodes; see ref 27. (37) (a) The Tsukamoto marine-derived *Aspergillus* sp.; Ding, Y.; de Wet, J. R.; Cavalcoli, J.; Li, S.; Greshock, T. J.; Miller, K. A.; Finefield, J. M.; Sunderhaus, J. D.; McAfoos, T.; Tsukamoto, S.; Williams, R. M.; Sherman, D. H. *J. Am. Chem. Soc.* **2010**, *132*, 12733–12740. (b) *Aspergillus versicolor* NRRL 35600; Li, S.; Finefield, J. M.; Tsukamoto, S.; Williams, R. M.; Sherman, D. H. Unpublished results. (38) (a) Stocking, E. M.; Sanz-Cervera, J. F.; Williams, R. M. *Angew. Chem., Int. Ed.* **1999**, *38*, 786–789. (b) Stocking, E. M.; Sanz-Cervera, J. F.; Williams, R. M. *J. Am. Chem. Soc.* **2000**, *122*, 9089–9098.

- (39) For related work on reverse prenylation, see: Balibar, C. J.; Howard-Jones, A. R.; Walsh, C. T. *Nature Chem. Biol.* **2007**, *3*, 584–592.
- (40) (a) Stocking, E.; Sanz-Cervera, J. F.; Williams, R. M.; Unkefer, C. J. *J. Am. Chem. Soc.* **1996**, *118*, 7008–7009; *J. Am. Chem. Soc.* **1997**, *119*, 9588 (Errata). (b) Stocking, E. M.; Sanz-Cervera, J. F.; Williams, R. M. *Angew. Chem., Int. Ed.* **2001**, *40*, 1296–1298. (c) Stocking, E. M.; Sanz-Cervera, J. F.; Unkefer, C. J.; Williams, R. M. *Tetrahedron* **2001**, *57*, 5303–5320. (d) Gray, C.; Sanz-Cervera, J. F.; Williams, R. M. *J. Am. Chem. Soc.* **2003**, *125*, 14692–14693.
- (41) Arigoni and Kellenberger studied the biosynthesis of  $\beta$ -methylproline in bottromycin and found this to be derived from S-proline and S-adenosyl methionine; see: Kellenberger, J. L. Ph.D. Thesis, ETH, 1997.
- (42) (a) Sanz-Cervera, J. F.; Williams, R. M. *J. Am. Chem. Soc.* **2002**, *124*, 2556–2559. (b) Stocking, E. M.; Sanz-Cervera, J. F.; Williams, R. M. *J. Am. Chem. Soc.* **2000**, *122*, 1675–1683.
- (43) Isolation of the asperparalines: (a) Hayashi, H.; Nishimoto, Y.; Nozaki, H. *Tetrahedron Lett.* **1997**, *38*, 5655–5658. (b) Hayashi, H.; Nishimoto, Y.; Akiyama, K.; Nozaki, H. *Biosci. Biotechnol. Biochem.* **2000**, *64* (1), 111–115. (c) Banks, R. M.; Blanchflower, S. E.; Everett, J. R.; Manger, B. R.; Reading, C. J. *Antibiot.* **1997**, *50*, 840–846.
- (44) For some reviews on the synthesis and biosynthesis of the prenylated indole alkaloids, see: (a) Williams, R. M.; Sanz-Cervera, J. F.; Stocking, E. *Topics in Current Chemistry, Volume on Biosynthesis - Terpenes and Alkaloids*; Leeper, F., Vederas, J. C., Eds.; Springer-Verlag: Berlin, 2000; Vol. 209, pp 97–173. (b) Williams, R. M. *Chem. Pharm. Bull.* **2002**, *50*, 711–740. (c) Cox, R. J.; Williams, R. M. *Acc. Chem. Res.* **2003**, *36*, 127–139. (d) Miller, K. A.; Williams, R. M. *Chem. Soc. Rev.* **2009**, *38*, 3160–3174. (e) Welch, T.; Williams, R. M. *Biomimetic Synthesis of Alkaloids Derived from Tryptophan: Dioxopiperazine Alkaloids*. In *Biomimetic Organic Synthesis*; Poupon, E., Nay, B., Eds.; Wiley-VCH: Weinheim, 2011; in press. (f) Sunderhaus, J. D.; Williams, R. M. *Isr. J. Chem.* **2011**.
- (45) Stocking, E.; Williams, R. M. *Angew. Chem., Int. Ed.* **2003**, *42*, 3078–3115.
- (46) For a review on the asymmetric synthesis of  $\alpha$ -amino acids, see: Williams, R. M. *Synthesis of Optically Active  $\alpha$ -Amino Acids*; Pergamon Press, Oxford, 1989; Vol. 7.
- (47) Vigneron, J. P.; Kagan, H.; Horeau, A. *Tetrahedron Lett.* **1968**, 5681–5683.
- (48) (a) Sinclair, P. J.; Zhai, D.; Reibenspies, J.; Williams, R. M. *J. Am. Chem. Soc.* **1986**, *108*, 1103–1104. (b) Williams, R. M.; Sinclair, P. J.; Zhai, D.; Chen, D. *J. Am. Chem. Soc.* **1988**, *110*, 1547–1557. (c) Williams, R. M.; Zhai, D.; Sinclair, P. J. *J. Org. Chem.* **1986**, *51*, 5021–5022.
- (49) (a) Williams, R. M.; Sinclair, P. J.; DeMong, D.; Chen, D.; Zhai, D. *Org. Synth.* **2003**, *80*, 18–30. (b) Williams, R. M.; Sinclair, P. J.; DeMong, D. E. *Org. Synth.* **2003**, *80*, 31–37.
- (50) (a) Weijlard, J.; Pfister, K.; Swanezy, E. F.; Robinson, C. A.; Tishler, M. *J. Am. Chem. Soc.* **1951**, *73*, 1216–1218. (b) For an improved, alternative resolution, see: Dastlik, K. A.; Sundermeier, U.; Johns, D. M.; Chen, Y.; Williams, R. M. *Syn. Lett.* **2005**, 693–696.
- (51) Sharpless-based methodology has been applied to the synthesis of these amino alcohols; see: Chang, H.-T.; Sharpless, K. B. *Tetrahedron Lett.* **1996**, *37*, 3219–3222.
- (52) A lipase-based resolution of benzoin has also been reported as a method to prepare (1R,2S)-erythro-2-amino-1,2-diphenylethanol: Aoyagi, Y.; Agata, N.; Shibata, N.; Horiguchi, M.; Williams, R. M. *Tetrahedron Lett.* **2000**, *41*, 10159–10162.
- (53) van den Nieuwendijk, A. M. C. H.; Warmerdam, E. G. J. C.; Brussee, J.; van der Gen, A. *Tetrahedron: Asymmetry* **1995**, *6*, 801–806.
- (54) (a) Williams, R. M. *Aldrichim. Acta* **1992**, *25*, 11–25. (b) Williams, R. M.; Hendrix, J. A. *Chem. Rev.* **1992**, *92*, 889–917. (c) Williams, R. M. *Advances in Asymmetric Synthesis*; Hassner, A., Ed.; JAI Press: Greenwich, 1995; Vol. 1, pp 45–94. (d) Burnett, C.; Williams, R. M. *Strategies Tactics Org. Synth.* **2008**, *7*, 268–327. (e) Burnett, C.; Williams, R. M. *New Tricks in Amino Acid Synthesis: Applications to Complex Natural Products*; Soloshonok, V. A., Izawa, K., Eds.; ACS Symposium Book Series; American Chemical Society: Washington, DC, 2009; Chapter 26, pp 420–442.
- (55) Williams, R. M.; Sinclair, P. J.; Zhai, W. *J. Am. Chem. Soc.* **1988**, *110*, 482–483.
- (56) Williams, R. M.; Im, M.-N.; Cao, J. *J. Am. Chem. Soc.* **1991**, *113*, 6976–6981.
- (57) Williams, R. M.; Fegley, G. J. *Tetrahedron Lett.* **1992**, *33*, 6755–6758.
- (58) Williams, R. M.; Fegley, G. J. *J. Am. Chem. Soc.* **1991**, *113*, 8796–8806.
- (59) Williams, R. M.; Yuan, C. *J. Org. Chem.* **1992**, *57*, 6519–6527.
- (60) Williams, R. M.; Colson, P.-J.; Zhai, W. *Tetrahedron Lett.* **1994**, *35*, 9371–9374.
- (61) Williams, R. M.; Yuan, C. *J. Org. Chem.* **1994**, *59*, 6190–6193.
- (62) (a) Sebahar, P.; Williams, R. M. *J. Am. Chem. Soc.* **2000**, *122*, 5666–5667. (b) Sebahar, P. R.; Osada, H.; Williams, R. M. *Tetrahedron* **2002**, *58*, 6311–6322.
- (63) Onishi, T.; Sebahar, P. R.; Williams, R. M. *Org. Lett.* **2003**, *5*, 3135–3137.
- (64) (a) Scott, J. D.; Williams, R. M. *Angew. Chem., Int. Ed.* **2001**, *40*, 1463–1465. (b) Williams, R. M.; Scott, J. D. *J. Am. Chem. Soc.* **2002**, *124*, 2951–2956. (c) Scott, J. D.; Tippie, T. N.; Williams, R. M. *Tetrahedron Lett.* **1998**, *39*, 3659–3662.
- (65) DeMong, D. E.; Williams, R. M. *Tetrahedron Lett.* **2001**, *42*, 3529–3532.
- (66) DeMong, D. E.; Williams, R. M. *J. Am. Chem. Soc.* **2003**, *125*, 8561–8565.
- (67) Jain, R. P.; Williams, R. M. *Tetrahedron* **2001**, *57*, 6505–6509.
- (68) Jain, R. P.; Williams, R. M. *Tetrahedron Lett.* **2001**, *42*, 4437–4440.
- (69) Jain, R. P.; Albrecht, B. K.; DeMong, D. E.; Williams, R. M. *Org. Lett.* **2001**, *24*, 4287–4289.
- (70) Jain, R. P.; Williams, R. M. *J. Org. Chem.* **2002**, *67*, 6361–6365.
- (71) Lane, J. W.; Chen, Y.; Williams, R. M. *J. Am. Chem. Soc.* **2005**, *127*, 12684–12690.
- (72) (a) Looper, R.; Williams, R. M. *Tetrahedron Lett.* **2001**, *42*, 769–771. (b) Looper, R. E.; Runnegar, M. T. C.; Williams, R. M. *Tetrahedron* **2006**, *62*, 4549–4562.
- (73) Looper, R. E.; Williams, R. M. *Angew. Chem., Int. Ed.* **2004**, *43*, 2930–2933.
- (74) Looper, R. E.; Runnegar, M. T. C.; Williams, R. M. *Angew. Chem., Int. Ed.* **2005**, *44*, 3879–3881.
- (75) (a) Ohtani, I.; Moore, R. E.; Runnegar, M. T. C. *J. Am. Chem. Soc.* **1992**, *114*, 7941–7942. (b) Moore, R. E.; Ohtani, I.; Moore, B. S.; deKoning, C. B.; Yoshida, W. Y.; Runnegar, M. T. C.; Carmichael, W. W. *Gazz. Chim. Ital.* **1993**, *123*, 329–336. (c) Norris, R. L.; Eaglesham, G. K.; Pierens, G.; Shaw, G. R.; Smith, M. J.; Chiswell, R. K.; Seawright, A. A.; Moore, M. R. *Environ. Toxicol.* **1999**, *14*, 163–165. (d) Li, R.; Carmichael, W. W.; Brittain, S.; Eaglesham, G. K.; Shaw, G. R.; Mahakhant, A.; Noparatnaraporn, N.; Yongmanitchai, W.; Kaya, K.; Watanabe, M. M. *Toxicol.* **2001**, *39*, 973–980. (e) Norris, R. L. G.; Eaglesham, G. K.; Shaw, G. R.; Senogles, P.; Chiswell, R. K.; Smith, M. J.; Davis, B. C.; Seawright, A. A.; Moore, M. R. *Environ. Toxicol.* **2001**, *16*, 391–396. (f) Griffiths, D. J.; Saker, M. L. *Environ. Toxicol.* **2003**, *18*, 78–93.
- (76) Harada, K.; Ohtani, I.; Iwamoto, K.; Suzuki, M.; Watanabe, M. F.; Watanabe, M.; Terao, K. *Toxicol.* **1994**, *32*, 73–84.
- (77) (a) Banker, R.; Carmeli, S.; Hadas, O.; Teltsch, B.; Porat, R.; Sukenik, A. *J. Phycol.* **1997**, *33*, 613–616. (b) Banker, R.; Teltsch, B.; Sukenik, A.; Carmeli, S. *J. Nat. Prod.* **2000**, *63*, 387–389.
- (78) Li, R. H.; Carmichael, W. W.; Brittain, S.; Eaglesham, G. K.; Shaw, G. R.; Liu, Y. D.; Watanabe, M. M. *J. Phycol.* **2001**, *37*, 1121–1126.
- (79) (a) Shaw, G. R.; Seawright, A. A.; Moore, M. R.; Lam, P. K. S. *Therapeutic Drug Monitoring* **2000**, *22*, 89–92. (b) Fessard, V.; Bernard, C. *Environ. Toxicol.* **2003**, *18*, 353–359.
- (80) (a) Shaw, G. R.; Seawright, A. A.; Moore, M. R.; Lam, P. K. S. *Therapeutic Drug Monitoring* **2000**, *22*, 89–92. (b) Fessard, V.; Bernard, C. *Environ. Toxicol.* **2003**, *18*, 353–359.



- (81) Banker, R.; Carmeli, S.; Werman, M.; Teltsch, B.; Porat, R.; Sukenik, A. *J. Toxicol. Environ. Health Part A* **2001**, *62*, 281–288.
- (82) (a) Runnegar, M. J. T.; Kong, S.-M.; Zhong, Y.-Z.; Ge, J.-L.; Lu, S. C. *Biochem. Biophys. Res. Commun.* **1994**, *201*, 235–241. (b) Runnegar, M. T.; Kong, S.-M.; Zhong, Y.-Z.; Lu, S. C. *Biochem. Pharmacol.* **1995**, *49*, 219–225.
- (83) (a) Shen, X. Y.; Lam, P. K. S.; Shaw, G. R.; Wickramasinghe, W. *Toxicol.* **2002**, *40*, 1499–1501. (b) Falconer, I. R.; Humpage, A. R. *Environ. Toxicol.* **2006**, *21*, 299–304.
- (84) Xie, C.; Runnegar, M. T. C.; Snider, B. B. *J. Am. Chem. Soc.* **2000**, *122*, 5017–5024.
- (85) Heintzelman, G. R.; Fang, W.-K.; Keen, S. P.; Wallace, G. A.; Weinreb, S. M. *J. Am. Chem. Soc.* **2001**, *123*, 8851–8853.
- (86) White, J. D.; Hansen, J. D. *J. Am. Chem. Soc.* **2002**, *124*, 4950–4951.
- (87) (a) Cui, C. B.; Kakeya, H.; Osada, H. *J. Antibiot.* **1996**, *49*, 832–835. (b) Cui, C. B.; Kakeya, H.; Osada, H. *Tetrahedron.* **1996**, *51*, 12651–12666.
- (88) For total syntheses of spirotryprostatin A, see: (a) Edmonson, S. D.; Danishefsky, S. J. *Angew. Chem., Int. Ed.* **1998**, *37*, 1138–1140. (b) Edmonson, S.; Danishefsky, S. J.; Sepp-Lorenzino, L.; Rosen, N. *J. Am. Chem. Soc.* **1999**, *121*, 2147–2155. (c) Onishi, T.; Sebahar, P. R.; Williams, R. M. *Org. Lett.* **2003**, *5*, 3135–3137. (d) Onishi, T.; Sebahar, P. R.; Williams, R. M. *Tetrahedron* **2004**, *60*, 9503–9515. (e) Miyake, F. Y.; Yakushijin, K.; Horne, D. A. *Org. Lett.* **2004**, *6*, 4249–4251.
- (89) For total syntheses of spirotryprostatin B, see: (a) von Nussbaum, F.; Danishefsky, S. J. *Angew. Chem., Int. Ed.* **2000**, *39*, 2175–2178. (b) Overman, L. E.; Rosen, M. D. *Angew. Chem., Int. Ed.* **2000**, *39*, 4596–4599. (c) Wang, H.; Ganesan, H. *J. Org. Chem.* **2000**, *65*, 4685–4693. (d) Bagul, T. D.; Lakshmaiah, G.; Kawataba, T.; Fujii, K. *Org. Lett.* **2002**, *4*, 249–251. (e) Meyers, C.; Carreira, E. M. *Angew. Chem., Int. Ed.* **2003**, *42*, 694–696. (f) Marti, C.; Carreira, E. M. *Eur. J. Org. Chem.* **2003**, 2209–2219. (g) Miyake, F. Y.; Yakushijin, K.; Horne, D. A. *Angew. Chem., Int. Ed.* **2004**, *43*, 5357–5360. (h) Marti, C.; Carreira, E. M. *J. Am. Chem. Soc.* **2005**, *127*, 11505–11515. (i) Trost, B. M.; Stiles, D. T. *Org. Lett.* **2007**, *9*, 2763–2766. For a review, see: (j) Lindel, T. *Nachrichten aus der Chemie* **2000**, *48*, 1498–1501.
- (90) See ref 62; see also: Sebahar, P. Ph.D. dissertation, Colorado State University, 2003.
- (91) See ref 63 and: Onishi, T.; Sebahar, P. R.; Williams, R. M. *Tetrahedron* **2004**, *60*, 9503–9515.
- (92) (a) Namba, K.; Greshock, T. J.; Sundermeier, U.; Li, H.; Williams, R. M. *Tetrahedron Lett.* **2010**, *51*, 6557–6559. See also: (b) Namba, K.; Kaihara, Y.; Yamamoto, H.; Imagawa, H.; Tanino, K.; Williams, R. M.; Nishizawa, M. *Chem.—Eur. J.* **2009**, *15*, 6560–6563.
- (93) (a) Kinnel, R. B.; Gehrken, H.-P.; Scheuer, P. J. *J. Am. Chem. Soc.* **1993**, *115*, 3376–3377. (b) Kinnel, R. B.; Gehrken, H.-P.; Swali, R.; Skoropowski, G.; Scheuer, P. J. *J. Org. Chem.* **1998**, *63*, 3281–3286.
- (94) For synthetic approaches to palau'amine and congeners, see references cited in ref 92a.
- (95) Seiple, I. B.; Su, S.; Young, I. S.; Lewis, C. A.; Yamaguchi, J.; Baran, P. S. *Angew. Chem., Int. Ed.* **2010**, *49*, 1095–1098.
- (96) (a) Buchanan, M. S.; Carroll, A. R.; Addepalli, R.; Avery, V. M.; Hooper, J. N. A.; Quinn, R. J. *J. Org. Chem.* **2007**, *72*, 2309–2317. (b) Grube, A.; Köck, M. *Angew. Chem., Int. Ed.* **2007**, *46*, 2320–2324.
- (97) Ahrendt, K. A.; Williams, R. M. *Org. Lett.* **2004**, *6*, 4539–4541.
- (98) Lo, M.M.-C.; Neumann, C. S.; Nagayama, S.; Perlstein, E. O.; Schreiber, S. L. *J. Am. Chem. Soc.* **2004**, *126*, 16077–16086.
- (99) Tomita, F.; Takahashi, K.; Tamaoki, T. *J. Antibiot.* **1984**, *37*, 1268–1272.
- (100) (a) Williams, R. M.; Glinka, T.; Flanagan, M. E.; Gallegos, R.; Coffman, H.; Pei, D. *J. Am. Chem. Soc.* **1992**, *114*, 733–740. (b) Williams, R. M.; Glinka, T.; Gallegos, R.; Ehrlich, P.; Flanagan, M. E.; Coffman, H.; Park, G. *Tetrahedron* **1991**, *47*, 2629–2642. (c) Williams, R. M.; Flanagan, M. E.; Tippie, T. *Biochemistry* **1994**, *33*, 4086–4092.
- (101) Flanagan, M. E.; Rollins, S. B.; Williams, R. M. *Chem. Biol.* **1995**, *2*, 147–156.
- (102) Flanagan, M. E.; Williams, R. M. *J. Org. Chem.* **1995**, *60*, 6791–6797.
- (103) (a) Vincent, G.; Williams, R. M. *Angew. Chem., Int. Ed.* **2007**, *46*, 1517–1520. (b) Vincent, G.; Chen, Y.; Lane, J. W.; Williams, R. M. *Heterocycles* **2007**, *72*, 385–398.
- (104) Fishlock, D.; Williams, R. M. *J. Org. Chem.* **2008**, *73*, 9594–9600.
- (105) Chan, C.; Heid, R.; Zheng, S. P.; Guo, J. S.; Zhou, B. S.; Furuuchi, T.; Danishefsky, S. J. *J. Am. Chem. Soc.* **2005**, *127*, 4596–4598.
- (106) Zheng, S.; Chan, C.; Furuuchi, T.; Wright, B. J. D.; Zhou, B.; Guo, J.; Danishefsky, S. J. *Angew. Chem., Int. Ed.* **2006**, *45*, 1754–1759.
- (107) Endo, A.; Yanagisawa, A.; Abe, M.; Tohma, S.; Kan, T.; Fukuyama, T. *J. Am. Chem. Soc.* **2002**, *124*, 6552–6554.
- (108) Williams, R. M.; Herberich, B. *J. Am. Chem. Soc.* **1998**, *120*, 10272–10273.
- (109) Hill, G. C.; Wunz, T. P.; Mackenzie, N. E.; Gooley, P. R.; Remers, W. A. *J. Med. Chem.* **1991**, *34*, 2079–2088.
- (110) (a) Garcia-Carbonero, R.; Supko, J. G.; Maki, R. G.; Manola, J.; Ryan, D. P.; Harmon, D.; Puchalski, T. A.; Goss, G.; Seiden, M. V.; Waxman, A.; Quigley, M. T.; Lopez, T.; Sancho, M. A.; Limeno, J.; Guzman, C.; Demetri, G. D. *J. Clin. Oncol.* **2005**, *23*, 5484–5492. (b) Garcia-Carbonero, R.; Supko, J. G.; Manola, J.; Seiden, M. V.; Harmon, D.; Ryan, D. P.; Quigley, M. T.; Merriam, P.; Canniff, J.; Goss, G.; Matulonis, U.; Maki, R. G.; Lopez, T.; Puchalski, T. A.; Sancho, M. A.; Gomez, J.; Guzman, C.; Jimeno, J.; Demetri, G. D. *J. Clinical Oncol.* **2004**, *22*, 1480–1490. (c) Hing, J.; Perea-Ruixo, J.; Stuyckens, K.; Soto-Matos, A.; Lopez-Lazaro, L.; Zannikos, P. *Clinical Pharmacol. Ther.* **2008**, *83*, 130–143.
- (111) Cuevas, C.; Perez, M.; Martin, M. J.; Chicharro, J. L.; Fernandez-Rivas, C.; Flores, M.; Francesch, A.; Gallego, P.; Zarzuelo, M.; de la Calle, F.; Garcia, J.; Polanco, C.; Rodriguez, I.; Manzanares, I. *Org. Lett.* **2000**, *2*, 2545–2548.
- (112) (a) Piel, J.; Hui, D.; Wen, G.; Butzke, D.; Platzer, M.; Fusetani, N.; Matsunaga, S. *Proc. Natl. Acad. Sci. U.S.A.* **2004**, *101*, 16222–7. (b) Sudek, S.; Lapanik, N. B.; Waggoner, L. E.; Hildebrand, M.; Anderson, C.; Liu, H.; Patel, A.; Sherman, D. H.; Haygood, M. G. *J. Nat. Prod.* **2007**, *70*, 67–74.
- (113) Paclitaxel, the generic name for Taxol, is a registered trademark of Bristol-Myers Squibb. Because of the greater familiarity with the word Taxol, this will be used throughout this article, and the trademark symbol has been deleted for the sake of clarity and brevity. For reviews, see: (a) Georg, G. I.; Ali, S. M.; Zygmunt, J.; Jayasinghe, L. R. *Exp. Opin. Ther. Patents* **1994**, *4*, 109–120. (b) A., N.; Jenkins, P. R.; Lawrence, N. J. *Contemp. Org. Synth.* **1994**, 47–75. (c) Nicolaou, K. C.; Dai, W.-M.; Guy, R. K. *Angew. Chem., Int. Ed.* **1994**, *33*, 15–44. (d) Guenard, D.; Gueritte-Voegelien, F.; Potier, P. *Acc. Chem. Res.* **1993**, *26*, 160–167. (e) Kingston, D. G. *Pharmacol. Ther.* **1991**, *52*, 1–34. (f) Swindell, C. S. *Org. Prep. Proc. Int.* **1991**, *23*, 465–543. (g) Floss, H. G.; Mocek, U. Biosynthesis of Taxol. In *Taxol: Science and Applications*; Suffness, M., Ed.; CRC Press: Boca Raton, FL, 1995. (h) Rohr, J. *Angew. Chem., Int. Ed.* **1997**, *36*, 2190–2195.
- (114) Wani, M. C.; Taylor, H. L.; Wall, M. E.; Coggon, P.; McPhail, A. T. *J. Am. Chem. Soc.* **1971**, *93*, 2325–2327.
- (115) For some leading references on the total synthesis of Taxol and synthetic approaches, see: (a) Holton, R. A.; Juo, R. R.; Kim, H. B.; Williams, A. D.; Harusawa, S.; Lowenthal, R. E.; Yogai, S. *J. Am. Chem. Soc.* **1988**, *110*, 6558–6560; (b) Wender, P. A.; Mucciario, T. P. *J. Am. Chem. Soc.* **1992**, *114*, 5878–5879; (c) Nicolaou, K. C.; Yang, Z.; Liu, J. J.; Nantermet, P. G.; Guy, R. K.; Claiborne, C. F.; Renaud, J.; Coulaudouros, E. A.; Paulvannan, K.; Sorensen, E. J. *Nature* **1994**, *367*, 630–634; (d) Nicolaou, K. C.; Nantermet, P. G.; Ueno, H.; Guy, R. K.; Coulaudouros, E. A.; Sorensen, E. J. *J. Am. Chem. Soc.* **1995**, *117*, 624–633; (e) Nicolaou, K. C.; Liu, J.-J.; Yang, Z.; Ueno, H.; Sorensen, E. J.; Claiborne, C. F.; Guy, R. K.; Hwang, C.-K.; Nakada, M.; Nantermet, P. G. *J. Am. Chem. Soc.* **1995**, *117*, 634–644; (f) K., C.; Yang, Z.; Liu, J.-J.; Nantermet, P. G.; Claiborne, C. F.; Renaud, J.; Guy, R. K.; Shibayama, K. *J. Am. Chem. Soc.* **1995**, *117*, 645–652; (g) Nicolaou, K. C.; Ueno, H.; Liu, J.-J.; Nantermet, P. G.; Yang, Z.; Renaud, J.

- Paulvannan, K.; Chadha, R. *J. Am. Chem. Soc.* **1995**, *117*, 653–659 and references cited therein; (h) Holton, R. A.; Somoza, C.; Kim, H.-B.; Liang, F.; Biediger, J.; Boatman, P. D.; Shindo, M.; Smith, C. C.; Kim, S.; Nadizadeh, H.; Suzuki, Y.; Tao, C.; Vu, P.; Tang, S.; Zhang, P.; Murthi, K. K.; Gentile, L. N.; Liu, J. H. *J. Am. Chem. Soc.* **1994**, *116*, 1597–1598; (i) *J. Am. Chem. Soc.* **1994**, *116*, 1599–1600. (j) Masters, J. J.; Link, J. T.; Snyder, L. B.; Young, W. B.; Danishefsky, S. J. *Angew. Chem., Int. Ed.* **1995**, *34*, 1723–1726. (k) Wender, P. A.; Badham, N. F.; Conway, S. P.; Floreancig, P. E.; Glass, T. E.; Granicher, C.; Houze, J. B.; Janichen, J.; Lee, D.; Marquess, D. G.; McGrane, P. L.; Meng, W.; Mucciario, T. P.; Muhlebach, M.; Natchus, M. G.; Paulsen, H.; Rawlins, D. B.; Satkofsky, J.; Shuker, A. J.; Sutton, J. C.; Taylor, R. E.; Tomooka, K. *J. Am. Chem. Soc.* **1997**, *119*, 2755–2756. (l) Wender, P. A.; Badham, N. F.; Conway, S. P.; Floreancig, P. E.; Glass, T. E.; Houze, J. B.; Krauss, N. E.; Lee, D.; Marquess, D. G.; McGrane, P. L.; Meng, W.; Natchus, M. G.; Shuker, A. J.; Sutton, J. C.; Taylor, R. E. *J. Am. Chem. Soc.* **1997**, *119*, 2757–2758. (m) Morihira, K.; Hara, R.; Kawahara, S.; Nishimori, T.; Nakamura, N.; Kusama, H.; Kuwajima, I. *J. Am. Chem. Soc.* **1998**, *120*, 12980–12981. (n) Paquette, L. A.; Wang, H.-L.; Su, Z.; Zhao, M. *J. Am. Chem. Soc.* **1998**, *120*, 5213–5225. (o) Mukaiyama, T.; Shiina, I.; Iwadare, H.; Saitoh, M.; Nishimura, T.; Ohkawa, N.; Sakoh, H.; Nishimura, K.; Tani, Y.; Hasegawa, M.; Yamada, K.; Saitoh, K. *Chem. Eur.* **1999**, *5*, 121–161.
- (116) Han, K.-H.; Fleming, P.; Walker, K.; Loper, M.; Chilton, W. S.; Mocek, U.; Gordon, M. P.; Floss, H. G. *Plant Sci.* **1994**, *95*, 187–196.
- (117) (a) Stierle, A.; Strobel, G.; Stierle, D. *Science* **1993**, *260*, 214–216. (b) Strobel, G.; Yang, X.; Sears, J.; Kramer, R.; Sidhu, R.; Hess, W. M. *Microbiol.* **1996**, *142*, 435–440. (c) Strobel, G. A.; Hess, W. M.; Ford, E.; Sidhu, R.; Yang, X. *J. Ind. Microbiol.* **1996**, *17*, 417–423. (d) Strobel, G. A.; Hess, W. M.; Li, J.-Y.; Ford, E.; Sears, J.; Sidhu, R. S.; Summerell, B. *Aust. J. Bot.* **1997**, *45*, 1073–1082. (e) Hoffman, A.; Khan, W.; Worapong, J.; Strobel, G.; Griffin, D.; Arbogast, B.; Barofsky, D.; Boone, R. B.; Ning, L.; Zheng, P.; Daley, L. *Spectroscopy* **1999**, *13*, 22–32. (f) Stierle, A.; Stierle, D.; Strobel, G.; Bignami, G.; Grothaus, P. Bioactive Metabolites of the Endophytic Fungi of Pacific Yew, *Taxus brevifolia*. *Taxane Anticancer Agents*; American Chemical Society: Washington, DC, 1995; Chapter 6, pp 82–97. (g) Shrestha, K.; Strobel, G. A.; Shrivastava, S. P.; Gewali, M. B. *Planta Med.* **2001**, *67*, 374–376. (h) Li, J. Y.; Sidhu, R. S.; Ford, E. J.; Long, D. M.; Strobel, G. A. *J. Ind. Microbiol. Biotech.* **1998**, *20*, 259–264. (i) Metz, A. M.; Haddad, A.; Worapong, J.; Long, D. M.; Ford, E. J.; Hess, W. M.; Strobel, G. A. *Microbiol.* **2000**, *146*, 2079–2089.
- (118) (a) Fleming, P. E.; Knaggs, A. R.; He, X.-G.; Mocek, U.; Floss, H. G. *J. Am. Chem. Soc.* **1994**, *116*, 4137–4138. (b) Fleming, P. E.; Mocek, U.; Floss, H. G. *J. Am. Chem. Soc.* **1993**, *115*, 805–807.
- (119) (a) Harrison, J. W.; Crowston, R. M.; Lythgoe, B. J. *Chem. Soc. C* **1966**, 1933–1945. See also: (b) Gueritte-Voegelien, F.; Guenard, D.; Potier, P. *J. Nat. Prod.* **1987**, *50*, 9–18.
- (120) (a) Koeppe, A. E.; Hezari, M.; Zajicek, J.; Vogel, B. S.; LaFever, R. E.; Lewis, N. G.; Croteau, R. *J. Biol. Chem.* **1995**, *270*, 8686–8690. (b) Hezari, M.; Lewis, N. G.; Croteau, R. *Arch. Biochem. Biophys.* **1995**, *322*, 437–444. (c) Lin, X.; Hezari, M.; Koeppe, A. E.; Floss, H. G.; Croteau, R. *Biochemistry* **1996**, *35*, 2968–2977. (d) Wildung, M. R.; Croteau, R. *J. Biol. Chem.* **1996**, *271*, 9201–9204. (e) Hezari, M.; Croteau, R. *Planta Med.* **1997**, *63*, 291–295.
- (121) Williams, D. C.; Carroll, B. J.; Jin, Q.; Rithner, C. D.; Lenger, S. R.; Floss, H. G.; Coates, R. A.; Williams, R. M.; Croteau, R. *Chem. Biol.* **2000**, *7*, 969–977.
- (122) (a) Rubenstein, S. M.; Williams, R. M. *J. Org. Chem.* **1995**, *60*, 7215–7223. (b) Rubenstein, S. M. Ph.D. dissertation, Elucidating the Biosynthetic Pathway to Taxol, Colorado State University, 1996. (c) Vazquez, A.; Williams, R. M. *J. Org. Chem.* **2000**, *65*, 7865–7869.
- (123) (a) Hefner, J.; Rubenstein, S. M.; Ketchum, R. E. B.; Gibson, D. M.; Williams, R. M.; Croteau, R. *Chem. Biol.* **1996**, *3*, 479–489. See also: (b) Borman, S. Researchers Probe Steps of Taxol Biosynthesis. *Chem. Eng. News* **1996**, No. July 1, 27–29.
- (124) (a) Walker, K.; Ketchum, R. E. B.; Hezari, M.; Gatfield, D.; Goleniowski, M.; Barthol, A.; Croteau, R. *Arch. Biochem. Biophys.* **1999**, *364*, 273–279. (b) Walker, K.; Croteau, R. *Proc. Natl. Acad. Sci. U.S.A.* **2000**, *97*, 583–587. (c) Walker, K.; Schoendorf, A.; Croteau, R. *Arch. Biochem. Biophys.* **2000**, *374*, 371–380.
- (125) For leading references, see: (a) Herbert, B. A., *The Biosynthesis of Secondary Metabolites*; Chapman and Hall: London, 1981. (b) Nakanishi, K.; Goto, T.; Ito, S.; Nozoe, S. *Natural Products Chemistry*; Kodansha, Ltd.: Tokyo, 1974; Vol. I. (c) *Recent Advances in Phytochemistry, Vol. 24: Biochemistry of the Mevalonic Acid Pathway to Terpenoids*; Towers, G. H. N., Stafford, H. A., Eds.; Plenum Press: New York, 1990. (d) Luckner, M. *Secondary Metabolism in Microorganisms, Plants and Animals*; Springer-Verlag: Berlin, 1990.
- (126) Jennewein, S.; Long, R. M.; Williams, R. M.; Croteau, R. *Chem. Biol.* **2004**, *11*, 379–387.
- (127) (a) Horiguchi, T.; Rithner, C. D.; Croteau, R.; Williams, R. M. *Tetrahedron* **2003**, *59*, 267–273. (b) Rubenstein, S. M.; Vazquez, A.; Williams, R. M. *J. Labelled Compd. Radiopharm.* **2000**, *43*, 481–491. (c) Horiguchi, T.; Rithner, C. D.; Croteau, R.; Williams, R. M. *J. Org. Chem.* **2002**, *67*, 4901–4903. (d) Horiguchi, T.; Li, H.; Croteau, R.; Williams, R. M. *Tetrahedron* **2008**, *64*, 6561–6567. (e) Tohru Horiguchi, T.; Rithner, C. D.; Croteau, R.; Williams, R. M. *J. Labelled Compd. Radiopharm.* **2008**, *51*, 325–328.
- (128) Chau, M.; Croteau, R. *Arch. Biochem. Biophys.* **2004**, *427*, 48–57.
- (129) Chau, M.; Jennewein, S.; Walker, K.; Croteau, R. *Chem. Biol.* **2004**, *11*, 663–672.
- (130) Croteau, R. Unpublished results.
- (131) Schoendorf, A.; Rithner, C. D.; Williams, R. M.; Croteau, R. *Proc. Natl. Acad. Sci. U.S.A.* **2001**, *98*, 1501–1506.
- (132) Jennewein, S.; Rithner, C. D.; Williams, R. M.; Croteau, R. *Proc. Natl. Acad. Sci. U.S.A.* **2001**, *98*, 13595–13600.
- (133) Kaspera, R.; Croteau, R. *Phytochem. Rev.* **2006**, *5*, 433–444.
- (134) (a) Ketchum, R. E. B.; Croteau, R. *Plant Metabolomics. Biotechnol. Agric. For.* **2006**, *57*, 291–309. (b) Ketchum, R. E. B.; Horiguchi, T.; Qiu, D.; Williams, R. M.; Croteau, R. *Phytochemistry* **2007**, *68*, 335–341.
- (135) (a) Uchida, I.; Takase, S.; Kayakiri, H.; Kiyoto, S.; Hashimoto, M.; Tada, T.; Koda, S.; Morimoto, Y. *J. Am. Chem. Soc.* **1987**, *109*, 4108–4109. (b) Iwami, M.; Kiyoto, S.; Terano, H.; Kohsaka, M.; Aoki, H.; Imanaka, H. *J. Antibiot.* **1987**, *40*, 589–593. (c) Kiyoto, S.; Shibata, T.; Yamashita, M.; Komori, T.; Okuhara, M.; Terano, H.; Kohsaka, M.; Aoki, H.; Imanaka, H. *J. Antibiot.* **1987**, *40*, 594–599. (d) Fujita, T.; Takase, S.; Otsuka, T.; Terano, H.; Kohsaka, M. *J. Antibiot.* **1988**, *41*, 392–394.
- (136) (a) Shimomura, K.; Hirai, O.; Mizota, T.; Matsumoto, S.; Mori, J.; Shibayama, F.; Kikuchi, H. *J. Antibiot.* **1987**, *40*, 600–606. (b) Hirai, O.; Shimomura, K.; Mizota, T.; Matsumoto, S.; Mori, J.; Kikuchi, H. *J. Antibiot.* **1987**, *40*, 607–611. (c) Shimomura, K.; Manda, T.; Mukumoto, S.; Masuda, K.; Nakamura, T.; Mizota, T.; Matsumoto, S.; Nishigaki, F.; Oku, T.; More, J.; Shibayama, F. *Cancer Res.* **1988**, *48*, 1116–1172. (d) Masuda, K.; Makamura, T.; Shimomura, K.; Shibata, T.; Terano, H.; Kohsaka, M. *J. Antibiot.* **1988**, *41*, 1497–1499. (e) Masuda, K.; Nakamura, T.; Mizota, T.; Mori, J.; Shimomura, K. *Cancer Res.* **1988**, *48*, 5172–5177. (f) Nakamura, T.; Masada, K.; Matsumoto, S.; Oku, T.; Manda, T.; Mori, J.; Shimomura, K. *Jpn. J. Pharmacol.* **1989**, *49*, 317–324.
- (137) (a) Naoe, Y.; Inami, M.; Matsumoto, S.; Nishigaki, F.; Tsujimoto, S.; Kawamura, I.; Miyayasu, K.; Manda, T.; Shimomura, K. *Cancer Chemother. Pharmacol.* **1998**, *42*, 31–36. (b) Naoe, Y.; Inami, M.; Kawamura, I.; Nishigaki, F.; Tsujimoto, S.; Matsumoto, S.; Manda, T.; Shimomura, K. *Jpn. J. Cancer Res.* **1998**, *89*, 666–672. (c) Naoe, Y.; Inami, M.; Takagaki, S.; Matsumoto, S.; Kawamura, I.; Nishigaki, F.; Tsujimoto, S.; Manda, T.; Shimomura, K. *Jpn. J. Cancer Res.* **1998**, *89*, 1047–1054. (d) Naoe, Y.; Inami, M.; Matsumoto, S.; Takagaki, S.; Fujiwara, T.; Yamazaki, S.; Kawamura, I.; Nishigaki, F.; Tsujimoto, S.; Manda, T.; Shimomura, K. *Jpn. J. Cancer Res.* **1998**, *89*, 1306–1317. (e) Naoe, Y.; Kawamura, I.; Inami, M.; Matsumoto, S.; Nishigaki, F.; Tsujimoto, S.; Manda, T.; Shimomura, K. *Jpn. J. Cancer Res.* **1998**, *89*, 1318–1325. (f) Furuse, K.; Hasegawa, K.; Kudo, S.; Niitaru, H. *Proc. Am. Soc. Clin. Oncol.* **1999**, *18*, 179a, Abstract 689. (g) Ravandi, F.; Wenske, C.; Royca, M.; Hoff, P.; Brito, R.; Zukowski, T.; Mekki, Q.; Pazdur, R. *Proc. Am. Soc. Clin. Oncol.* **1999**, *18*, 225a, Abstract 867.



- (138) (a) Beijnen, J. H.; Lingeman, H.; Underberg, W. J. M.; Vanmunster, H. A. *J. Pharm. Biomed. Anal.* **1986**, *4*, 275. (b) Tomasz, M. *Chem. Biol.* **1995**, *2*, 575–579.
- (139) (a) For a comprehensive review on DNA cross-linking agents, see: Rajsiki, S. R.; Williams, R. M. *Chem. Rev.* **1998**, *98*, 2723–2796. (b) For an excellent review of oxyl radical-based damage to DNA, see: Breen, A. P.; Murphy, J. A. *Free Radical Biol. Med.* **1995**, *18*, 1033–1076.
- (140) (a) Baluna, R.; Rizo, J.; Gordon, B. E.; Ghetie, V.; Vitetta, E. *Proc. Natl. Acad. Sci. U.S.A.* **1999**, *96*, 3957–3962. (b) Rafi-Janajreh, A. Q.; Chen, Dawai; Schmits, Rudolf, Mak, T. W.; Grayson, R. L.; Sponenberg, D. P.; Nagarkatti, M.; Nagarkatti, P. S. *J. Immunol.* **1999**, *163*, 1619–1627. (c) Baluna, R.; Vitetta, E. *Immunopharmacol.* **2001**, *37*, 117–132. (d) Teelucksingh, S.; Padfield, P. L.; Edwards, C. R. W. Q. *J. Med.* **1990**, *75*, 515–524. (e) Barnadas, M. A.; Cisteros, A.; Dolores, S.; Pascual, E.; Puig, X.; de Moragas, J. M. *J. Am. Acad. Dermatol.* **1995**, *32*, 364–366.
- (141) (a) Williams, R. M.; Rajsiki, S. R.; Rollins, S. B. *Chem. Biol.* **1997**, *4*, 127–137. (b) Huang, H.; Rajsiki, S. R.; Williams, R. M.; Hopkins, P. B. *Tetrahedron Lett.* **1994**, *35*, 9669–9672.
- (142) (a) Fukuyama, T.; Xu, L.; Goto, S. *J. Am. Chem. Soc.* **1992**, *114*, 383–385. (b) Schkeryantz, J. M.; Danishefsky, S. J. *J. Am. Chem. Soc.* **1995**, *117*, 4722–4723. (c) Katoh, T.; Itoh, E.; Yoshino, T.; Terashima, S. *Tetrahedron Lett.* **1996**, *37*, 3471–3474. (d) Yoshino, T.; Nagata, Y.; Itoh, E.; Hashimoto, M.; Katoh, T.; Terashima, S. *Tetrahedron Lett.* **1996**, *37*, 3475–3478. (e) Katoh, T.; Yoshino, T.; Nagata, Y.; Nakatani, S.; Terashima, S. *Tetrahedron Lett.* **1996**, *37*, 3479–3482. (f) Katoh, T.; Itoh, E.; Yoshino, T.; Terashima, S. *Tetrahedron* **1997**, *53*, 10229–10238. (g) Yoshino, T.; Nagata, Y.; Itoh, E.; Hashimoto, M.; Katoh, T.; Terashima, S. *Tetrahedron* **1997**, *53*, 10239–10252. (h) Katoh, T.; Nagata, Y.; Yoshino, T.; Nakatani, S.; Terashima, S. *Tetrahedron* **1997**, *53*, 10253–10270. (i) Katoh, T.; Terashima, S. *J. Synth. Org. Chem. Jpn.* **1997**, *55*, 946–957. (j) Fellows, I. M.; Kaelin, D. E., Jr.; Martin, S. F. *J. Am. Chem. Soc.* **2000**, *122*, 10781–10787. (k) Ducray, R.; Ciufolini, M. A. *Angew. Chem., Int. Ed.* **2002**, *41*, 4688–4691. (l) Suzuki, M.; Kambe, M.; Tokuyama, H.; Fukuyama, T. *Angew. Chem., Int. Ed.* **2002**, *41*, 4686–4688. (m) Paleo, M. R.; Aurrecochea, N.; Jung, K.-Y.; Rapoport, H. *J. Org. Chem.* **2003**, *68*, 130–138. (n) Trost, B. M.; O'Boyle, B. M. *Org. Lett.* **2008**, *10*, 1369–1372.
- (143) Judd, T.; Williams, R. M. *Angew. Chem., Int. Ed.* **2002**, *41*, 4683–4685.
- (144) (a) Rollins, S. B.; Williams, R. M. *Tetrahedron Lett.* **1997**, *38*, 4033–4036. (b) Williams, R. M.; Rollins, S. B.; Judd, T. C. *Tetrahedron* **2000**, *56*, 521–532. (c) Judd, T.; Williams, R. M. *Org. Lett.* **2002**, *4*, 3711–3714.
- (145) (a) Tepe, J. J.; Williams, R. M. *Angew. Chem., Int. Ed.* **1999**, *38*, 3501–3503. (b) Tepe, J. J.; Kosogof, C.; Williams, R. M. *Tetrahedron* **2002**, *58*, 3553–3559.
- (146) Williams, R. M.; Tepe, J. *J. Am. Chem. Soc.* **1999**, *121*, 2951–2955. (b) Kosogof, C.; Tepe, J. J.; Williams, R. M. *Tetrahedron Lett.* **2001**, *42*, 6641–6643.
- (147) Subramanian, V.; Ducept, P.; Williams, R. M.; Luger, K. *Chem. Biol.* **2007**, *14*, 553–563.
- (148) (a) Beckerbauer, L.; Tepe, J.; Cullison, J.; Reeves, R.; Williams, R. M. *Chem. Biol.* **2000**, *7*, 805–812. (b) Beckerbauer, L.; Tepe, J. J.; Eastman, R. A.; Mixer, P.; Williams, R. M.; Reeves, R. *Chem. Biol.* **2002**, *8*, 427–441.
- (149) (a) Mao, Y.; Varoglu, M.; Sherman, D. H. *Chem. Biol.* **1999**, *6*, 251–263. (b) Varoglu, M.; Mao, Y.; Sherman, D. H. *J. Am. Chem. Soc.* **2001**, *123*, 6712–6713. (c) Sheldon, P. R.; Mao, Y.; He, M.; Sherman, D. H. *J. Bacteriol.* **1999**, *181*, 2199–2208. (d) Belcourt, M. F.; Penketh, P. G.; Hodnick, W. F.; Johnson, D. A.; Sherman, D. H.; Rockwell, S.; Sartorelli, A. C. *Proc. Natl. Acad. Sci. U.S.A.* **1999**, *96*, 10489–10494. (e) He, M.; Sheldon, P.; Sherman, D. H. *Proc. Natl. Acad. Sci. U.S.A.* **2001**, *98*, 926–931. (f) Martin, T. W. Z.; Dauter, Y.; Devedjev, P.; Sheffield, M.; He, M.; Sherman, D. H.; Derewenda, Z. S.; Derewenda, U. *Structure* **2002**, *10*, 933–942.
- (150) Chamberland, S.; Sherman, D. H.; Williams, R. M. *Org. Lett.* **2009**, *11*, 791–794.
- (151) Taunton, J.; Hassig, C. A.; Schreiber, S. L. *Science* **1996**, *272*, 408–11.
- (152) Grozinger, C. M.; Hassig, C. A.; Schreiber, S. L. *Proc. Natl. Acad. Sci. U.S.A.* **1999**, *96*, 4868–4873.
- (153) Minucci, S.; Pelicci, P. G. *Nature Rev. Cancer* **2006**, *6*, 38–51.
- (154) Johnstone, R. W. *Nature Rev. Drug Discovery* **2002**, *1*, 287–299.
- (155) McLaughlin, F.; La Thangue, N. B. *Current Drug Targets: Inflammation Allergy* **2004**, *3*, 213–219.
- (156) Lin, H. S.; Hu, C. Y.; Chan, H. Y.; Liew, Y. Y.; Huang, H. P.; Lepescheux, L.; Bastianelli, E.; Baron, R.; Rawadi, G.; Clement-Lacroix, P. *Br. J. Pharmacol.* **2007**, *150*, 862–872.
- (157) Avila, A. M.; Burnett, B. G.; Taye, A. A.; Gabanella, F.; Knight, M. A.; Hartenstein, P.; Cizman, Z.; Di Prospero, N. A.; Pellizzoni, L.; Fischbeck, K. H.; Sumner, C. J. *J. Clin. Invest.* **2007**, *117*, 659–671.
- (158) Cao, H.; Stamatoyannopoulos, G. *Am. J. Hematol.* **2006**, *81*, 981–983.
- (159) Hockley, E.; Richon, V. M.; Woodman, B.; Smith, D. L.; Zhou, X.; Rosa, E.; Sathasivam, K.; Ghazi-Noori, S.; Mahal, A.; Lowden, P. A. S.; Steffan, J. S.; Marsh, J. L.; Thompson, L. M.; Lewis, C. M.; Marks, P. A.; Bates, G. P. *Proc. Natl. Acad. Sci. U.S.A.* **2003**, *100*, 2041–2046.
- (160) Meinke, P. T.; Liberator, P. *Curr. Med. Chem.* **2001**, *8*, 211–235.
- (161) Rodriguez, M.; Aquino, M.; Bruno, I.; De Martino, G.; Taddei, M.; Gomez-Paloma, L. *Curr. Med. Chem.* **2006**, *13*, 1119–1139.
- (162) Piekarczyk, R. L.; Frye, A. R.; Wright, J. J.; Steinberg, S. M.; Liewehr, D. J.; Rosing, D. R.; Sachdev, V.; Fojo, T.; Bates, S. E. *Clin. Cancer Res.* **2006**, *12*, 3762–3773.
- (163) Shah, M. H.; Binkley, P.; Chan, K.; Xiao, J.; Arbogast, D.; Collamore, M.; Farra, Y.; Young, D.; Grever, M. *Clin. Cancer Res.* **2006**, *12*, 3997–4003.
- (164) (a) Curtin, M.; Glaser, K. *Curr. Med. Chem.* **2003**, *10*, 2373–2392. (b) Remiszewski, S. W. *Curr. Med. Chem.* **2003**, *10*, 2393–2402.
- (165) (a) Xu, W. S.; Parmigiani, R. B.; Marks, P. A. *Oncogene* **2007**, *26*, 5541–5552. (b) Kelly, W. K.; Marks, P. A. *Nature Clin. Practice Oncol.* **2005**, *2*, 150–157. (c) Glozak, M. A.; Seto, E. *Oncogene* **2007**, *26*, 5420–5432. (d) Yang, X.-J.; Gregoire, S. *Mol. Cell. Biol.* **2005**, *25*, 2873–2884. (e) Grozinger, C. M.; Schreiber, S. L. *Chem. Biol.* **2002**, *9*, 3–16.
- (166) Li, K. W.; Wu, J.; Xing, W.; Simon, J. A. *J. Am. Chem. Soc.* **1996**, *118*, 7237–7238.
- (167) Johns, D. M.; Greshock, T. J.; Noguchi, Y.; Williams, R. M. *Org. Lett.* **2008**, *10*, 613–616.
- (168) (a) Taori, K.; Paul, V. J.; Luesch, H. *J. Am. Chem. Soc.* **2008**, *130*, 1806–1807. (b) Taori, K.; Paul, V. J.; Luesch, H. *J. Am. Chem. Soc.* **2008**, *130*, 13506–13506.
- (169) Bowers, A.; West, N.; Taunton, J.; Schreiber, S. L.; Bradner, J. E.; Williams, R. M. *J. Am. Chem. Soc.* **2008**, *130*, 11219–11222.
- (170) (a) Ying, Y.; Taori, K.; Kim, H.; Hong, J.; Luesch, H. *J. Am. Chem. Soc.* **2008**, *130*, 8455–8459. (b) Chen, F.; Gao, A.-H.; Li, J.; Nan, F.-J. *Chem. Med. Chem.* **2010**, *53*, 4654–4667. (c) Ying, Y.; Liu, Y.; Byeon, S. R.; Kim, H.; Luesch, H.; Hong, J. *Org. Lett.* **2009**, *10*, 4021–4024. (d) Numajiri, Y.; Takahashi, T.; Takagi, M.; Shin-ya, K.; Doi, T. *Synlett* **2008**, 2483–2486. (e) Ghosh, A.; Kulkarni, S. *Org. Lett.* **2008**, *10*, 3907–3909. (f) Seiser, T.; Kamena, F.; Cramer, N. *Angew. Chem., Int. Ed.* **2008**, *47*, 6483–6485. (g) Seiser, T.; Cramer, N. *Chimia* **2009**, *63*, 19–22. (h) Naveschuk, C. G.; Ungermannova, D.; Liu, X.; Phillips, A. J. *Org. Lett.* **2008**, *10*, 3595–3598. (i) Ren, Q.; Dai, L.; Zhang, H.; Tan, W.; Xu, Z.; Ye, T. *Synlett* **2008**, 2379–2383.
- (171) Greshock, T. J.; Noguchi, Y.; West, N.; Schreiber, S. L.; Wiest, O.; Bradner, J. E.; Williams, R. M. *J. Am. Chem. Soc.* **2009**, *131*, 2900–2905.
- (172) Bowers, A. L.; West, N.; Newkirk, T. L.; Troutman-Youngman, A. E.; Schreiber, S. L.; Wiest, O.; Bradner, J. E.; Williams, R. M. *Org. Lett.* **2009**, *11*, 1301–1304.